Universitat Autònoma de Barcelona

Understanding the physiological mechanisms of drought-induced decline in Scots pine (Pinus sylvestris L.)

David Aguadé Vidal

Universitat Autònoma de Barcelona

CREAF

Understanding the physiological mechanisms of drought-induced decline in Scots pine (*Pinus sylvestris* L.)

PhD Thesis by

David Aguadé Vidal

Supervised by

Dr. Jordi Martínez-Vilalta **Dr. Rafael Poyatos López**

Universitat Autònoma de Barcelona, December 2016

Universitat Autònoma de Barcelona

CREAF

Understanding the physiological mechanisms of drought-induced decline in Scots pine (*Pinus sylvestris* L.)

PhD Thesis by

David Aguadé Vidal

To be eligible for the Doctor degree

With the approval of the supervisors

Dr. Jordi Martínez-Vilalta **Dr. Rafael Poyatos López**

Programa de doctorat en Ecologia Terrestre

CREAF & Departament de Biologia Animal, Biologia Vegetal i Ecologia

Facultat de Biociències

Universitat Autònoma de Barcelona, December 2016

Table of contents

Resum

El canvi climàtic provocat per l'emissió antropogènica de gasos d'efecte hivernacle ha esdevingut una preocupació a nivell global. Durant les darreres dècades, com a conseqüència d'aquest canvi climàtic, s'ha observat un augment dels períodes de sequera i d'onades de calor, que es preveu que s'intensifiqui en els pròxims decennis. Tot i que les plantes tenen mecanismes per evitar l'estrès provocat per aquests fenòmens severs, tant a curt com a llarg termini, darrerament s'han documentat arreu del món múltiples casos de mortalitat forestal produïda per sequera i és probable que aquests augmentin en el futur, particularment en aquelles zones on la disponibilitat d'aigua és ja limitada. Aquests episodis de decaïment forestal poden causar canvis sobtats en l'estructura i funcionament dels ecosistemes. Per tant, a causa de l'estreta interacció entre els boscos i l'atmosfera, és important estudiar els mecanismes fisiològics implicats en la mortalitat per tal de poder millorar els models que preveuen la dinàmica forestal. L'objectiu principal d'aquesta tesi doctoral és el d'aprofundir en els mecanismes fisiològics que intervenen en els processos de decaïment induït per sequera. Els estudis s'han fet en una població de pi roig (*Pinus sylvestris* L.) dins el Paratge Natural d'Interès Nacional (PNIN) de Poblet (a les Muntanyes de Prades, Tarragona). Diferents episodis de mortalitat per sequera en el pi han sigut documentats en aquesta població, on, a més a més, l'alzina (*Quercus ilex* L.) és una clara candidata a substituir el pi roig en els propers anys ja que és l'actual espècie dominant del sotabosc i tendeix a ocupar-ne els rodals afectats per mortalitat de pins.

En aquesta tesi m'he centrat en estudiar els dos principals mecanismes fisiològics que s'han proposat com a principals desencadenants de la mortalitat forestal produïda per sequera: l'esgotament de les reserves de carboni i la fallida hidràulica. Tenint en compte que la defoliació és un símptoma del decaïment forestal i que està associada a un major risc de mortalitat, he caracteritzat les conseqüències fisiològiques de la defoliació en el pi roig, comparant els patrons estacionals de flux de saba, els potencials hídrics foliars i la conductància hidràulica de la planta entre pins defoliats i pins sans (no defoliats) (Capítol 2), per a testar la hipòtesi que els pins defoliats serien més sensibles a la sequera. En el Capítol 3, s'ha mesurat la vulnerabilitat a l'embolisme en branques i arrels, l'estacionalitat en l'embolisme nadiu i els nivells de les reserves de carbohidrats no estructurals en pins defoliats i no defoliats amb l'objectiu de testar si la defoliació s'associa més amb processos de fallida hidràulica o d'inanició per manca de carboni. A més, també s'ha analitzat el paper dels fongs patògens com a possible factor implicat en la defoliació. Posteriorment, he utilitzat dades de microvariacions del radi del xilema per a estudiar la resposta a la sequera de la resistència hidràulica subterrània i de la seva contribució a la

resistència total en pins defoliats i no defoliats (Capítol 4). Finalment, s'han estudiat les respostes a la sequera de pins roig i alzines en boscos mixtos i purs (Capítol 5) per tal de determinar possibles diferències fisiològiques que influeixin en la competència entre les dues espècies en un escenari de substitució del pi roig per l'alzina.

Els resultats d'aquesta tesi mostren que els pins defoliats són més sensibles a la sequera que els pins no defoliats i presenten una major reducció de la seva transpiració com a conseqüència del tancament estomàtic, associat també a una reducció de la conductància hidràulica al llarg de tot l'arbre. Per tant, la defoliació es podria interpretar més aviat com una conseqüència de la sequera que no pas com una estratègia per combatre-la (Capítol 2). A més a més, les arrels dels arbres defoliats presenten una major vulnerabilitat a l'embolisme (Capítol 3), a banda de tindre també menys reserves de carbohidrats no estructurals en tots els òrgans sobretot en els mesos d'estiu (Capítol 3). Això, combinat amb el paper dels fongs patògens, fa que sigui molt difícil esbrinar quin és el mecanisme precís que porta a la mortalitat produïda per sequera degut a la complexa interconnexió entre ells. D'altra banda, observem en el Capítol 4 com la resistència hidràulica radicular juga un paper important amb l'augment de la sequera, però, en aquest cas, observem que els pins no defoliats són els que pateixen majors constriccions en el transport d'aigua en la zona radicular en condicions de sequera. Finalment, en el Capítol 5 observem una major resistència a la sequera de l'alzina en comparació amb el pi roig, malgrat una certa tendència en l'alzina a patir un risc més elevat de fallida hidràulica durant sequeres intenses. Aquesta resistència a la sequera de l'alzina, tant en masses pures com mixtes co-habitant amb el pi roig, suggereix que el procés de substitució del pi roig per l'alzina continuarà en el futur.

Abstract

Climate change caused by anthropogenic emissions of greenhouse gases has become a global concern. In recent decades, as a result of this climate change, there has been an increase in the frequency of drought periods and heat waves, which is expected to intensify in the coming decades. Although plants present mechanisms to prevent severe stress caused by these phenomena, both in the short and long term, several episodes of drought-induced mortality have recently been reported and they are likely to increase in the future, particularly in those areas where water is already limiting. These episodes of forest decline can cause sudden changes in the structure and functioning of ecosystems. Therefore, due to the close interaction between forests and the atmosphere, it is important to study the physiological mechanisms involved in mortality in order to improve models that predict forest dynamics. The main objective of this thesis is to delve into the physiological mechanisms involved in drought-induced forest decline. The studies were carried out in a population of Scots pine (*Pinus sylvestris* L.) within PNIN (Paratge Natural d'Interès Nacional) of Poblet (Prades Mountains, Catalonia). Different episodes of Scots pine drought-induced mortality have been documented in this population where, in addition, holm oak (*Quercus ilex* L.) is a clear candidate to replace pine in the coming years as it is the current dominant understorey species and tends to occupy the gaps opened by pine mortality.

In this thesis I focused on the study of the two main physiological mechanisms that have been proposed as major triggers of drought-induced tree mortality: depletion of carbon stores and hydraulic failure. Given that defoliation is a symptom of forest decline and that it is associated with an increased mortality risk, I characterised the physiological consequences of Scots pine defoliation, by comparing the seasonal patterns of sap flow, leaf water potentials and plant hydraulic conductance among defoliated and healthy (non-defoliated) pines (Chapter 2), to test the hypothesis that defoliated pines would be more sensitive to drought. In Chapter 3, I measured vulnerability to embolism in roots and branches and the seasonality of native embolism and non-structural carbohydrates reserves in defoliated and non-defoliated pines, in order to test whether defoliation was more associated with hydraulic failure or carbon starvation processes. In addition, I also analysed the role of pathogenic fungi as a possible factor involved in mortality. Subsequently, I used data on the microvariations of xylem radius to study the drought response of belowground hydraulic resistance and its contribution to total resistance in defoliated and non-defoliated pines (Chapter 4). Finally, I studied the drought responses in Scots pine trees and holm oaks in mixed and pure stands (Chapter 5), in order to determine possible physiological

differences influencing competition between both species in a scenario of Scots pine substitution by holm oak.

The main results of this thesis showed that defoliated pines were more sensitive to drought than non-defoliated ones and that they showed a transpiration reduction as a result of stomatal closure, which associated with a reduction in tree hydraulic conductance. Thus, defoliation may be more adequately seen as an inevitable consequence of drought than as a strategy to cope with water stress (Chapter 2). Furthermore, roots of defoliated trees showed greater vulnerability to embolism (Chapter 3), besides also having less nonstructural carbohydrate stores in all organs, especially in summer months (Chapter 3). This, combined with the role of pathogenic fungi, makes it very difficult to identify the precise mechanisms triggering drought-induced mortality due to the complex interconnection between them. I highlight, in Chapter 4, how root hydraulic resistance played an important role with increasing drought, but in this case, non-defoliated pines suffered higher constraints on water transport in the root zone under drought conditions. Finally, in Chapter 5, I observed a higher drought resistance in holm oak compared to Scots pine, despite holm oak tending to suffer a higher risk of hydraulic failure under intense droughts. This drought resistance of holm oak, both in pure and mixed stands coexisting with Scots pine, suggests that the process of substitution of Scots pine by holm oak will continue in the future.

Chapter 1

General introduction

Forests under pressure

Forests cover approximately 30% of world's land surface, throughout tropical, temperate and boreal regions (Bonan 2008). Forests should not be seen only as a group of trees living in the same habitat where animals can shelter in, as they provide a variety of ecosystem services to humankind. Broadly speaking, ecosystem services are defined as the benefits that humanity obtains from the proper functioning of ecosystems. Ecosystem services can be grouped into four categories depending on the type of benefit, including provisioning (e.g., food, medicines, timber…), regulating (e.g., purification of air and water, carbon sequestration…), cultural (e.g., aesthetics, spiritual, recreational…) and supporting services (these are necessary for the existence of all other services; e.g., primary production…) (Naidoo et al. 2008). Focusing on forests' ecosystem services, their prominent role on Earth's biogeochemical cycles should be emphasised. For instance, forests are a key driver in the global carbon cycle, as they currently store about 861 ± 66 Pg C (Pan et al. 2011) and absorb around one-fourth of the total anthropogenic carbon emissions (Le Quéré et al. 2014). In general, there is a tight interdependence between forests and the atmosphere, as forests also regulate local and global weather through their influence on the water and energy balances (Alkama and Cescatti 2016).

Globally, human activities and particularly land use, driven by socio-economic factors, are currently a major determinant of forest cover dynamics and functioning. Even though forests are in expansion in some regions because of the abandonment of agropastoral activities, particularly in less productive and remote areas from developed countries (Navarro and Pereira 2012), they are also critically endangered in other regions. For example, woodlands suffer strong pressures due to the rapid expansion of population and economy in tropical countries, thereby altering forest distribution and composition as a consequence of activities like logging (Achard et al. 2002; Broadbent et al. 2008) and croplands expansion (Gibbs et al. 2010; Morton et al. 2006), or by changes in the atmospheric composition (Sicard et al. 2016).

The global distribution of forests is determined, to a large extent, by climate (Woodward 1987). Therefore, climate change produced by the anthropogenic increase in greenhouse gas concentration in the atmosphere (IPCC 2014) is having and will have a major impact on forest function and dynamics. These changes in atmospheric composition have already had direct effects on Earth's climate, causing an increase of the global temperature (~0.85°C over the period 1880-2012) and also altering the seasonality of extreme weather events (e.g., the frequency of heat waves has increased in some areas) (IPCC 2014). Drought conditions are likely to be exacerbated

by global warming (Trenberth et al. 2014) and extreme drought events may in turn reduce the carbon sink potential of ecosystems (Reichstein et al. 2013). Basically, all model projections forecast that temperatures will continue to rise with more frequent hot and fewer cold temperature extremes and more extreme droughts in some regions (IPCC 2014). Thus, understanding and predicting the impacts of climate change on forests have become fundamental aims for global change scientists and ecologists.

Drought-induced tree mortality and its physiological mechanisms

Tree mortality is an ecological process driven by the interaction of biotic and abiotic factors (Franklin et al. 1987). However, it was not until the 1980's acid rain crisis that the link between causal mortality factors and physiological mechanisms contributing to tree death began to be investigated (Johnson and Siccama 1983). More recently, events of forest decline have been related to climate change and, in particular, to the physiological stress suffered by trees as a consequence of drought, elevated temperatures and related pathogen outbreaks and more frequent wildfires (Allen et al. 2015; Allen et al. 2010). Moreover, in some areas, drought-induced forest decline processes may be aggravated by forest densification resulting from the abandonment of forest management (Linares et al. 2009). This multi-causal nature of drought-induced tree decline precludes our ability to predict tree mortality within communities and across landscapes (Anderegg et al. 2012a), thus hampering the performance of dynamic global vegetation models used to predict the future impacts of climate change on forests (McDowell et al. 2011).

Drought stress on trees can be produced by soil water exhaustion, by an increase in evaporative demand of the air surrounding leaves, or both. Vegetation in general, and trees in particular, have developed different mechanisms to cope with these stressful conditions. Tree responses can take place in the short or long term depending on the intensity and duration of the drought and the plant organ involved (Abrams 1990). For instance, in the long term, plants can increase their belowground biomass in order to explore a new portion of soil and exploit new water sources (Hendrick and Pregitzer 1996) or they can also reduce their leaf area in order to diminish transpiration water loss and improve the water status of the remaining crown (Mencuccini and Grace 1995; Pataki et al. 1998). Regarding the short-term mechanisms, the most important one is stomatal regulation. Stomata are the pores in the leaves where gas exchange takes place, including the entrance of carbon dioxide (CO_2) and the outflow of water (H_2O) and

oxygen (O_2). Trees will normally close stomata during a drought period to avoid excessive loss of water through transpiration, but they will also inevitably reduce the CO_2 supply needed for photosynthesis. However, the stomatal sensitivity to drought varies greatly across species. According to the classic view, isohydric plants are those that keep their internal water status reasonably constant (relatively high xylem water potentials) during drought by having very sensitive stomata and rapid stomatal closure in face of water stress (Jones 1998; Tardieu and Simonneau 1998). On the contrary, anisohydric plants reach more negative xylem water potentials and tend to show slower stomatal responses under drought (Jones 1998; Tardieu and Simonneau 1998).

McDowell et al. (2008) were among the first who tried to formalise the physiological mechanisms underlying drought-induced tree mortality based on a hydraulic framework. Their hypotheses were based on stomatal regulation of water loss during a drought period of a given intensity and duration and the distinction between isohydric or anisohydric behaviours. According to their framework, isohydric plants will not be able to maintain photosynthesis under drought due to prolonged stomatal closure. If the water shortage is long enough, reduced (or ceased) assimilation together with continuing carbon demands for growth and maintenance could cause a depletion of non-structural carbohydrates (NSCs) and, eventually, tree death by carbon starvation (McDowell et al. 2008; McDowell et al. 2011). On the other hand, during an intense drought, anisohydric plants could reach very high xylem tensions (low water potentials), which could trigger the entrance of air bubbles into their xylem conduits, initiating a cavitation process that would eventually result in hydraulic failure (i.e., the cessation of water transport from roots to leaves in the xylem) (McDowell et al. 2008; McDowell et al. 2011). Biotic agents, which are frequently amplified by high temperatures and drought (Desprez-Loustau et al. 2006), could have a key role into drought-induced decline by amplifying the effects of the aforementioned drought-induced responses (Gaylord et al. 2013; Oliva et al. 2014).

Testing physiological mechanisms of drought-induced tree mortality: 1000 ways to die

Despite the huge scientific effort devoted to explore the precise mechanisms implicated in drought-induced tree mortality in the last decade, the physiological mechanisms remain insufficiently understood, mainly because of the difficulty to demonstrate them in nature (Sala et al. 2010). However, several important developments have occurred since the seminal work by McDowell et al. (2008) in the study of the carbon and water economy of plants, and their

interactions, under extreme drought. Adams et al. (2009) were amongst the first authors, after the McDowell et al. (2008) paper, to identify carbon starvation as the most likely mechanism triggering drought-induced tree mortality, although their work was not immune to criticism (Leuzinger et al. 2009; Sala 2009). Later on, McDowell and Sevanto (2010) highlighted the importance of partitioning the different mechanisms that trigger drought-induced tree mortality for a better understanding of the mortality process itself. With regard to the carbon starvation hypothesis, several studies have demonstrated a clear association between low reserves of NSCs and drought-induced tree decline (Adams et al. 2013; Galiano et al. 2011; Mitchell et al. 2013; O'Brien et al. 2014). However, this carbon role during tree die-off does not seem to be universal and it is difficult to extrapolate to other similar tree decline events, since NSCs dynamics are highly variable even between species of the same genus (Piper 2011) or between different organs within a species (Hartmann et al. 2013b). Furthermore, NSCs stores can also strongly depend on the intensity of drought and the precise moment when tree's tissues are sampled (Martínez-Vilalta et al. 2016; McDowell 2011). On the other hand, regarding the hydraulic failure hypothesis and its association to drought-induced tree mortality by the formation of xylem embolism, high levels of hydraulic dysfunction have been reported in most species under extreme or terminal drought (Anderegg et al. 2013b; Hoffmann et al. 2011; Nardini et al. 2013). However, the detailed mechanisms of hydraulic dysfunction are far from being completely understood, and embolism repair after drought cessation remains a controversial issue (Brodersen and McElrone 2013; Delzon and Cochard 2014).

Added to carbon starvation and hydraulic failure as the main mechanisms implicated in drought-induced mortality, the occurrence of phloem impairment (Sala et al. 2010) may also have a key role by implying the possibility of local carbon starvation even if overall plant NSCs stores are substantial, thus hindering the study of NSCs depletion as a mechanism in drought-induced tree decline (Hartmann et al. 2013b; Sevanto et al. 2014). Recently, some authors have stressed the need to adopt a more integrated approach focusing on the interrelations between plant hydraulics and carbon stores if we are to fully understand the process of tree mortality (Hartmann et al. 2015; McDowell 2011; McDowell et al. 2011; McDowell and Sevanto 2010; Sala et al. 2012).

Recent modelling studies suggest that different mechanisms of mortality may occur in nature and it may be impossible to disentangle them in practice (Mencuccini et al. 2015). On the other hand, the general use of the dichotomy between iso- and anisohydric behaviour to study the responses of species to drought may be problematic because stomata responses to environmental conditions take place in a continuum (Klein 2014; Martínez-Vilalta et al. 2014) and

their association with water potential regulation is not as clear as previously assumed (Garcia-Forner et al. 2016a; Martínez-Vilalta and Garcia-Forner 2016).

Hydraulics as a key factor underlying drought-induced decline

Regardless of the precise mechanism leading to tree death under extreme drought, there is a growing consensus that most plant responses under drought, including stomatal responses, are triggered by hydraulic mechanisms (e.g., Sperry and Love 2015). The difference between the water potentials under which a plant is operating under certain conditions and the critical values leading to hydraulic dysfunction is termed hydraulic safety margin (Choat et al. 2012a; Meinzer et al. 2009), which has been proven as a good proxy for vulnerability to drought-induced tree mortality (Anderegg et al. 2016; McDowell et al. 2016). Consequently, the addition of precise hydraulic mechanisms and species specific thresholds in dynamic global vegetation models could help us to better forecast tree mortality (Anderegg et al. 2015a). On the other hand, NSCs threshold below which tree mortality occurs have not been identified (but see indirect evidence in Martínez-Vilalta et al. 2016), reflecting our limited understanding of NSCs distribution and storage along the plant (Hartmann and Trumbore 2016).

Hydraulic resistances are distributed along the tree's hydraulic pathway, equivalent to an electrical circuit (Tyree and Ewers 1991). Increases in hydraulic resistance as a consequence of the formation of embolism can take place in any plant's organ, though it is still unclear which part of the plant's hydraulic pathway is more vulnerable to xylem embolism relative to the water potentials it experiences (Bartlett et al. 2016). Plant roots have been proven to be more vulnerable than other plant organs during drought (Domec et al. 2009; Hacke et al. 2000; Martínez-Vilalta et al. 2002; Rodríguez-Calcerrada et al. 2016), with the only possible exception of leaves (Sack and Holbrook 2006). Furthermore, differential responses of root and rhizosphere hydraulic resistances to varying soil water supply (Domec et al. 2009) and/or evaporative demand (Martínez-Vilalta et al. 2007) may also be involved in determining tree survival under extreme drought. Nevertheless, most of the studies on tree hydraulics during drought-induced tree decline have focused on the mechanisms occurring within aboveground tissues (Anderegg et al. 2015a) and a more detailed picture of hydraulic resistance dynamics in the rizhosphere is urgently needed.

Southern Scots pine populations as a model system

Scots pine (*Pinus sylvestris* L.) is one of the most widely distributed species of the world (Critchfield and Little 1966), and can be found from the far east of Siberia to the European side of the Mediterranean basin; with some of its southernmost populations located in the Iberian Peninsula (Figure 1). This enormous distribution implies that Scots pine species has to face highly contrasted climatic conditions along a wide environmental gradient. Scots pine has been categorised as an isohydric species (Irvine et al. 1998; Poyatos et al. 2008; Zweifel et al. 2007) and presents a high capacity to adjust its hydraulic architecture to contrasting atmospheric and soil conditions, primarily through changes in its leaf-to-sapwood area ratio (Martínez-Vilalta et al. 2009; Poyatos et al. 2007). In spite of this high plasticity, several episodes of Scots pine die-off have been reported and associated to extreme drought and heat events (and the associated insect pathogens outbreaks) across Europe, mostly located in dry parts of its distribution, such as the Swiss dry Rhone Valley (Bigler et al. 2006; Dobbertin et al. 2007; Wermelinger et al. 2008), Spain (Galiano et al. 2010; Martínez-Vilalta and Piñol 2002; Navarro Cerrillo et al. 2007), Tyrol (Oberhuber 2001) and the Italian Aosta Valley (Vertui and Tagliaferro 1998) (Figure 1). An additional factor compromising the viability of southernmost Scots pine populations is the fact that recruitment is frequently very low or absent, particularly in those populations with higher rates of mortality (Vilà-Cabrera et al. 2013). As a result, Scots pine is being replaced by other species, particularly oaks (*Quercus* spp.) in some parts of its distribution (Galiano et al. 2010; Rigling et al. 2013).

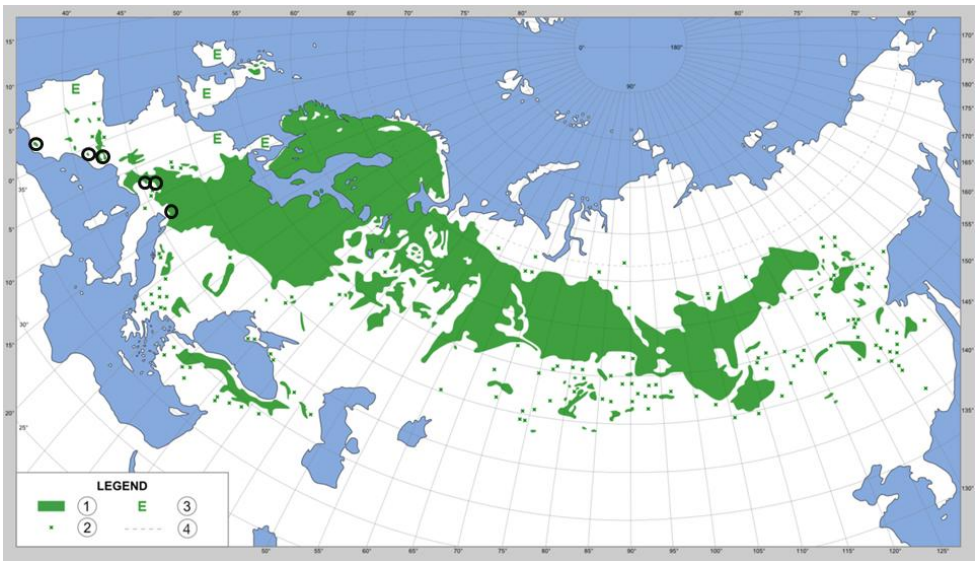

Figure 1. Current distribution of Scots pine (*Pinus sylvestris* L.) across Eurasia. The regions where evident drought-induced tree decline episodes have been reported and studied are marked in black circles. Legend: 1) main distribution; 2) isolated populations; 3) extinct populations by humans; 4) Arctic circle.

Populations of Scots pine in Spain are among the southernmost ones and have experienced several episodes of drought-induced decline in the last decades, since climate change have altered the normal patterns of drought and wildfires in this region (Lloret 2012; Martínez-Vilalta et al. 2012a). The study of populations at the limits of the current species' distribution is of significance because current climatic extremes, which are causing tree mortality episodes, could take place in more northern populations in the coming decades (Hampe and Petit 2005). Furthermore, southern populations are a great reservoir of within species diversity (Hampe and Petit 2005) that could help to mitigate widespread tree mortality.

Despite the global increase of Scots pine basal area growth in the whole of Catalonia throughout the 20th century, probably caused by fertilisation effects (CO_2, N) and a lengthening of the growing season, a negative impact of warming at the driest populations in Catalonia has been reported, particularly in the last decades (Martínez-Vilalta et al. 2008; Martínez-Vilalta et al. 2012c). Competition for resources amongst trees, as well as shallow soils and low local water availability have been shown to exacerbate the demographic effects of drought (Galiano et al. 2010; Martínez-Vilalta et al. 2012c; Vilà-Cabrera et al. 2013; Vilà-Cabrera et al. 2011). The mortality process in Scots pine is associated with long-term declines in radial growth, which can start decades before mortality occurs (Hereş et al. 2012). The period (~few years) immediately preceding mortality is normally characterised by substantial leaf loss, which can be highly heterogeneous within populations (Galiano et al. 2011). Leaf loss has been associated with reduced growth and low NSCs reserves, which in turn has been shown to increase mortality risk under subsequent droughts (Galiano et al. 2011). At the same time, previous studies have shown that different levels of drought-induced mortality between Scots pine populations were associated to differences in hydraulic conductivity per unit of leaf area, but not to vulnerability to xylem embolism (Martínez-Vilalta and Piñol 2002). The role of biotic agents in Scots pine mortality has been studied only at a few sites, including the effect of blue-stain fungal pathogens in the Alps (Heiniger et al. 2011), and the effect of mistletoe infection in the Pyrenees (Galiano et al. 2011).

Structure and main objectives of the thesis

The main aim of the present thesis is to understand the mechanisms of drought-induced tree decline in Scots pine. We focus on one of the southernmost populations of Scot pine in Spain, located in Prades Mountains (NE Iberian Peninsula), where several episodes of Scots pine drought-induced mortality have been reported since the 1990's (Hereş et al. 2012; Martínez-

Vilalta and Piñol 2002). Our studied population was located in a NW-facing hillside in Tillar Valley, within the Poblet Forest Natural Reserve (41° 19'N, 1° 00'E; 990m above sea level). The climate is typically Mediterranean, with hot and dry summers, mild winters and most of the rainfall concentrated in spring and autumn. The soils are mostly Xerochrepts with fractured schist and clay loam texture, although outcrops of granitic sandy soils are also present (Hereter and Sánchez 1999). Our population was located on a very shallow and unstable soil due to the high stoniness and steep slopes (35° on average). The dominant species are Holm oak (*Quercus ilex* L.) and Scots pine. This latter species is suffering drought-induced decline, but the health status of trees is highly variable, and defoliated trees (<< 50% of green needles) in the process of dying (cf. above) coexist with apparently healthy individuals (>> 50% of green needles) and dead stumps (Figure 2). Scots pine recruitment is extremely low in our study population, and Holm oak is becoming the canopy dominant species in those sites with higher Scots pine mortality (Vilà-Cabrera et al. 2013). More detailed information about the study area can be found in Hereter& Sánchez (1999).

Figure 2. Aerial photography taken at Tillar Valley. Defoliated, non-defoliated and dead Scots pine trees coexist in the same population. Author: Richard Martin Vidal.

We focused on three main habitats at Tillar Valley: 1) Pure Holm oak stand, which mainly dominates the valley's lowlands, 2) pure Scots pine forests in the upper valley and 3) a mixed Holm oak-Scots pine forest in mid-altitude within the valley (Figure 3).

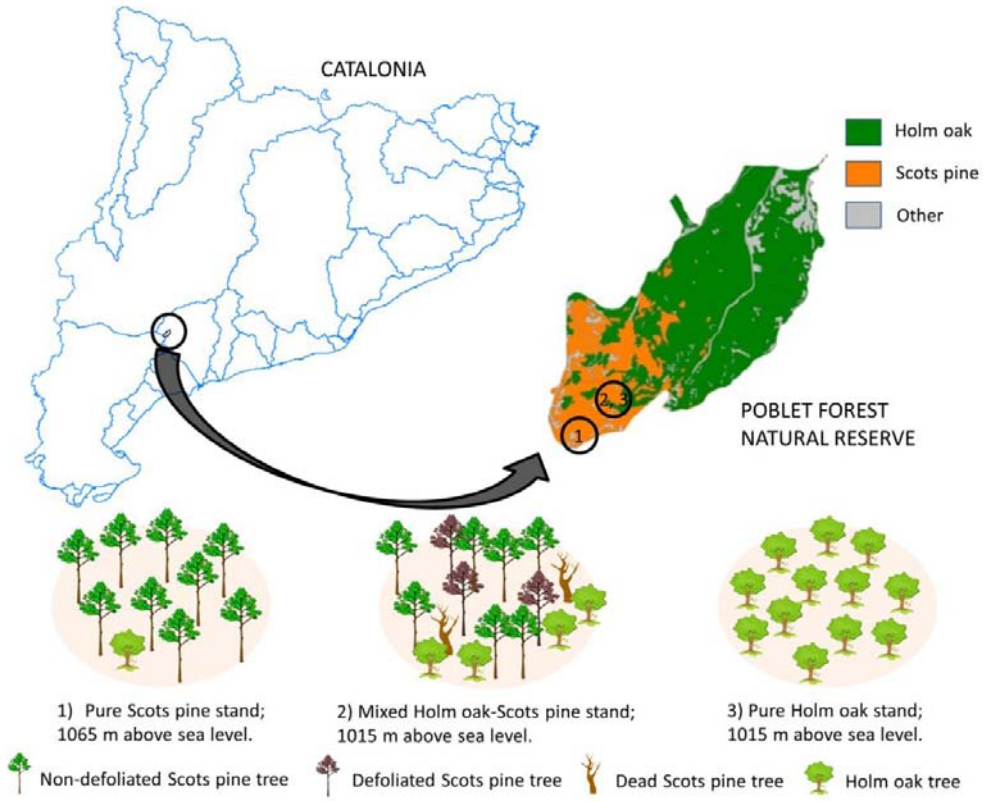

Figure 3. Diagram showing the three main stands studied in the present thesis within the Poblet Forest Natural Reserve and its location in Catalonia. The main watersheds are drawn in the map of Catalonia.

The present thesis is divided into 4 main chapters, each of which has different objectives:

Chapter 2: We analysed the patterns of seasonal sap flow, needle water potentials and whole-tree leaf-specific conductance in Scots pines affected by drought-induced defoliation compared with that of apparently healthy pines in Prades Mountains. The coexistence of healthy and defoliated Scots pines in the study area provides an ideal model system to explore the physiological implications of drought-induced defoliation and the mechanisms underlying eventual tree death and possible C starvation (Galiano et al. 2011). We hypothesised that: (1) defoliated and non-defoliated pines would display similar regulation of leaf water potential, with minimum values of ca. -2.5 MPa (Martínez-Vilalta et al. 2009); (2) the maximum values of sap flow per unit of leaf area and soil-to-leaf hydraulic conductance in spring would be higher in defoliated than in non-defoliated pines, but (3) both variables would show stronger declines during the summer in defoliated pines, indicating higher sensitivity to increasing soil and atmospheric drought. We finally postulated that, in terms of C gain (4) the increased hydraulic capacity during spring in defoliated pines would not compensate for their reduced canopy leaf area and the prolonged periods with near-zero gas exchange, leading to more strongly depleted carbohydrate reserves and increased mortality risk associated with drought-induced defoliation.

Chapter 3: Field studies on mature trees examining all three hypothesised mechanisms of drought-induced mortality are still scarce and rarely explore explicitly the interactions between different mechanisms and their occurrence in different plant organs. Here we compare the hydraulic properties and the dynamics of NSC and embolism as a function of defoliation and infection by fungal pathogens in Scots pine trees growing together in a site affected by drought-induced decline (Hereş et al. 2012; Martínez-Vilalta and Piñol 2002) and close to the dry limit of the distribution of the species. Previous studies have shown that defoliation precedes drought-induced mortality in Scots pine trees from the same or similar sites (Galiano et al. 2011; Poyatos et al. 2013), and that defoliation seems to be an inevitable consequence of drought in the most susceptible individuals rather than an (effective) strategy to cope with it (Poyatos et al. 2013). In this context, we address the following questions: (1) are defoliated Scots pines intrinsically more vulnerable to xylem embolism than non-defoliated ones, providing evidence in favour of hydraulic failure as an important component of the decline process? If so, do defoliated trees experience higher levels of native embolism under dry summer conditions? (i.e., are leaf area reductions enough to compensate for their intrinsically higher vulnerability?) (2) Do defoliated pines have lower seasonal NSC concentrations in all organs, supporting carbon starvation being involved in the mortality process? (3) Is infection by fungal pathogens likely to enhance hydraulic dysfunction through increased levels of native embolism, or carbon depletion directly or indirectly lowering NSC levels through increased consumption, reduced sapwood depth or low growth?

Chapter 4: We monitored sap flow, xylem radius variations and leaf water potentials in Scots pine trees from a mountain Mediterranean forest where episodes of drought-induced decline have been reported since the 1990's (Hereş et al. 2012; Martínez-Vilalta and Piñol 2002). Our main objective was to estimate the below-crown hydraulic resistance (R_{bc}) and its contribution to whole-tree hydraulic resistance and explore their seasonal dynamics in a declining Scots pine population at the dry-edge of its distribution. We hypothesised that (1) R_{bc} will increase in summer in all trees studied due to the higher vulnerability to embolism of roots, (2) the summer increase in R_{bc} will be more acute in defoliated pines, and (3) $\%R_{bc}$ will increase in summer in both defoliated and non-defoliated pines due to the greater contribution of roots relative to leaves to hydraulic resistance during acute drought.

Chapter 5: We compare the physiological responses of coexisting Scots pine and holm oak trees to two major components of drought: vapour pressure deficit (VPD) and soil water content (SWC), both in pure and mixed stands, in an area where Scots pine has been affected by drought-induced mortality (Aguadé et al. 2015; Martínez-Vilalta and Piñol 2002; Poyatos et al. 2013) and

where this species is being replaced by holm oak as the canopy-dominant species (Vilà-Cabrera et al. 2013). An important aspect of this study is that, unlike much previous work comparing conifers with angiosperms, it compares species with the same leaf habit. We hypothesise that (1) Scots pine would close stomata at higher (closer to zero) water potentials than holm oak and, therefore, it would experience lower losses of xylem hydraulic conductivity and greater reductions of NSC concentrations during drought, and (2) holm oak would suffer higher water stress in pure stands than in mixed ones, limiting the capacity of holm oak to become the canopy-dominant species in the long term.

Chapter 2

Drought-induced defoliation and long periods of near-zero gas exchange play a key role in accentuating metabolic decline of Scots pine[1]

Poyatos, R., Aguadé, D., Galiano, L., Mencuccini, M. and Martínez-Vilalta, J.

[1]Published in *New Phytologist* (DOI: 10.1111/nph.12278)

Abstract

Drought-induced defoliation has recently been associated with the depletion of carbon reserves and increased mortality risk in Scots pine (*Pinus sylvestris* L.). We hypothesise that defoliated individuals are more sensitive to drought, implying that potentially higher gas exchange (per unit of leaf area) during wet periods may not compensate for their reduced photosynthetic area. We measured sap flow, needle water potentials and whole-tree hydraulic conductance to analyse the drought responses of co-occurring defoliated and non-defoliated Scots pines in northeast Spain during typical (2010) and extreme (2011) drought conditions.

Defoliated Scots pines showed higher sap flow per unit leaf area during spring, but were more sensitive to summer drought, relative to non-defoliated pines. This pattern was associated with a steeper decline in soil-to-leaf hydraulic conductance with drought and an enhanced sensitivity of canopy conductance to soil water availability. Near-homeostasis in midday water potentials was observed across years and defoliation classes, with minimum values of -2.5 MPa. Enhanced sensitivity to drought and prolonged periods of near-zero gas exchange were consistent with low levels of carbohydrate reserves in defoliated trees. Our results support the critical links between defoliation, water and carbon availability and their key roles in determining tree survival and recovery under drought.

Keywords: canopy defoliation, hydraulic limits, non-structural carbohydrates, *Pinus sylvestris*, sap flow, stomatal conductance, tree mortality, water potential

2.1. Introduction

Forests are key regulators of land-atmosphere interactions at the global scale, including energy balance processes and carbon (C) and water cycles (Bonan 2008). Among all the abiotic factors constraining forest functioning, water availability is often the most limiting factor in many forest ecosystems (Boisvenue and Running 2006). Under extreme and/or chronic drought, partial canopy dieback and increased tree mortality may occur (Bréda et al. 2006). These phenomena are being increasingly reported worldwide (Allen et al. 2010; Carnicer et al. 2011) and can ultimately lead to the collapse of many forest-related ecosystem services (Breshears et al. 2011). Drought-induced dieback is a complex multifactor process (McDowell 2011) in which climate change emerges as a key element (Van Mantgem et al. 2009), but often in combination with other

interacting drivers, such as forest densification (Vilà-Cabrera et al. 2011). This complexity and our limited understanding of the physiological mechanisms involved in drought-induced dieback processes (Sala et al. 2010) hinder our capacity to predict the potential feedbacks between global change and forest ecosystems (McDowell et al. 2011).

Tree growth and survival largely depend on an adequate supply of water to transpiring leaves via root absorption and xylem transport in a tension-driven hydraulic continuum. Physiological and structural responses to fluctuations in water availability have been observed at various time scales and organisational levels, resulting in an operative range of water potentials for the plant (Maseda and Fernández 2006). In the short term, stomatal closure regulates the decrease in leaf water potential that results from the rates of evaporative loss to the atmosphere and water supply by soils (Oren et al. 1999). The mode of stomatal regulation is tightly co-ordinated with whole-plant hydraulic architecture to prevent the impairment of xylem transport as a result of excessive cavitation, whilst maximising water extraction from the soil (Sperry et al. 2002). Under long-term drought conditions, some tree species reduce their leaf area so that they can maintain moderate transpiration rates without increasing tension in the xylem. As a result, the capacity of their hydraulic system to transport water to the canopy (whole-plant leaf-specific hydraulic conductance, $k_{S\text{-}L}$) can be maintained, or even increased (Maseda and Fernández 2006; Mencuccini 2003). At the whole-tree scale, experimental partial leaf removal usually leads to hydraulically mediated improvements in the water balance of the remaining leaves and subsequent increases in stomatal conductance (Pataki et al. 1998; Quentin et al. 2011).

Pines are particularly plastic in their patterns of biomass allocation to leaves (Delucia et al. 2000; Martínez-Vilalta et al. 2004). Within pine species, the leaf-to-sapwood area ratio (A_L:A_S) decreases with increased climatic aridity in field-grown populations (Maherali and DeLucia 2001; Mencuccini and Grace 1995). These plastic hydraulic adjustments (Creese et al. 2011) enhance $k_{S\text{-}L}$ and allow pines in drier populations to display higher transpiration rates per unit leaf area than their mesic counterparts, without increasing the water potential gradient between soil and canopy (Maherali and DeLucia 2001). Likewise, in long-term experimental studies, treatments with comparatively reduced water availability show lower leaf areas and higher leaf-specific transpiration rates, especially when soil water is plentiful (Cinnirella et al. 2002).

Scots pine (*Pinus sylvestris* L.) thrives under contrasting water balance conditions across its wide geographic distribution, largely because of an efficient hydraulic adjustment via reductions in A_L:A_S and enhanced stomatal control in response to evaporative demand (Martínez-Vilalta et al.

2009; Poyatos et al. 2007). In addition, an enhanced sensitivity to soil water availability has been shown in warm and dry sites, also related to low A_L:A_S (Poyatos et al. 2007). Despite these adjustments, Scots pine drought-induced dieback is being increasingly reported throughout southern Europe and the Mediterranean basin (Bigler et al. 2006; Galiano et al. 2010; Martínez-Vilalta and Piñol 2002), which points to the biological costs and limits to the plasticity of the species in response to drought.

Defoliation in drought-exposed Scots pine populations (Dobbertin et al. 2010; Galiano et al. 2010) has been related to reduced canopy development (Dobbertin et al. 2010) and low growth rates (Galiano et al. 2011). Crown defoliation and associated symptoms can thus be regarded as indicators of low vigour, although it appears to be reversible once water stress is relieved (Dobbertin et al. 2010). In chronically dry sites, however, reduced leaf area coupled with Scots pine's characteristic isohydric stomatal control (Duursma et al. 2008; Irvine et al. 1998; Poyatos et al. 2008; Zweifel et al. 2007) may lead to increased reliance on recent assimilation (Eilmann et al. 2010). The continued metabolic demand may eventually deplete carbohydrate reserves, a situation that has been associated with increased mortality risk in Scots pine (Galiano et al. 2011). This scenario is consistent with the carbon starvation hypothesis (McDowell et al. 2008; McDowell 2011). However, it still remains to be tested whether whole-plant hydraulic capacity in field-grown declining trees maintains its integrity and its ability to recover in response to extreme drought. If defoliated trees display an enhanced physiological sensitivity to water deficits, extreme reductions in leaf area may be regarded more as an unavoidable symptom of drought stress rather than as a strategy for long-term tree survival.

Here, we analysed the patterns of seasonal sap flow, needle water potentials and whole-plant hydraulic conductance in Scots pines affected by drought-induced defoliation compared with that of apparently healthy trees in one of the first sites in which drought-induced dieback was reported for Scots pine (Martínez-Vilalta and Piñol 2002). The coexistence of healthy and defoliated Scots pines in the study area provides an ideal model system to explore the physiological implications of drought-induced defoliation and the mechanisms underlying eventual tree death and possible C starvation (Galiano et al. 2011). We hypothesised that (1) defoliated and non-defoliated pines would display similar regulation of leaf water potential, with minimum values of ca. -2.5 MPa (Martínez-Vilalta et al. 2009); (2) the maximum values of sap flow per unit of leaf area and soil-to-leaf hydraulic conductance in spring would be higher in defoliated than in non-defoliated pines, but (3) both variables would show stronger declines during the summer in defoliated pines, indicating higher sensitivity to increasing soil and atmospheric

drought. We finally postulated that, in terms of C gain (4) the increased hydraulic capacity during spring in defoliated pines would not compensate for their reduced canopy leaf area and the prolonged periods with near-zero gas exchange, leading to more strongly depleted carbohydrate reserves and increased mortality risk associated with drought-induced defoliation.

2.2. Materials and methods

Study site

The study was conducted on a northwest-facing hillside within the Tillar valley, at the Poblet nature reserve (Prades Mountains, northeast Spain). The climate is Mediterranean, with a mean annual rainfall of 664 mm, peaking in spring and autumn, and mean annual temperature of 11.3°C (period 1951-2010), according to a spatially explicit climatic database (cf. Ninyerola et al. 2007a; Ninyerola et al. 2007b). The experimental area (41°19'58.05"N, 1°0'52.26"E; 1015 m asl) is located on a 35° hillslope, on fractured schist, which results in fairly rocky and shallow (ca. 40 cm deep) xerochrept soils with a loamy texture and a high gravel content of ca. 46% (Barba et al. 2013). Additional information about the study site can be found in Hereter and Sánchez (1999). In this valley, holm oak (*Quercus ilex* L.) coppiced woodland occupies lower elevations (below 800 m asl), whereas Scots pine stands dominate the upper areas (Gutiérrez Merino 1989).

Our study focuses on a Scots pine population which is at least 150 years old and has remained unmanaged for the past 30 years (Hereş et al. 2012). The studied area has been affected by severe drought episodes since the 1990s (Martínez-Vilalta and Piñol 2002). Average standing mortality and crown defoliation in the Tillar valley are 12% and 52%, respectively, whereas Scots pine regeneration is very low (Vilà-Cabrera et al. 2013). In some parts of the forest, standing mortality is > 20% and cumulative mortality is as high as 50% in the last 20 years (J. Martínez-Vilalta, unpublished). Our study plot is located in one of these areas (Table 2), in which defoliated Scots pines survive side by side with non-defoliated individuals and holm oak growing in the understorey.

Meteorological and soil moisture measurements

A data acquisition system (CR1000 datalogger and AM16/32 multiplexers, Campbell Scientific Inc., Logan, UT, USA) was used to store 15-min means of meteorological variables, soil moisture and sap flow sampled every 30 seconds. Sensors for measuring air temperature and air relative humidity (CS215, Campbell Scientific Inc.), precipitation (52203, R.M. Young Company, Traverse City, MI, USA), total solar radiation (SP1110, Skye Instruments Ltd., Llandrindod Wells, Powys, UK) and wind speed (05103-5, R.M. Young Company) were installed at the top of a 16-m-tall tower within 20 m of the plot centre. Average volumetric soil water content (θ; SWC) in the upper 30 cm of soil was monitored using six frequency domain reflectometers (CS616, Campbell Scientific Inc.) randomly distributed within the plot. Volumetric soil water contents measured in soil samples within the plot were regressed against θ to correct values from automatic sensors, which were strongly affected by soil stoniness. The measurement period lasted from the end of April 2010 until December 2011.

Sap flow of defoliated and non-defoliated pines

In November 2009, we selected 10 non-defoliated and 11 defoliated Scots pines of similar size for sap flow measurements (see Table S1 available in Supplementary Material 1 Section), within a maximum distance of 70 m from the centre of the plot. Defoliation was expressed as the percentage of green leaves and was visually estimated relative to a healthy canopy of a similar sized tree in the same population (Galiano et al. 2010). Those Scots pines which had 50% or less leaves were considered defoliated (see Table S1 available in Supplementary Material 1 Section). The foliage of two of the defoliated pines (35% green leaves) had turned completely brown by March 2010, and hence these trees were not included in our analyses.

Sap flow density was measured with constant heat dissipation sensors (Granier 1985) manufactured in our laboratory. All sensors (n = 38) were installed in April 2010. Probe pairs (length, 2 cm) were inserted into the xylem at breast height, with a vertical separation of 12 cm, and were covered with reflective bubble wrap to minimise natural temperature gradients. Two sensors were installed in all pines, on the north- and south-facing sides of the main stem.

Periods during which the sensors were not powered (on average 46 days per tree) were used to estimate natural temperature gradients in the stem. Upper (95%) and lower (5%) quantiles of natural gradients were 0.24 ± 0.02 and -0.20 ± 0.02°C (across trees mean ± SE), respectively;

therefore, their effect on sap flow measurements could be considered very low (Do and Rocheteau 2002). Nevertheless, a multiple regression model of natural temperature gradients was fitted using environmental variables (including lags) as predictors, for each individual probe. On average, these models explained 30% of the variance in natural temperature gradients and were used to correct the signal from Granier sensors. Sap flow density in the outer xylem was then calculated according to the original calibration (Granier 1985), estimating the maximum temperature difference under zero-flow conditions (ΔT_{max}) only for those nights on which the temperature difference between the probes was stable (2-hour running coefficient of variation < 0.5%) and vapour pressure deficit (D, kPa) was low (2-hour running minimum D < 0.2 kPa). When these conditions were not met, ΔT_{max} was linearly interpolated from neighbouring days (Oishi et al. 2008).

Sap flow measurements made using single-point sensors installed in the outer sapwood were integrated to the entire xylem depth using measured radial profiles of sap flow (Nadezhdina et al. 2002). We measured sap flow at six depths in the xylem using the heat field deformation (HFD) method (Nadezhdina et al. 2006), in three defoliated and three non-defoliated Scots pines, during at least 7 days per tree. Two HFD sensors with 8 and 10 mm spacing between measuring points were used (RP20/8-10, Dendronet, Brno, Czech Republic). The shallowest measuring point was always located at 5 mm beneath the cambium, and therefore sap flow could be measured up to a depth of 45-55 mm into the sapwood. Sap flow was expressed as percentage of maximum sap flow, which usually occurred in the shallowest measuring point. Radial profiles of relative sap flow (% of maximum) were fitted to Gaussian functions (Microsoft Excel 2007 Solver and Microsoft VBA) using the relative xylem radius as the explanatory variable (Ford et al. 2004). Radial correction coefficients (C_r) were obtained as the ratio between the integrated radial profile over the shallowest 2 cm of sapwood and that integrated over the entire sapwood. For each tree in which radial patterns of sap flow had been measured, we applied the corresponding C_r to obtain whole-tree sap flow on a sapwood area basis (J_S). For the rest, we used an average value for each crown defoliation class (C_r, defoliated = 0.58 ± 0.05; C_r, non-defoliated = 0.41 ± 0.04).

Sapwood and needle analyses

In November 2009, the main stems of 15 defoliated and 15 non-defoliated Scots pines in the studied population were cored with a Pressler increment borer (5 mm in diameter; Suunto, Vantaa, Finland). The sapwood depth was visually delimited in the field and then used to calculate tree sapwood area (A_S, cm^2). The relationship between tree basal area (A_B, cm^2) and tree sapwood

area was A_S = 0.406 · A_B - 83.145 (adjusted R^2 = 0.76, n = 30) and did not differ between crown defoliation classes (P = 0.91; not shown). In the same cores, sapwood non-structural carbohydrates (NSCs) were analysed according to Galiano et al. (2011) and expressed as a percentage of dry matter. In addition, for the same sampled pines $\delta^{13}C$ and nitrogen (N) content (%DW) were measured in 20-30 mid-canopy current-year needles using standard methods (Galiano et al. 2011).

Leaf area and shoot parameters

In order to obtain allometric equations to estimate the total leaf area of the measured trees, we followed the approach used by Martínez-Vilalta et al. (2007). In September 2010, a total of 13 (2.9-5 cm in diameter) and 12 (3.2-14.3 cm in diameter) primary branches were harvested from defoliated and non-defoliated trees, respectively. Once in the laboratory, we selected three representative twigs per branch and measured annual shoot growth. We also measured the number of needles, their projected area (Licor 3100 Leaf Area Meter, Licor Inc. Lincoln, NE, USA) and dry weight (oven dried for 48 h at 60°C) separately for cohorts of years 2008 (and older), 2009 and 2010. The rest of the needles for each branch were dried and weighed, converting whole-branch needle dry biomass to projected, one-sided needle area using branch-specific values of specific leaf area (SLA).

A predictive model of branch-level needle area ($A_{L,br}$, m^2) was built using branch diameter (d_{br}, cm) and defoliation class as explanatory variables (adjusted R^2 = 0.69, n = 25). Defoliation class was represented by parameter C in the following equation (C = 5.56 for defoliated trees and C = 6.07 for non-defoliated trees):

$$\log A_{\mathrm{L,br}} = 1.62 \cdot d_{\mathrm{br}} + C \qquad \text{Equation 1}$$

This relationship was used to estimate the leaf area of all the primary branches of pines monitored with sap flow sensors. The basal diameter of primary branches of these trees was measured from the ground using large callipers with laser pointers (Mantax Black and Gator Eyes, Haglöf, Sweden). Laser-measured branch diameters showed a tight 1:1 relationship with tape-measured values (R^2 = 0.95), with the slope and intercept not significantly different from one and zero, respectively.

Leaf water potential

Leaf water potentials were measured monthly from June to October (except for September 2011) using a pressure chamber (PMS Instruments, Corvallis, OR, USA). Measurements were taken at predawn (ψ_{PD}; just before sunrise at 03:00-05:00 h, solar time) and at midday (ψ_{MD}; 11:00-13:00 h, solar time). On each sampling date, one exposed shoot tip was excised with a pruning pole from four to seven trees of each crown defoliation category, from those monitored with sap flow sensors. Once sampled, shoot tips were stored in a plastic bag with moist paper towels to avoid leaf water loss during the time lag between shoot excision and measurement in the field, which was typically < 2 hours.

Whole-tree sap flow, canopy conductance and hydraulic conductance

Whole-tree sap flow rates were obtained by multiplying J_S (average of radially corrected sap flow density measured by north- and south-facing sensors) by A_S, and expressed on a leaf-area basis (J_L) by dividing J_T by A_L. According to on-site phenological observations, Scots pine A_L was assumed to increase linearly from mid-May to mid-July and to decline linearly from August to November to two-thirds of its maximum value (Bealde et al. 1982). Sap flow data was then aggregated to daytime averages (R_S > 1 W m^{-2}), yielding sap flow per tree ($J_{T,dt}$, kg H_2O d^{-1}), sap flow per unit sapwood ($J_{S,dt}$, g H_2O $cm^{-2}d^{-1}$) and sap flow per unit leaf area ($J_{L,dt}$, kg H_2O m^{-2} d^{-1}). Daytime averages were used to avoid problems related to lags between transpiration and water uptake.

Midday canopy stomatal conductance ($G_{s,md}$) was calculated with the simplified Penman-Monteith equation for aerodynamically rough canopies (Whitehead and Jarvis 1981):

$$G_{\mathrm{s,md}} = \frac{\gamma \lambda J_{\mathrm{L,md}}}{\rho c_p D_{\mathrm{md}}} \qquad \text{Equation 2}$$

where γ is the psychrometric constant (kPa K^{-1}), λ is latent heat of vaporisation of water (J kg^{-1}), ρ is air density (kg m^{-3}), c_p is specific heat of air at constant pressure (J kg^{-1} K^{-1}), D_{md} is midday vapour pressure deficit (averaged between 11:00 and 14:00) (kPa), and $J_{L,md}$ is midday leaf-area based sap flow converted to molar units (mmol m^{-2} s^{-1}). We used midday values so that canopy stomatal conductance was more representative of instantaneous stomatal regulation, and lag effects were minimised (Irvine et al. 2004).

We also used $J_{L,md}$ to calculate whole-tree leaf-specific hydraulic conductance ($k_{S\text{-}L}$, mmol m^{-2} MPa^{-1} s^{-1}), assuming that trees had reached equilibrium with the soil during the night, and that ψ_{PD} represents an estimate of soil water potential (Irvine et al. 2004):

$$k_{S-L} = \frac{J_{L,md}}{\psi_{PD} - \psi_{MD}} \qquad \text{Equation 3}$$

Data analysis

All variables, with their symbols and units, are described in Table 1. All analyses, unless otherwise stated, were carried out with R Statistical Software version 2.12.0 (R Core Team, 2009). Seasonal sap flow data, leaf water potential and hydraulic conductance data were analysed using linear mixed-effects models (lme function, package nlme) with tree as a random factor (Pinheiro and Bates 2000). Fixed factors included date (or seasonal period) and defoliation class. Shoot and needle parameters were similarly analysed, introducing cohort and defoliation class as fixed factors and branch as a random factor. We thus tested for differences in $J_{L,dt}$, $J_{S,dt}$, ψ_{PD}, ψ_{MD} and $k_{S\text{-}L}$ across defoliation classes and periods (hypotheses 1 and 2). Differences in relationships between continuous variables in defoliated versus non-defoliated pines were analysed using generalised least squares (gls function, package nlme), in order to account for variance heterogeneity and temporal autocorrelation, when present. Here, we tested how defoliation influenced the effects of θ_d on ψ_{PD} and $k_{S\text{-}L}$ (hypothesis 3), the regulation of ψ_{MD} with respect to ψ_{PD} (hypothesis 1) and controls on $G_{s,md}$ by ψ_{PD} (hypothesis 3). Differences in NSC, leaf $\delta^{13}C$ and N content between defoliation classes were assessed using *t*-tests or Mann-Whitney-Wilcoxon tests (hypothesis 4).

Differences in the environmental controls on sap flow of defoliated and non-defoliated pines were assessed by examination of the functional response of $J_{L,dt}$ to evaporative demand and soil water availability (hypotheses 2 and 3). The asymptotic relationship between $J_{L,dt}$ and average daytime *D* (D_{dt}) was analysed using an exponential saturation function (Ewers et al. 2002):

$$J_{L,dt} = a \cdot \left(1 - e^{b \cdot D_{dt}}\right) \qquad \text{Equation 4}$$

where *a* is related to maximum sap flow and *b* is the initial increase in sap flow with respect to D_{dt}. Only data with daytime-averaged radiation ($R_{S,dt}$) > 150 W m^{-2} and daily soil moisture (θ_d) > 0.20 cm^3 cm^{-3} were used to fit the function. The nonlinear reduction in sap flow with decreasing θ_d was described by a three-parameter sigmoid (based on results by Duursma et al. 2008):

$$J_{L,dt} = \frac{J_{L,asym}}{1+\exp\left[(\theta_{mid} - \theta_d)/\theta_{scal}\right]} \qquad \text{Equation 5}$$

fitted to data when $R_{S,dt}$ > 150 W m^{-2} and D_{dt} > 0.8 kPa, with $J_{L,asym}$ being the asymptote, θ_{mid} the inflection point (for which $J_{L,dt} = J_{L,asym}/2$) and θ_{scal} a scaling parameter. Both functions were fitted to individual tree $J_{L,dt}$ and environmental data using nonlinear mixed-effects models (nlme, package nlme), with tree as random factor and defoliation class as fixed factor.

In all cases, model selection was based on the Akaike information criterion (AIC), including the selection of appropriate random effects, variance structures and autocorrelation parameters. Model assessment was carried out by visual inspection of residual plots. The significance of fixed effects was assessed using *F*-tests. *Post-hoc* tests were carried out with the general linear hypothesis function (glht) in the package multcomp (Hothorn et al. 2008).

The relationship between $G_{s,md}$ and D_{md} (hypothesis 3) was analysed using boundary-line analysis, fitting the following model using quantile regression (Cade and Noon 2003):

$$G_{\mathrm{s,md}} = G_{\mathrm{s,ref}} - m \,\mathrm{Log}_e\, D_{\mathrm{md}} \qquad \text{Equation 6}$$

We assumed that the linear regression results for the 95th quantile were representative of the relationship between $G_{s,md}$ and $\log_e D_{md}$ when other factors were not limiting (Cade and Noon 2003) and identified the resulting intercept and slope with the model parameters $G_{s,ref}$ (reference $G_{s,md}$ at D_{md} = 1 kPa) and m (sensitivity to vapour pressure deficit, $-dG_{s,md}/d\log_e D$) respectively. Only data with D_{md} > 0.6 kPa were analysed to avoid potential errors in $G_{s,md}$ estimation under low evaporative demand (Ewers and Oren 2000).

2.3. Results

Seasonal course of environmental variables and sap flow

Over the study period, meteorology was typical of low-elevation Mediterranean mountain climate, with occasional cold spells in winter (daytime minimum of -3.8°C), moderately high temperature and evaporative demand during summer (maximum of 26.6°C and 3.0 kPa, respectively) and irregular precipitation (Figure 1). The two growing seasons studied were not exceptional in terms of temperature, with May-October average values of 15.9 and 17.0°C for 2010 and 2011, respectively, compared with a climatic average (1951-2010) value of 16.6°C. Likewise, a normal drought period occurred in 2010, with 333 mm of total precipitation recorded from May to October (92% of the climatic average). However, the drought in 2011 was especially acute, with just 113 mm of rain between May and October, representing only 31% of the climatic

average. Accordingly, soil water content remained below 0.10 cm^3 cm^{-3} between July and mid-October in 2011 (Figure 1c).

Sap flow was higher during spring and decreased strongly after June for both years. Rainy periods in late summer and autumn raised soil water availability, leading to a recovery in sap flow rates in 2010, but not in 2011 (Figures 1d, e). In general, sap flow during peak summer and autumn drought was lower for 2011 relative to 2010 (Figures 1d, e; see Table S2 available in Supplementary Material 1 Section). Non-defoliated pines showed similar sap flow per unit sapwood area ($J_{S,dt}$) to defoliated pines (Figure 1d; see Table S2 available in Supplementary Material 1 Section). This pattern changed when sap flow was expressed per unit leaf area ($J_{L,dt}$) and, especially during late spring and early summer, $J_{L,dt}$ was considerably higher for defoliated pines relative to non-defoliated pines (hypothesis 2). However, in response to summer drought, $J_{L,dt}$ was more strongly reduced in defoliated pines, eventually reaching similar near-zero values to those found for non-defoliated pines (Figure 1e; see Table S2 available in Supplementary Material 1 Section), consistent with hypothesis 3. Tree-level water use was consistently lower in defoliated pines, but the difference was not statistically significant when averaged over seasonal periods, except for the summer of 2010 (see Table S2 available in Supplementary Material 1 Section).

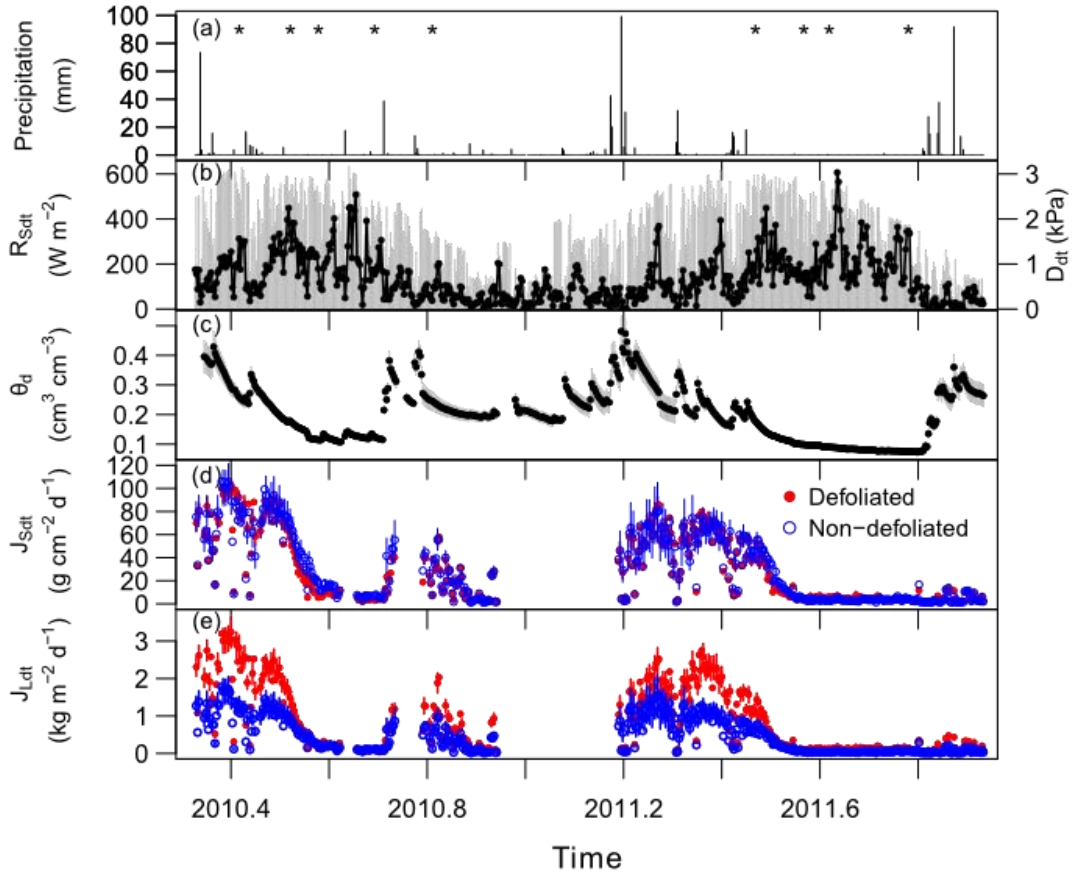

Figure 1. Seasonal course of environmental variables and Scots pine sap flow over the study period: (a) daily precipitation, (b) daytime-averaged solar radiation ($R_{S,dt,}$ grey bars) and vapour pressure deficit (D_{dt}, solid dots), (c) mean volumetric soil water content (θ_d cm^3 cm^{-3}, solid circles) and standard errors (grey bars), (d) across-trees mean of daytime sap flow per unit sapwood area ($J_{S,dt}$) and (e) per unit leaf area ($J_{L,dt}$) in defoliated (closed circles and continuous line) and non-defoliated (open circles and dashed line) pines. Coloured bars depict standard errors. Asterisks in panel (a) show the sampling dates for water potential measurements. Gaps in the time series are a result of power failures. Note that labels on the x axis represent year in decimal format (i.e., January 2011 is 2011.0).

Environmental responses of sap flow in defoliated and non-defoliated pines

The increase in $J_{L,dt}$ with D_{dt} was well described by the exponential saturation function employed (Figure 2). Defoliated and non-defoliated pines differed in their maximum $J_{L,dt}$, with higher *a* values for defoliated individuals, but not in the initial increase in $J_{L,dt}$ with D_{dt} (parameter *b*) (Figure 2, Table 3). Sap flow started to decline appreciably at values of $\theta_d \approx 0.25$ cm^3 cm^{-3} and was almost zero below $\theta_d \approx 0.10$ cm^3 cm^{-3} (Figure 2). The analysis of the response of $J_{L,dt}$ to θ_d showed that defoliated pines displayed a higher $J_{L,asym}$ and also a slightly higher θ_{mid} (Table 3), implying a steeper decline of $J_{L,dt}$ with θ_d.

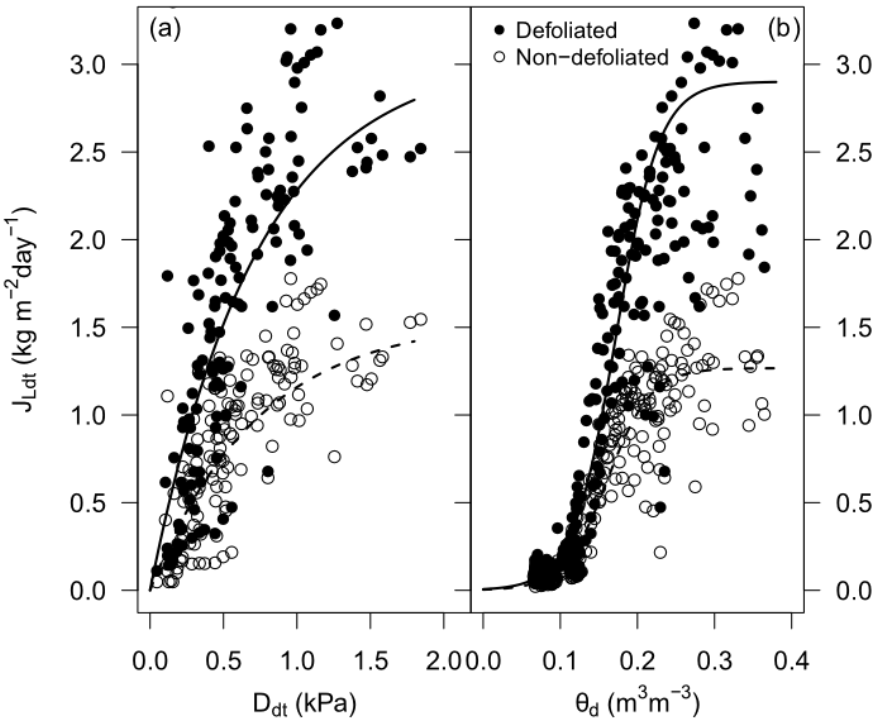

Figure 2. Responses of daytime averages of leaf area-related sap flow ($J_{L,dt}$) to vapour pressure deficit (D_{dt}) (a) and soil water content (θ_d) (b) in Scots pine. Average values for defoliated (closed circles) and non-defoliated (open circles) pines are shown. Standard errors are not displayed to improve clarity. Different fits for defoliated (solid line) and non-defoliated (dashed line) pines reflect the significance of the defoliation effect in the nonlinear mixed models of individual tree $J_{L,dt}$ data (Table 3).

Water potentials and hydraulic conductance

Leaf water potentials gradually decreased from late spring/early summer to early autumn for both years (Figure 3). Across dates, non-defoliated pines showed slightly higher water potentials (ca. 0.1 MPa higher), both when measured before dawn and at midday. The water potential difference varied with date ($P < 0.001$; not shown), but not with defoliation class ($P = 0.41$; not shown), although a significant interaction of date and defoliation class was found ($P = 0.038$; not shown).

The lowest ψ_{PD} values were measured in September and October for 2010 and 2011, respectively. In 2011, they reached a significantly lower seasonal minimum value (-2.2 MPa) relative to 2010 (-1.6 MPa), for both defoliated and non-defoliated pines (both $P < 0.001$; Figure 3). Likewise, seasonal ψ_{PD} values were lower in 2011 (October, -2.5 MPa) relative to 2010 (August, -2.3 MPa) (both $P < 0.001$; Figure 3). Ψ_{PD} declined with decreasing θ_d following a nonlinear relationship (Figure 4a), with similar slopes but different intercepts for defoliated and non-defoliated trees (Table 4), implying that, at a given θ_d, ψ_{PD} was lower in defoliated trees.

Whole-tree leaf-specific hydraulic conductance ($k_{S\text{-}L}$) decreased as the drought progressed (Figures 3e, f) and did not show a short-term recovery in response to precipitation. In 2010, $k_{S\text{-}L}$ still showed very low values after a rainy period in early autumn which raised θ_d above 0.20 cm^3 cm^{-3} (Figure 3e). Nevertheless, early summer values of $k_{S\text{-}L}$ in 2011 did recover, although, apparently, not at the same level as the maximum values in 2010. This was probably caused by a delayed first measurement of $k_{S\text{-}L}$ in 2011. Defoliated pines displayed higher values of $k_{S\text{-}L}$ early in the growing season, but, in response to drought, $k_{S\text{-}L}$ dropped to values similar to those found in non-defoliated pines (Figures 3e, f; significant interaction between date and defoliation class $P = 0.016$).

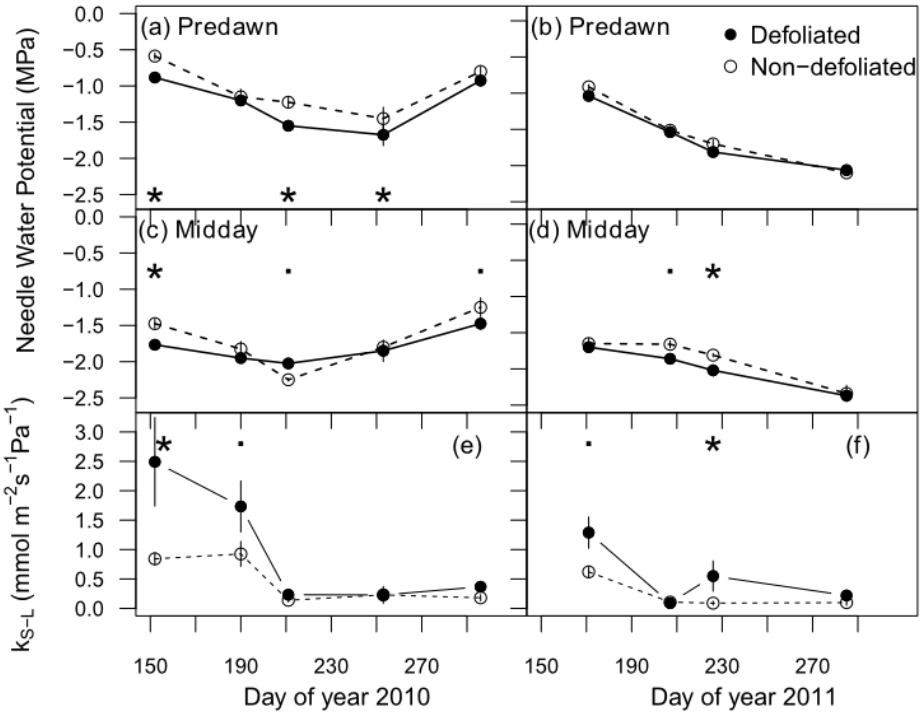

Figure 3. Seasonal course of predawn water potential (a, b), midday water potential (c, d) and soil-to-leaf hydraulic conductance (k_{S-L}) in defoliated (closed circles) and non-defoliated (open circles) Scots pines for 2010 and 2011. Different line patterns depict significant differences between defoliated and non-defoliated pines for the entire study period according to linear mixed-effects models (cf. Materials and methods). Where a significant interaction between time and defoliation class was present, asterisks ($P < 0.05$) or dots ($0.05 < P < 0.1$) identify significant differences between defoliation classes.

Despite the decoupling observed between k_{S-L} and θ_d in autumn 2010, k_{S-L} was positively related to θ_d for the rest of the dates (Figure 4b). This relationship differed for defoliated and non-defoliated pines (Table 4), with the rate of decline in k_{S-L} with decreasing θ_d being higher for defoliated pines (hypothesis 3). The capacity of Scots to supply its canopy leaves with water was greatly reduced when θ_d fell below ca. 0.10 cm^3 cm^{-3} (Figure 4b).

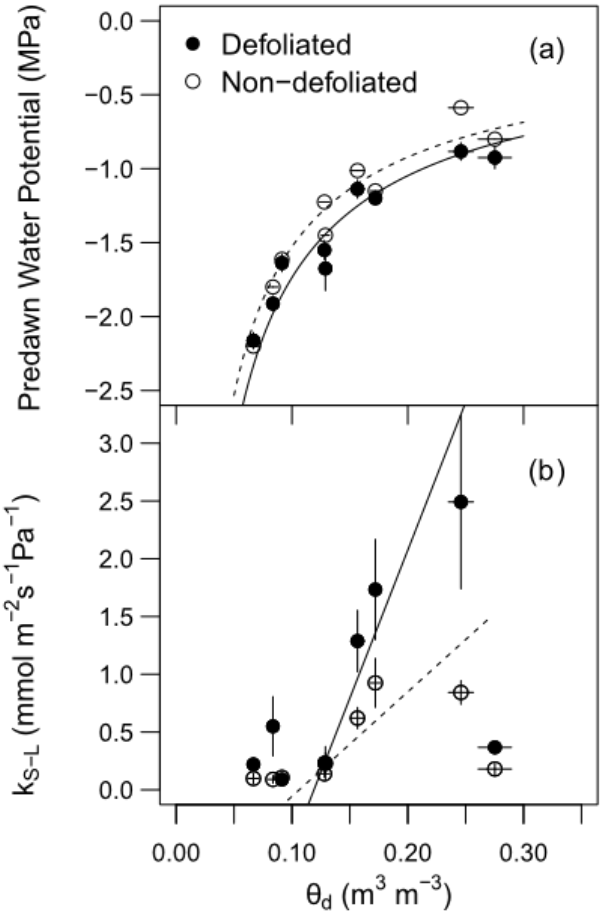

Figure 4. Relationships between daily average soil water content (θ_d) and (a) predawn water potential and (b) soil-to-leaf hydraulic conductance (k_{S-L}) in defoliated (closed circles) and non-defoliated (open circles) Scots pine. Different line patterns depict significant differences ($P < 0.05$; Table 4) between defoliated (solid) and non-defoliated (dashed) pines. The two low values of k_{S-L} at high soil moisture values correspond to a lack of recovery in k_{S-L} after autumn rains in 2010, and were not used to fit the regression lines (cf. Results section).

Stomatal control in defoliated and non-defoliated pines

Defoliated and non-defoliated pines shared a common relationship between ψ_{PD} and ψ_{MD} (Figure 5a, Table 4). However, defoliated and non-defoliated Scots pines showed differences in the response of $G_{s,md}$ to ψ_{PD} (Figure 5b). The function relating $G_{s,md}$ and log(-ψ_{PD}) showed different intercepts and marginally higher slopes, in absolute value, for defoliated pines (Table 4).

Reference canopy stomatal conductance was generally higher for defoliated than for non-defoliated trees, except for one individual (Figure 6); $G_{s,ref}$ was higher in defoliated trees (*t*-test, $P = 0.006$), showing an average of 255 ± 27 mmols m^{-2} s^{-1} relative to 139 ± 31 mmols m^{-2} s^{-1}

observed for non-defoliated pines. The sensitivity of $G_{s,md}$ to vapour pressure deficit (m) shared the same proportionality with respect to $G_{s,ref}$ across defoliation classes, with a slope of 0.79 ± 0.02 mmols m^{-2} s^{-1} log_e kPa^{-1} and a nonsignificant intercept (P = 0.841).

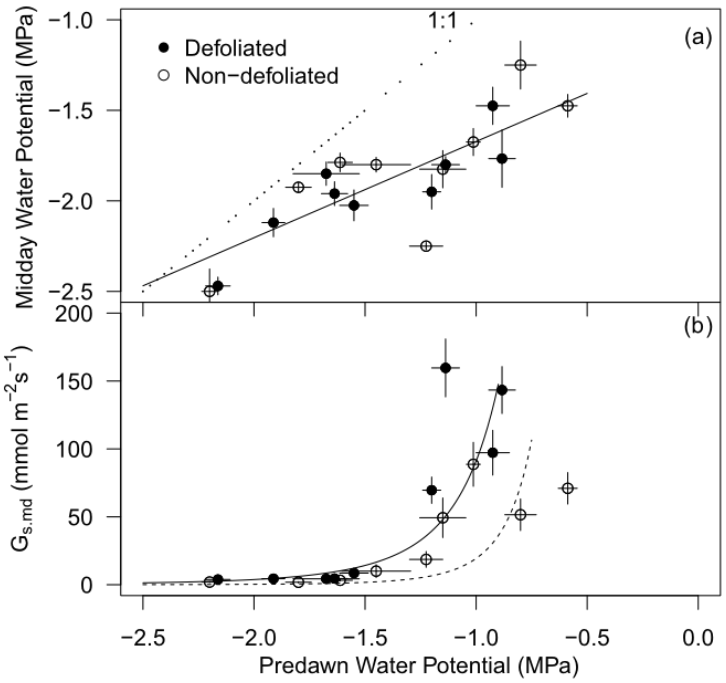

Figure 5. Relationships between predawn water potential and (a) midday water potential and (b) canopy stomatal conductance measured at midday ($G_{s,md}$) in defoliated (closed circles) and non-defoliated (open circles) Scots pine. Different line patterns depict significant differences (P < 0.05; Table 4) between defoliated (solid) and non-defoliated (dashed) pines. The 1:1 line is also shown.

Shoot and leaf parameters and sapwood non-structural carbohydrates

The patterns in shoot and leaf parameters (see Table S3 available in Supplementary Material 1 Section) revealed higher growth constraints for defoliated pines. Shoot growth was 42% higher for non-defoliated pines in 2009 and 2010, relative to that of defoliated pines, but no significant difference was observed in 2008. Most of the needle-level differences were observed for the 2010 cohort, when non-defoliated pines had 20% more needles and lower SLA compared to defoliated pines (see Table S3 available in Supplementary Material 1 Section). Average needle retention was ca. 3 years for both defoliation classes (not shown).

At the leaf level, no differences in either $^{13}\delta C$ or leaf N content were found between defoliated and non-defoliated pines, and leaf N content was not correlated with either $^{13}\delta C$ or sapwood NSC (not shown). Finally, defoliated pines displayed similar sapwood density to that of non-defoliated

pines, and significantly lower (33%) sapwood NSC levels (Table 2), a result consistent with hypothesis 4.

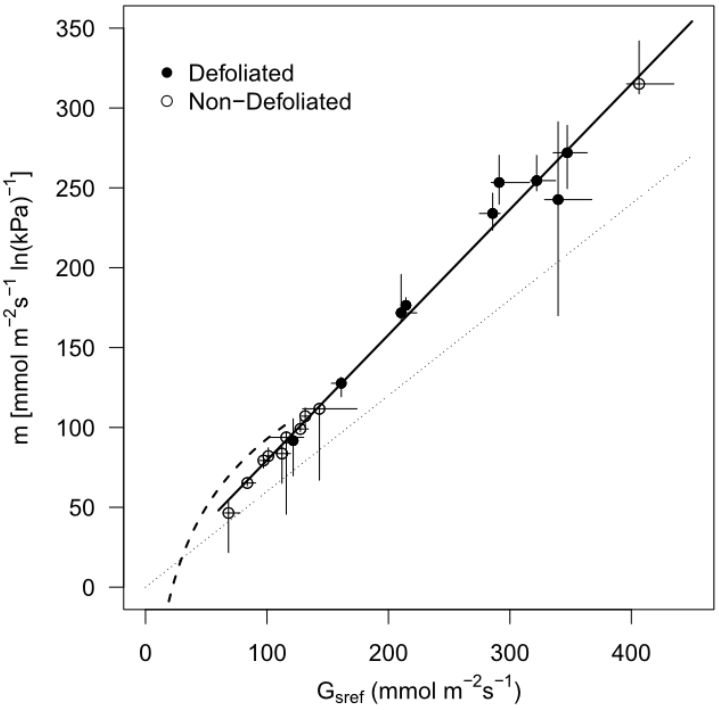

Figure 6. Stomatal sensitivity to vapour pressure deficit parameters for defoliated (closed circles) and non-defoliated (open circles) Scots pines. The solid line represents the common relationship between reference stomatal conductance ($G_{s,ref}$) and sensitivity to vapour pressure deficit (m) across defoliation classes (cf. Results section). The dotted line has a slope of 0.6 and zero intercept, representing the predicted relationship for species showing an isohydric control of leaf water potential (Oren et al. 1999). The dashed line depicts the fit between $G_{s,ref}$ and m observed across Scots pine populations (Poyatos et al. 2007).

Table 1. List of abbreviations used for measured variables and parameters in this study. Fitted parameters are shown in bold.

Symbol	Description	Units
a	**Asymptote of the relationship between $J_{L,dt}$ and D_{dt}**	**kg H_2O m^{-2} d^{-1}**
A_B	Tree basal area	cm^2
A_L	Tree leaf area	m^2
A_L:A_S	Leaf-to-sapwood area ratio	m^2 cm^{-2}
$A_{L,br}$	Leaf area of primary branch	m^2
A_S	Tree sapwood area	cm^2
b	**Initial increase in $J_{L,dt}$ with D_{dt}**	**Adimensional**
C	**Defoliation class coefficient in the $A_{L,br}$model**	**Adimensional**
c_p	Specific heat of air at constant pressure	J kg^{-1} K^{-1}
C_r	**Coefficient for radial integration of sap flow density**	**Adimensional**
d_{br}	Branch diameter	cm
D	Instantaneous (15-min) vapour pressure deficit of the air	kPa
D_{dt}	Daytime averaged vapour pressure deficit of the air	kPa
D_{md}	Midday averaged vapour pressure deficit of the air	kPa
$G_{s,md}$	Canopy stomatal conductance at midday	mmol m^{-2} s^{-1}
$G_{s,ref}$	**Reference $G_{s,md}$at D_d=1 kPa**	**mmol m^{-2} s^{-1}**
J_L	Instantaneous (15-min) sap flow per unit leaf area	kg H_2O m^{-2} s^{-1}
$J_{L,dt}$	Daytime-averaged sap flow per unit leaf area	kg H_2O m^{-2} d^{-1}
$J_{L,asym}$	**Asymptote of response of $J_{L,dt}$to θ_d**	**kg H_2O m^{-2} d^{-1}**
$J_{L,md}$	Leaf-area based sap flow during midday	mmol m^{-2} s^{-1}
J_S	Instantaneous (15-min) sap flow per unit sapwood	kg H_2O m^{-2} s^{-1}
$J_{S,dt}$	Daytime-averaged sap flow per unit sapwood	g H_2O cm^{-2} d^{-1}
J_T	Instantaneous (15-min) sap flow per tree	kg H_2O s^{-1}
$J_{T,dt}$	Daytime-averaged sap flow per tree	kg H_2O d^{-1}
k_{S-L}	Whole-tree hydraulic conductance	mmol m^{-2} MPa^{-1} s^{-1}
m	**Sensitivity of $G_{s,md}$ to D_d**	**mmol m^{-2} MPa^{-1} s^{-1} (log_e kPa)$^{-1}$**
NSC	Non-structural carbohydrates	% DW
R_S	Total solar radiation	W m^{-2}
$R_{S,dt}$	Daytime average of total solar radiation	W m^{-2}
SLA	Specific leaf area	cm^2 g^{-1}
ΔT_{max}	Temperature difference measured by sap flow probes under zero-flow conditions	°C
γ	Psychrometric constant	kPa K^{-1}
$\delta^{13}C$	Carbon stable isotopic composition	‰
θ	Instantaneous (15-min) soil water content	cm^3 cm^{-3}
θ_d	Daily average of soil water content	cm^3 cm^{-3}
θ_{mid}	**Inflection point in the response of $J_{L,dt}$ to θ_d**	**cm^3 cm^{-3}**
θ_{scal}	**Scaling parameter in the response of $J_{L,dt}$ to θ_d**	**cm^3 cm^{-3}**
λ	Latent heat of vaporisation of water	J kg^{-1}
ρ	Air density	kg m^{-3}
ψ_{MD}	Midday water potential	MPa
ψ_{PD}	Predawn water potential	MPa
ψ_{50}	Water potential causing 50% loss of hydraulic conductivity	MPa

Table 2. Characteristics of the studied stand, together with leaf and sapwood parameters of defoliated and non-defoliated Scots pines.

	Scots pine		**Holm oak**	**Other**
	Defoliated	**Non-defoliated**		
Plot level				
Density (stems ha^{-1})	106	151	1736	242
DBH (cm)	37.90±3.0	26.65±5.3	8.4±0.4	6.7±1.2
Basal area (m^2 ha^{-1})	12.33	11.46	24.86	2.9
Height (m)	13.4±0.5	14.8±0.8		
LAI (m^2 m^{-2})	0.16	0.42	1.39	n. a.
Tree level				
Sapwood density	0.46±0.01 [a]	0.44±0.01 [a]		
Trunk sapwood NSC % DW	0.70±0.09 [a]	1.05±0.06 [b]		
Leaf $^{13}\delta$‰	-26.7±0.66 [a]	-26.4±0.33 [a]		
Leaf N % dry mass	1.19±0.04 [a]	1.37±0.06 [a]		

Stand-level variables were measured in two 18.2 x 18.2 m^2 plots (J. Barba, unpublished). LAI was estimated from the tree-level leaf area obtained by site-specific allometric relationships (cf. Materials and methods section). Differences in tree-level traits were assessed with *t*-tests or Mann-Whitney-Wilcoxon tests for non-normally distributed variables. Different lowercase letters represent statistically significant differences ($P < 0.05$) between defoliated and non-defoliated trees. See Table 1 for abbreviation and symbol descriptions. DBH, tree diameter at breast height; LAI, Leaf area index.

Table 3. Summary of the nonlinear mixed models relating daytime values of Scots pine sap flow per unit leaf area ($J_{L,dt}$) with vapour pressure deficit (D_{dt}) and soil water content (θ_d).

Model	Parameter	Estimate	SE	*t*	*P*
$J_{L,dt} = a \cdot (1 - e^{b \cdot D_{dt}})$	***a:* non-defoliated**	**1.548**	**0.331**	**4.677**	**<0.0001**
	***a:* defoliated**	**1.539**	**0.482**	**3.196**	**0.0010**
	b	-1.438	0.097	14.896	<0.0001
$J_{L,dt} = \frac{J_{L,asym}}{1 + \exp[(\theta_{mid} - \theta_d)/\theta_{scal}]}$	**$J_{L,asym}$*:* non-defoliated**	**1.267**	**0.257**	**4.934**	**<0.0001**
	$J_{L,asym}$:defoliated	**1.634**	**0.363**	**4.501**	**<0.0001**
	θ_{mid}*:* non-defoliated	**0.161**	**0.003**	**51.491**	**<0.0001**
	θ_{mid} :defoliated	**0.011**	**0.003**	**3.098**	**0.0020**
	θ_{scal}	0.028	0.002	16.977	<0.0001

Defoliation class (defoliated, ≤ 50% green leaves; non-defoliated, > 50% green leaves) was introduced as a factor in the models; non-defoliated is used as the reference level. Parameters with a significant effect of defoliation class are shown in bold. See Table 1 for abbreviation and symbol descriptions.

Table 4. Coefficients and summary statistics for some relevant relationships among environmental and ecophysiological variables related to whole-plant water status in Scots pines.

Response variable	Model terms	Estimate	SE	*t*	*P*
$k_{S\text{-}L}$	Intercept	-0.962	0.366	-2.628	0.0144
	θ_d: Non-defoliated	**9.048**	**2.690**	**3.364**	**0.0024**
	Defoliated	**-2.086**	**0.860**	**-2.426**	**0.0225**
	θ_d:Defoliated	**16.557**	**6.514**	**2.542**	**0.0173**
$\log(-\psi_{PD})$	Intercept	-1.255	0.131	-9.579	<0.0001
	$\log(\theta_d)$	-0.729	0.062	-11.681	<0.0001
	Defoliated	**0.128**	**0.056**	**2.27**	**0.0380**
Ψ_{MD}	Intercept	-1.141	0.087	-13.14	<0.0001
	ψ_{pd}	0.531	0.059	8.992	<0.0001
$\log(G_{s,md})$	Intercept	2.777	0.568	4.888	<0.0001
	$\log(-\psi_{l,pd})$:Non-defoliated	**-1.260**	**0.534**	**-2.360**	**0.0212**
	Defoliated	**1.103**	**0.223**	**4.952**	**<0.0001**
	$\log(-\psi_{pd})$:Defoliated	-0.879	0.460	-1.910	0.0605

Defoliation class (Defoliated, ≤ 50% green leaves; non-defoliated, > 50% green leaves) was also introduced as a factor in the linear models; non-defoliated is used as the reference level. All models were fitted using generalised least squares to account for variance heterogeneity and temporal autocorrelation, where necessary. Parameters with a significant effect of defoliation class are shown in bold. See Table 1 for abbreviation and symbol descriptions.

2.4. Discussion

Seasonal patterns of sap flow in Scots pine at its dry limit

The present study portrays a detailed picture of the water relation of Scots pine at the dry edge of its distribution and under exceptionally dry conditions. The study area experienced the driest growing season on record, as the driest May-October period since 1951 had received 195 mm of rain (in 2007), compared with the value of 113 mm for the same period in 2011. Accordingly, the seasonal course of sap flow showed that Scots pine at this dry site is extremely sensitive to summer drought. Moreover, reduced precipitation during winter and the associated lack of recharge of soil water reserves (Figure 1) may limit the amount of water available to meet evaporative demand during summer (Llorens et al. 2010).

We observed a steep decline in sap flow rates at soil water content values below ca. 0.25 cm^3 cm^{-3} (Figures 1, 2), consistent with similar threshold-like responses observed elsewhere (Duursma et al. 2008; Irvine et al. 1998; Lagergren and Lindroth 2002; Poyatos et al. 2008). However, here,

we found that extremely low sap flow rates continued for over 2 months in 2010 and > 5 months in 2011, a more persistent drought response than that observed in other drought-affected populations (Zweifel et al. 2009). The sensitivity analysis of $G_{s,md}$ with respect to D_{md} also showed a strict stomatal closure in response to increasing evaporative demand in the studied Scots pine population. Stomatal sensitivity to D_{md} (m) was proportional to gas exchange capacity ($G_{s,ref}$) but the slope of the relationship between m and $G_{s,ref}$ was greater than the value of 0.6 found for mesic tree species with an isohydric regulation of leaf water potential (Oren et al. 1999). These results suggest a hypersensitive stomatal regulation with respect to D in this Scots pine population, as recently found for other species (Ogle et al. 2012).

Sap flow in defoliated pines is more sensitive to summer drought

Defoliated Scots pines showed higher $J_{L,dt}$ and $k_{S\text{-}L}$, consistent with hypothesis 2, and in agreement with the patterns observed along climatic gradients in Scots pine (Poyatos et al. 2007) and other pine species (Maherali and DeLucia 2001). This increased transport capacity determined higher water use per unit leaf area in defoliated than in non-defoliated pines, especially under well-watered conditions (Figure 1, see Table S2 available in Supplementary Material 1 Section). Accordingly, the hydraulic capacity per unit sapwood area was similar across defoliation classes (Figure 1, see Table S2 available in Supplementary Material 1 Section), as also reported for drought-adapted *Pinus ponderosa* Douglas ex C. Lawson relative to mesic populations (Maherali and DeLucia 2000). Likewise, artificial defoliation resulted in a perfect compensatory increase in transpiration of the remaining leaves in *Pinus taeda* L. (Pataki et al. 1998), although this response may not occur in other conifers (Brooks et al. 2003).

Here, we also showed that defoliated pines were more sensitive to summer drought (hypothesis 3), as shown by the steeper decline in $J_{L,dt}$ with decreasing θ_d (Figure 2, Table 3), and the enhanced sensitivity of $G_{s,md}$ to ψ_{PD} (Figure 5b, Table 4). Defoliated pines were also more sensitive to D_{dt} in absolute, but not relative, terms (Table 4, Figure 2) (cf. Poyatos et al. 2007). This pattern was confirmed by the analysis of $G_{s,md}$, whereby defoliated and non-defoliated pines shared the same proportionality between maximum gas exchange and its response to D_{dt} (Figure 6). The slope of the m vs. $G_{s,ref}$ relationship was similar to the population-averaged value of $m/G_{s,ref}$ (0.81) found for another Mediterranean Scots pine stand (Vallcebre, Eastern Pyrenees), in which no drought-driven mortality has so far been reported so far (Poyatos et al. 2007). In that study, however, m tended to plateau with increasing $G_{s,ref}$ across populations along a climatic

gradient spanning from Scandinavia to southern Spain. Here, we found a linear relationship between both parameters for trees with contrasting A_L:A_S within a site. This discrepancy and the higher $G_{s,ref}$ values observed for defoliated pines compared to those found across a climatic gradient suggest that the mechanisms behind climate-driven hydraulic adjustments across populations differ from those leading to spatially diffuse defoliation patterns in a declining stand.

Near-homeostasis in needle water potential across years and crown condition

Minimum needle water potentials were at the lower limit of the range reported for European Scots pine populations, including some drought-exposed sites (Martínez-Vilalta et al. 2009). However, a perfect homeostasis in midday leaf water potentials could not be strictly maintained under the extremely dry conditions in 2011 (Figsures 3c, d). Hypothesis 1 was only partly confirmed, as a perfect homeostasis in ψ_{MD} was not observed either across defoliation classes, as defoliated pines displayed (slightly but) consistently lower ψ_{MD} in comparison to non-defoliated pines (Figures 3c, d).

Despite this lack of perfect regulation, ψ_{MD} values were still far from site-specific estimates of branch-level ψ_{50} (water potential causing 50% loss of xylem conductivity), which did not vary with crown condition (-3.01 MPa, Aguadé et al. 2015). However, for both defoliation classes, root xylem was comparatively more vulnerable to embolism (ψ_{50} = -1.87 MPa), with roots of defoliated trees showing a steeper vulnerability curve (Aguadé et al. 2015). Hence, assuming that ψ_{PD} is representative of root water potential (Figures 3a, b), defoliated pines would have lost 61% of root xylem conductivity during peak drought in 2011, compared with 53% loss in non-defoliated pines. This result suggests that small hydraulic differences between defoliation classes could contribute to their differential water use and, ultimately, to a greater risk of mortality in defoliated individuals (cf. Galiano et al. 2011).

Soil-to-leaf hydraulic conductance declines more rapidly with drought in defoliated pines

Leaf-specific hydraulic capacity in both defoliated and non-defoliated Scots pines declined with drought and failed to recover quickly after the autumn rains in 2010 (Figures 3e, f). This seasonal pattern was also observed in *Pinus palustris* Mill. (Addington et al. 2004) and is consistent with the lack of an immediate recovery in transpiration after drought in *Pinus pinaster* Aiton (Duursma et al. 2008). The faster decline of $k_{S\text{-}L}$ in response to drought in defoliated pines (hypothesis 3) may

reflect differences in local water availability, as suggested by the lower ψ_{PD} value in defoliated than in non-defoliated pines (Figure 4b). A combination of slightly higher θ_{md} in the vicinity of the roots of non-defoliated pines, together with their slightly higher resistance to xylem embolism, probably explains the differences in $k_{S\text{-}L}$ dynamics observed in this study (Figure 3). Overall, these results are consistent with the negative association between defoliation and soil parameters related to increased water-holding capacity observed in another declining Scots pine population (Galiano et al. 2010).

Soil heterogeneity may also mediate root acclimation to local soil hydraulic properties (Addington et al. 2006) differently across crown condition classes, which would explain the higher ψ_{PD} at a given soil moisture observed for non-defoliated pines (Figure 4a). However, a recent study on a similarly drought-exposed Scots pine population, showing that crown transparency did not affect either root standing crop or root morphology (Brunner et al. 2009), does not support this explanation. Alternatively, fungal infection-driven impairment of stems and/or roots may underlie their steeper seasonal decline in $k_{S\text{-}L}$ (Croise et al. 2001; Heiniger et al. 2011), a possibility that remains to be explored in our study population.

Defoliation and physiological mechanisms underlying drought-induced mortality

Defoliated trees showed reduced needle number, shoot length and branching, and increased SLA (see Table S2 available in Supplementary Material 1 Section), in accordance with drought-induced constraints on canopy development reported elsewhere for Scots pine (Dobbertin et al. 2010; Irvine et al. 1998; Thabeet et al. 2009). For these trees, reduced leaf area, enhanced sensitivity to drought and a lack of compensatory increase in needle photosynthetic capacity (as inferred from leaf N content and gas exchange data; Table 2, Y. Salmon, unpublished results) all probably contribute to reduced NSCs relative to non-defoliated pines (hypothesis 4). Moreover, the long periods (up to 5 months) of severely restricted gas exchange do not appear to be compensated at the tree level by more favourable conditions for C assimilation because of the increased hydraulic capacity during spring. In any case, regardless of crown condition, NSCs were very low compared to those measured in more mesic Scots pine stands (Gruber et al. 2012; Hoch et al. 2003). Although more detailed observations on the dynamics of NSCs across multiple plant tissues and over longer time periods are required, our results suggest that persistent constraints on C gain during long droughts may be critical to determine the survival of pines. *Pinus edulis* Engelm. has been reported to recover after < 4 months of restricted gas exchange (Breshears et

al. 2009), but longer droughts may act as contributing factors preceding tree death (Breshears et al. 2009; Plaut et al. 2012). A recent study in another Scots pine population affected by drought-induced decline in the Central Pyrenees found a close association between defoliation, similarly low stem NSC values as those reported here and increased mortality risk in the event of a new drought (Galiano et al. 2011).

Our results are consistent with the C starvation hypothesis (Galiano et al. 2011; McDowell et al. 2008), although the numerous feedbacks between plant hydraulics and C availability and translocation within the plant (Sala et al. 2010) preclude the identification of the ultimate factor(s) triggering tree death (McDowell 2011). For the studied drought-exposed Scots pine population, reduced NSCs mediated by poor crown condition and prolonged stomatal closure may feed back on tree survival and resilience under drought by (1) limiting leaf production through bud impairment (Bréda et al. 2006), (2) increasing vulnerability to pathogen attacks (Wermelinger et al. 2008) and (3) preventing the recovery of hydraulic function after drought. Radial growth is severely restricted in our study area (Hereş et al. 2012), especially in defoliated pines (Vilà-Cabrera et al. 2014). As post-drought recovery of $k_{S\text{-}L}$ in conifers is highly dependent on new xylem growth (Brodribb et al. 2010), reduced C allocation to xylem growth might also constrain the hydraulic capacity of drought-exposed trees. Moreover, enhanced C limitations in defoliated pines may render them more vulnerable to fungal infections (Heiniger et al. 2011), and associated hydraulic dysfunction (Croise et al. 2001). Finally, other mesic-adapted tree species have shown continuous C investment to fine roots to compensate for increased fine root mortality under drought (Meier and Leuschner 2008), possibly enhancing the depletion of local carbohydrate reserves.

Concluding remarks

In conclusion, this study shows that drought-induced defoliation may be more adequately seen as an inevitable consequence of drought in inherently vulnerable trees than as a strategy to cope with water stress. This distinction is important in the context of climate change and the widespread increase in defoliation recently observed in many Southern European forests, including Scots pine populations (Carnicer et al. 2011). Extreme hydraulic adjustments may allow short-term survival, but jeopardise future resilience in response to drought. In this regard, Mediterranean populations of Scots pine may be especially vulnerable to the longer droughts projected for the region (Bates et al. 2008). The replacement of Scots pine by more drought-

resistant vegetation will eventually depend on other demographic processes, past management history, site factors (Vilà-Cabrera et al. 2013) and species interactions (Lloret et al. 2012).

Acknowledgments

Thanks to J. Llagostera, X. Buqueras, A. Vallvey and all the staff at PNIN de Poblet for allowing us to carry out research at the “Barranc del Tillar” nature reserve and for their logistic support in the field. We also acknowledge the field and laboratory support by J. Barba, J. Curiel, M. Mejía-Chang, P. García, P. Llorens, A. Vilà, H. Romanos, B. Ros and E. Sànchez. M. Ninyerola and M. Batalla (Unitat de Botànica, UAB) provided the climatic database (CGL2006-01293, Spanish Ministry of Science and Innovation, MICINN) and E. Marimon some meteorological data (www.meteoprades.net). The comments by David Ackerly and two anonymous reviewers greatly improved the manuscript. This research was funded by MICINN via competitive grants CGL2007-60120, CGL2010-16373, CSD2008-0004, a Juan de la Cierva postdoctoral fellowship awarded to R.P., Natural Environment Research Council (NERC) grant NE/I011749/1 to M.M. and an FPI doctoral fellowship awarded to L.G. D.A. was supported by an FPU doctoral fellowship from the Spanish Ministry of Education.

Chapter 3

The role of defoliation and root rot pathogen infection in driving the mode of drought-related physiological decline in Scots pine (*Pinus sylvestris* L.)[1]

Aguadé, D., Poyatos, R., Gómez, M., Oliva, J. and Martínez-Vilalta, J.

[1]Published in *Tree Physiology* (DOI: 10.1093/treephys/tpv005)

Abstract

Drought-related tree die-off episodes have been observed in all vegetated continents. Despite much research effort, however, the multiple interactions between carbon starvation, hydraulic failure and biotic agents in driving tree mortality under field conditions are still not well understood. We analysed the seasonal variability of non-structural carbohydrates (NSCs) in four organs (leaves, branches, trunk and roots), the vulnerability to embolism in roots and branches, native embolism (percentage loss of hydraulic conductivity (PLC)) in branches and the presence of root rot pathogens in defoliated and non-defoliated individuals in a declining Scots pine (*Pinus sylvestris* L.) population in the NE Iberian Peninsula in 2012, which included a particularly dry and warm summer.

No differences were observed between defoliated and non-defoliated pines in hydraulic parameters, except for a higher vulnerability to embolism at pressures below -2 MPa in roots of defoliated pines. No differences were found between defoliation classes in branch PLC. Total NSC (TNSC, soluble sugars plus starch) values decreased during drought, particularly in leaves. Defoliation reduced TNSC levels across tree organs, especially just before (June) and during (August) drought. Root rot infection by the fungal pathogen *Onnia* P. Karst spp. was detected but it did not appear to be associated to tree defoliation. However, *Onnia* infection was associated with reduced leaf-specific hydraulic conductivity and sapwood depth, and thus contributed to hydraulic impairment, especially in defoliated pines. Infection was also associated with virtually depleted root starch reserves during and after drought in defoliated pines. Moreover, defoliated and infected trees tended to show lower basal area increment.

Overall, our results show the intertwined nature of physiological mechanisms leading to drought-induced mortality and the inherent difficulty of isolating their contribution under field conditions.

Keywords: die-off, fungi pathogen, global change, hydraulic failure, non-structural carbohydrates

3.1. Introduction

Drought-induced tree die-off is emerging as a global phenomenon, affecting a great variety of species and ecosystems in all vegetated continents of the world (Allen et al. 2010). Recent episodes of crown defoliation and tree mortality have been related to an increase of mean annual temperature and a decrease of annual rainfall in southern European forests (Carnicer et al. 2011) and with increasing severe droughts in the southwestern USA (Van Mantgem et al. 2009; Williams et al. 2012). Extreme drought events are expected to become more frequent (IPCC 2013), which could accelerate drought-related tree mortality. These responses can be amplified in many regions by current trends towards increased stand basal area, associated with changes in forest management (Martínez-Vilalta et al. 2012b). There are important feedback loops between forest dynamics and climate due to the key role of forests on the global water and carbon cycles (Bonan 2008) and thus widespread forest mortality can have rapid and drastic consequences for ecosystems (Anderegg et al. 2013a). Nonetheless, and despite these potential effects on ecosystem functioning, the mechanisms causing tree die-off are still poorly understood (McDowell 2011; McDowell et al. 2011; Sala et al. 2010).

McDowell et al. (2008) introduced a framework with three main, non-exclusive mechanisms that could cause drought-induced mortality in trees: (1) carbon starvation, (2) hydraulic failure and (3) biotic agents. They also hypothesised that plants with a strict control of water loss through stomatal closure (isohydric species) would be more likely to die of carbon starvation during a long drought, whereas anisohydric species would more likely experience hydraulic failure during intense droughts, due to more negative xylem water potentials (McDowell et al. 2008). However, the evidence for or against these proposed mortality mechanisms is inconclusive, and recent reports have urged adoption of a more integrated approach focusing on the interrelations between plant hydraulics and the economy and transport of carbon in plants (McDowell 2011; McDowell et al. 2011; McDowell and Sevanto 2010; Sala et al. 2010; Sala et al. 2012).

Xylem vulnerability to embolism has been found to place a definitive limit on the physical tolerance of conifers (Brodribb and Cochard 2009) and angiosperms (Urli et al. 2013) to desiccation. A recent global synthesis has shown that many tree species operate within relatively narrow hydraulic safety margins in all major biomes of the world (Choat et al. 2012b). Although structural and physiological acclimation to drought may result in large safety margins from hydraulic failure preceding death (Plaut et al. 2012), high levels of hydraulic dysfunction associated with drought-induced desiccation have been reported (Hoffmann et al. 2011; Nardini

et al. 2013). In addition, evidence of hydraulic failure linked to canopy and root mortality has been found in declining trembling aspen (*Populus tremuloides* Michx.), without evidence of depletion of carbohydrate reserves (Anderegg et al. 2012b), and in some *Eucalyptus* L'Hér. species (Mitchell et al. 2013).

The dynamics and role of non-structural carbohydrate (NSC) stores during drought are still under debate, but some agreement is emerging in that NSC concentrations tend to increase under moderate drought because growth ceases before photosynthesis, whereas they may decline sharply if drought conditions become extreme (McDowell 2011). Recent reports show that the same drought conditions can have contrasting effects on NSC concentrations even on species of the same genus (*Nothofagus* Blume) (Piper 2011). On the other hand, Galiano et al. (2011) reported extremely low NSC concentrations in the stem of defoliated Scots pine (*Pinus sylvestris* L.) trees and higher probability of drought-induced mortality in pines with lower NSC concentrations. Also, Adams et al. (2013) observed an association between tree mortality and reduced NSC levels in leaves in a drought simulation experiment on piñon pine (*Pinus edulis* Engelm.). In addition, drought-related reductions in stored NSC pools may affect tree organs differentially. For instance, Hartmann et al. (2013a) showed a reduction of NSC in Norway spruce (*Picea abies* (L.) Karst.) roots but not in leaves, which could be attributed to changes in carbon allocation.

Biotic agents and drought can interact to accelerate tree mortality. Drought-stressed trees may be more vulnerable to infection by fungal pathogens (Desprez-Loustau et al. 2006; La Porta et al. 2008) or to insect attacks (Gaylord et al. 2013; Matthias et al. 2007). Although pathogens can directly kill trees through the production of toxic metabolites, they can also induce hydraulic failure, e.g., via occlusion of the xylem, or carbon starvation by altering NSC demand or supply. The interactions between pathogen infection and the physiological mechanisms of drought-induced mortality depend on the trophic interaction (biotrophic, necrotrophic or vascular wilts) established with the tree (Oliva et al. 2014). For instance, blue-stain fungi infection can cause outright hydraulic failure via xylem occlusion (Hubbard et al. 2013) while root rot fungi may lead to a gradual tree decline and eventually to death because of chronic growth reductions and subsequent constraints on water transport (Oliva et al. 2012). In addition, root rot fungi can reduce carbon reserves by fungal consumption of stored carbohydrates or by the induction of carbon-expensive defences, causing tree growth reductions (Cruickshank et al. 2011).

Field studies on mature trees examining all three hypothesised mechanisms of drought-induced mortality are still scarce and rarely explore explicitly the interactions between different mechanisms and their occurrence in different plant organs. Here we compare the hydraulic properties and the dynamics of NSC and embolism as a function of defoliation and infection by fungal pathogens in Scots pine trees growing together in a site affected by drought-induced decline (Hereş et al. 2012; Martínez-Vilalta and Piñol 2002) and close to the dry limit of the distribution of the species. Previous studies have shown that defoliation precedes drought-induced mortality in Scots pine trees from the same or similar sites (Galiano et al. 2011; Poyatos et al. 2013), and that defoliation seems to be an inevitable consequence of drought in the most susceptible individuals rather than an (effective) strategy to cope with it (Poyatos et al. 2013). In this context, we address the following questions: (1) are defoliated Scots pines intrinsically more vulnerable to xylem embolism than non-defoliated ones, providing evidence in favour of hydraulic failure as an important component of the decline process? If so, do defoliated trees experience higher levels of native embolism under dry summer conditions? (i.e., are leaf area reductions enough to compensate for their intrinsically higher vulnerability?), (2) do defoliated pines have lower seasonal NSC concentrations in all organs, supporting carbon starvation being involved in the mortality process?, and (3) is infection by fungal pathogens likely to enhance hydraulic dysfunction through increased levels of native embolism, or carbon depletion directly or indirectly lowering NSC levels through increased consumption, reduced sapwood depth or low growth?

3.2. Materials and methods

Study site

The study was conducted in Tillar valley (41°19'N, 1°00'E; 990 m above sea level) within Poblet Forest Natural Reserve (Prades Mountains, NE Iberian Peninsula). The climate is typically Mediterranean, with a mean annual precipitation of 664 mm (spring and autumn being the rainiest seasons and with a marked summer dry period), and moderately warm temperatures (11.3°C on average) (Poyatos et al. 2013). The soils are mostly Xerochrepts with fractured schist and clay loam texture, although outcrops of granitic sandy soils are also present (Hereter and Sánchez 1999). Our experimental area is mostly located on a NW-facing hillside with a very shallow and unstable soil due to the high stoniness and steep slopes (35° on average). More detailed information about the study area can be found in Hereter and Sánchez (1999).

The dominant canopy tree species in the study site is Scots pine and the understorey consists mainly of the Mediterranean evergreen holm oak (*Quercus ilex* L.). Severe droughts have affected the study site since the 1990s (Hereş et al. 2012; Martínez-Vilalta and Piñol 2002). Scots pine average standing mortality and crown defoliation in the Tillar valley are currently 12 and 52%, respectively. However, in some parts of the forest standing mortality is > 20% and cumulative mortality is as high as 50% in the last 20 years (J. Martínez-Vilalta, unpublished). The Scots pine population studied is more than 150 years old and has remained largely unmanaged for the past 30 years (Hereş et al. 2012). No major insect infestation episode associated with the forest decline in the area has been detected (M. Rojo, Catalan Forest Service, personal communication).

A mixed holm oak-Scots pine stand with a predominantly northern aspect was selected for this study where defoliated and non-defoliated pines were living side by side. A total of 10 defoliated and 10 non-defoliated Scots pine trees were sampled (see Table S1 in Supplementary Material 2 Section). In order to minimise unwanted variation, all trees had a diameter at breast height (DBH) between 25 and 50 cm (average DBH 36.08 ± 1.53 cm; similar between defoliation classes (P > 0.05; data not shown) and the distance between sampled trees was always > 5 m (the average minimum distance was 41.99 ± 13.74 m). In this study, defoliation was visually estimated relative to a completely healthy tree in the same population (cf. Galiano et al. 2011). A tree was considered as non-defoliated if the percentage of green needles was > 60% (average green leaves of the sampled non-defoliated trees = 77%) and defoliated if the percentage of green needles was < 40% (average green leaves of the sampled defoliated trees = 26%). The average height of Scots pines in the population studied was 14.1 ± 0.5 m (Poyatos et al. 2013). All measurements, in combination with a continuous monitoring of the main meteorological variables and soil moisture (cf. Poyatos et al. 2013 for details), were carried out during 2012. Sampling from defoliated trees avoided dead or dying branches (i.e., those with no green leaves), so our sampling can be considered representative only of the living part of the crown.

Non-structural carbohydrates sampling and analysis

Trees were sampled in March (late winter), June (late spring), August (mid-summer) and October (early autumn). Four organs (leaves, branches, trunk and coarse roots) were sampled from every tree to measure NSCs. Sun-exposed branches (0.5–1 cm of diameter with bark removed) were excised with a pole pruner around noon (12:00 pm – 03:00 pm, local time) to minimise the impact of diurnal variation in NSC concentrations due to photosynthetic activity

(Gruber et al. 2012; Li et al. 2008). One-year-old leaves were sampled from these branches. Trunk xylem at breast height and coarse roots at 5-10 cm soil depth were cored to obtain sapwood. Sapwood portion was visually estimated in situ from all the extracted cores. We also used these cores to measure the basal area increment (BAI) corresponding to the three most recent annual rings (see Table S1 available in Supplementary Material 2 Section). All samples were placed immediately in paper bags and stored in a portable cooler containing cold accumulators. One of the defoliated Scots pine trees (tree 1637; see Table S1 available in Supplementary Material 2 Section) died during the study period and leaves could not be sampled in August and October, whereas branches could be sampled in August but not in October.

At the end of every sampling day, samples were microwaved for 90 s in order to stop enzymatic activity and oven-dried for 72 h at 65°C. Samples were then ground to fine powder in the laboratory. Total NSC (TNSC) was defined as including free sugars (glucose and fructose), sucrose and starch, and were analysed following the procedures described by Hoch et al. (2002) with some minor variations (cf. Galiano et al. 2011). Approximately 12-14 mg of sample powder was extracted with 1.6 ml distilled water at 100°C for 60 min. After centrifugation, an aliquot of the extract was used for the determination of soluble sugars (glucose, fructose and sucrose), after enzymatic conversion of fructose and sucrose into glucose (invertase from *Saccharomyces cerevisae* Meyen ex E.C. Hansen) and glucose hexokinase (GHK assay reagent, I4504 and G3293, Sigma-Aldrich, Madrid, Spain). Another aliquot was incubated with an amyloglucosidase from *Aspergillus niger* van Tieghem at 50°C overnight, to break down all NSC (starch included) to glucose. The concentration of free glucose was determined photometrically in a 96-well microplate reader (Sunrise Basic Tecan, Männedorf, Switzerland) after enzymatic (GHK assay reagent) conversion of glucose to gluconate-6-phospate. Starch was calculated as TNSC minus soluble sugars. All NSC values are expressed as percent dry matter. Throughout the manuscript NSC is used to refer generically to NSCs, while TNSC is used to refer specifically to the total value of NSC (sum of starch and soluble sugars). The relationship between soluble sugars (SS) and TNSC will be expressed as SS:TNSC. Finally, we note that due to the current uncertainty in NSC quantification methodologies (Quentin et al. 2015), our results should be considered valid in relative terms (as used here) but not necessarily comparable to the values obtained by other laboratories or using different methods.

Hydraulic conductivity and vulnerability to xylem embolism

Hydraulic measurements were taken on the same Scots pine individuals as NSCs, except for one defoliated tree that could not be sampled for hydraulics. Branches and roots were sampled in April and May 2012, respectively, for determining xylem vulnerability curves. We selected branches and roots containing internodal segments 0.4–1.1 cm in diameter and ~15 cm in length. Branches were always sampled from the exposed part of the canopy and were 3-5 years old. Root samples were taken at a soil depth of ~20 cm and always from the down slope side of the trunk, in order to control for differences in water availability or soil properties. Sampled branches and roots were always longer than 40 cm and were immediately wrapped in wet cloths and stored inside plastic bags until they were transported to the laboratory on the same day. Once in the laboratory, samples were stored at 4°C until their vulnerability curves were established within < 3 weeks. Right before that, all leaves distal to the measured branch segments were removed and their total area measured with a Li-Cor 3100 Area Meter (Li-Cor Inc., Lincoln, NE, USA).

Vulnerability curves relating the percentage loss of hydraulic conductivity (PLC) as a function of xylem water potential were established using the air injection method (Cochard et al. 1992). Hydraulic conductivity (water flow per unit pressure gradient) was measured using the XYL'EM embolism meter (Bronkhorst, Montigny-Les-Cormeilles, France) using deionised, degassed water (Liqui-Cel Mini-Module degassing membrane) and a pressure head of 4.5 kPa. The bark was removed from all measurement segments and their ends were cleanly shaved with a sharp razor blade before connecting to the XYL'EM apparatus.

Branch segments were rehydrated with deionised, degassed water prior to determining maximum hydraulic conductivity (K_{max}) (Espino and Schenk 2011), leading to stable and consistent K_{max} measurements. Afterwards, all segments (four to six each time) were placed inside a multi-stem pressure chamber with both ends protruding. Then, we raised the pressure inside the chamber to 0.1 MPa (basal value) during 10 min, lowered the pressure, waited 10 min to allow the system to equilibrate and measured hydraulic conductivity under a low pressure head (4.5 kPa). Stable conductivity readings were usually achieved within 3 min. These measurements were considered to represent the maximum hydraulic conductivity (K_{max}) and were used as reference conductivity (PLC = 0) for the purpose of establishing vulnerability curves. We repeated this process, raising the injection pressure stepwise by 0.5 MPa (roots) or 1 MPa (branches), until the actual conductivity of the segment was < 20% of K_{max}, or when we reached 4 MPa. Due to technical limitations, we could not increase the pressure in the chamber over 4 MPa, but only five

samples (out of 38) had not reached 80% PLC at this pressure. We fitted vulnerability curves with the following function (Pammenter and Van Der Willigen 1998):

$$\mathrm{PLC} = \frac{100}{1+\exp\left(\mathrm{a}(P-P_{50})\right)} \qquad \text{Equation 1}$$

In this equation, PLC is the percentage loss of hydraulic conductivity, P the applied pressure, P_{50} the pressure (i.e., –ψ) causing a 50% PLC and a is related to the slope of the curve. Parameters were estimated with nonlinear least squares regression. Some vulnerability curves lead to inconsistent results, due to technical problems, and were removed from the analyses. Final sample size was 15 roots (six from defoliated and nine from non-defoliated trees) and 15 branches (seven from defoliated and eight from non-defoliated trees).

Measurements of K_{max} were used for calculating specific hydraulic conductivity (K_S, in m^2 MPa^{-1} s^{-1}), as the ratio between maximum hydraulic conductivity and mean cross-sectional area of the segment (without bark), and leaf specific conductivity (K_L, in m^2 MPa^{-1} s^{-1}), as the quotient between maximum hydraulic conductivity and distal leaf area. Finally, we calculated the ratio between distal leaf area and cross-sectional area (A_L:A_S) of each branch segment.

Monitoring water potentials and native embolism

We sampled one exposed branch from each of the trees that had been sampled for vulnerability curves (9 defoliated and 10 non-defoliated individuals) monthly from May to August and in October 2012. Midday and predawn leaf water potentials were usually measured in situ on nearby defoliated and healthy pines on the same sampling dates. We selected branches at least 40 cm long and containing internodal segments of 4-10 cm length (0.3-0.9 cm in diameter). Immediately following excision, branch samples were placed in plastic bags with a small piece of damp paper towel, stored in a bigger bag containing cold accumulators and transported to the laboratory within 3 hours. All branches were sampled before 8 a.m., solar time.

Once in the laboratory, we measured shoot water potential on one terminal shoot per sampled branch using a Scholander-type pressure chamber (PMS Instruments, Corvallis, OR, USA) (except for the initial, May sampling). To measure native embolism, we cut wood segments (4-10 cm in length) underwater from each sampled branch. The bark was removed from the measurement segments and their ends were cleanly shaved with a sharp razor blade before connecting them to the tubing system of the XYL'EM apparatus to measure native hydraulic

conductivity (K_i) under a pressure head of ~4.5 kPa. Measurement samples were rehydrated overnight and their maximum hydraulic conductivity (K_{max}) was measured with the XYL'EM apparatus as described above. The PLC due to embolism was computed as:

$$\mathrm{PLC} = 100 \left(1 - \frac{K_\mathrm{i}}{K_\mathrm{max}} \right) \qquad \text{Equation 2}$$

Root rot pathogens

We focused on root and butt rot pathogens as possible contributors to the decline process observed in the forest studied. From each tree, we extracted two cores with an increment borer, one at stump height and the other in one of the large roots. Decay presence was noted and cores were kept in sterile conditions. Within 48 h, they were placed onto Hagem medium amended with benomyl (10 mg l^{-1}) and cloramphenicol (200 mg l^{-1}). Plates were checked weekly during the following 3 months, and any mycelia growth was sub-cultured. Identification of fungal isolates was first attempted by sequencing the ITS region. Some of our isolates showed an equally low similarity (95%) to other isolates classified as either *Onnia tomentosa* (Fr.) P. Karst. or *O. circinata* (Fr.) P. Karst. in reference databases such as Genbank or UNITE. We identified our cultures as *Onnia* P. Karst spp., as morphological characters in culture and comparison with reference cultures from CBS-KNAW Fungal Biodiversity Centre (CBS 246.30 *O*. *circinata*, CBS 278.55 *O*. *tomentosa*) did not yield a conclusive identification.

We found signs of fungi infection after the cultivation of the extracted cores in seven pines; three of them were non-defoliated and the other four were defoliated (see Table S1 available in Supplementary Material 2 Section). One defoliated and one non-defoliated tree were infected by a heart rot fungi (*Porodaedalea pini* (Brot.) Murrill). These fungi mainly cause heartwood decay with no major known physiological effects (Garbelotto 2004), so we considered these two trees as "non-infected" in our analyses. The other trees (two non-defoliated and three defoliated) were infected by *Onnia* sp., which causes root rot and physiological impairment, and we considered those trees as "infected" in subsequent analyses.

Data analysis

We used different types of linear models to test the effects of defoliation and fungal infection on the measured response variables. In each case we included the main covariates (measured organ and sampling month, as appropriate) and the most biologically plausible interactions. Note that model complexity, in terms of the number of interactions that could be included, is subject to sample size limitations. Preliminary analyses showed that DBH effects were never significant in the models and therefore were not included in the final models reported here. General linear models were fitted to study the effects of defoliation class (two levels: defoliated or non-defoliated) and infection occurrence (two levels: infected or non-infected) on K_L, A_L:A_S, BAI and root and trunk sapwood depths. Separate linear models were fitted for each of the five response variables (see Eq. (S1) available in Supplementary Material 2 Section). Linear mixed models were used to analyse vulnerability-curve parameters (a andP_{50}) and K_S as a function of defoliation class, organ (branch or root) and infection occurrence. Tree identity was included in the models as a random factor (see Eq. (S2) available in Supplementary Material 2 Section). Similar mixed models were used to analyse shoot water potential, PLC, TNSC and SS:TNSC as a function of defoliation class, sampling date, organ (only for TNSC and SS:TNSC), and infection occurrence, including again tree identity as a random factor (see Eqs (S3) and (S4) available in Supplementary Material 2 Section). Finally, starch concentration in roots was also analysed using similar models (without the organ effect) to study in detail the impact of root rot pathogens on this NSC fraction and how it developed over time (and hence in this model we included the interaction between defoliation class, infection occurrence and sampling date) (see Eq. (S5) available in Supplementary Material 2 Section).

Variables K_S, K_L, A_L:A_S, TNSC and root and trunk sapwood depth were log-transformed, and starch concentration in roots was square root-transformed, to achieve normality prior to all analyses. All analyses were carried out with R Statistical Software version 3.1.0 (R Core Team, 2014) using the lm and lme functions.

3.3. Results

Meteorological conditions

The summer of 2012 was particularly dry and warm compared to the climatic average for the period 1951-2010: average air temperature (June-August) was 20.56°C and total precipitation only 56 mm (Figure 1), compared with climatic values (1951-2010) of 19.30°C and 135.23 mm, respectively. High values of daytime-averaged temperatures and vapour pressure deficits (VPDs) occurred in mid-August, followed by very low soil water content (SWC) values (~0.08 m^3 m^{-3}) at the beginning of September, compared with a spring maximum soil moisture of 0.33 m^3 m^{-3} (Figure 1).

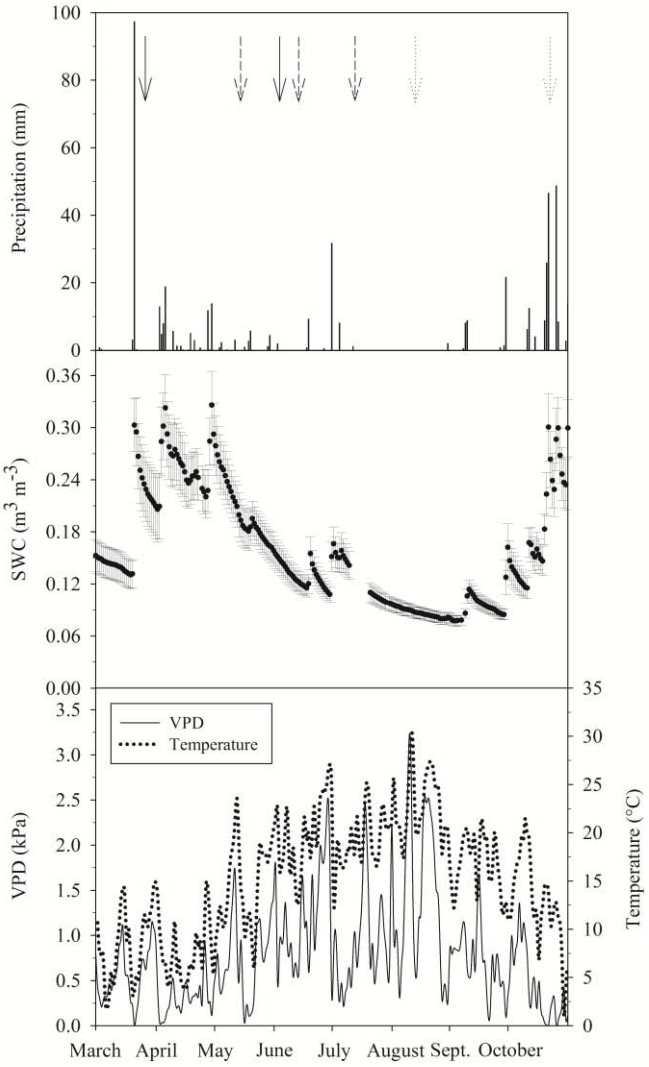

Figure 1. Seasonal course of daily precipitation, soil water content (SWC), vapour pressure deficit (VPD) and temperature during the study period. Error bars indicate ± 1 SE. Arrows in the upper panel indicate sampling days (carbohydrates sampling, solid arrow; carbohydrates + embolism sampling, dotted arrow; embolism sampling, dashed arrow).

Non-structural carbohydrates

Concentrations of total NSCs varied among tree organs, in the following order: TNSC (leaves) > TNSC (branches) > TNSC (roots) > TNSC (trunk) (Figure 2, Table 1). In general, non-defoliated Scots pine trees showed higher concentrations of TNSC throughout the study period and across all organs (Figure 2). Total non-structural carbohydrate values increased from March to June (except for leaves of defoliated pines) to reach a seasonal peak and then declined in August. Seasonal variation in TNSC was greater in leaves, especially for non-defoliated pines, which showed a more than fourfold decline in TNSC between the June peak and the minimum value in August. Post-drought October TNSC only slightly increased in trunks and leaves (Figure 2). Infection by fungal pathogens was not associated with significant differences in TNSC levels in any organ or month (Table 1).

The ratio of soluble sugars to TNSC (SS:TNSC) differed among tree organs but showed consistent seasonal dynamics across organs (Figure 2, Table 1). The value of SS:TNSC declined slightly from March to June, it increased in August, especially in leaves, and then declined in October. In August, SS:TNSC values were > 0.8 for all organs and defoliation classes, indicating that most of the TNSC were in the form of soluble sugars (Figure 2). Starch levels at peak drought were virtually depleted in leaves (i.e., SS:TNSC was nearly 1). Moreover, there were significant differences in SS:TNSC between defoliation classes in some organs and months, whereby defoliated pines tended to show higher SS:TNSC values before the onset of drought but similar or lower values in August (Figure 2, Table 1). No differences in SS:TNSC were observed associated to fungi infection (Table 1).

Throughout the season, root starch tended to be lower in defoliated pines compared to non-defoliated ones (Figure 3). Root rot infection was associated with higher root starch levels in non-defoliated pines, but this effect was not observed in defoliated pines (Figure 3, Table 1). The triple interaction between month, defoliation and infection was statistically significant (Table 1). Interestingly, our results show that root starch concentration in October was virtually depleted in infected, defoliated pines, and it was much lower than in non-infected ones (Figure 3).

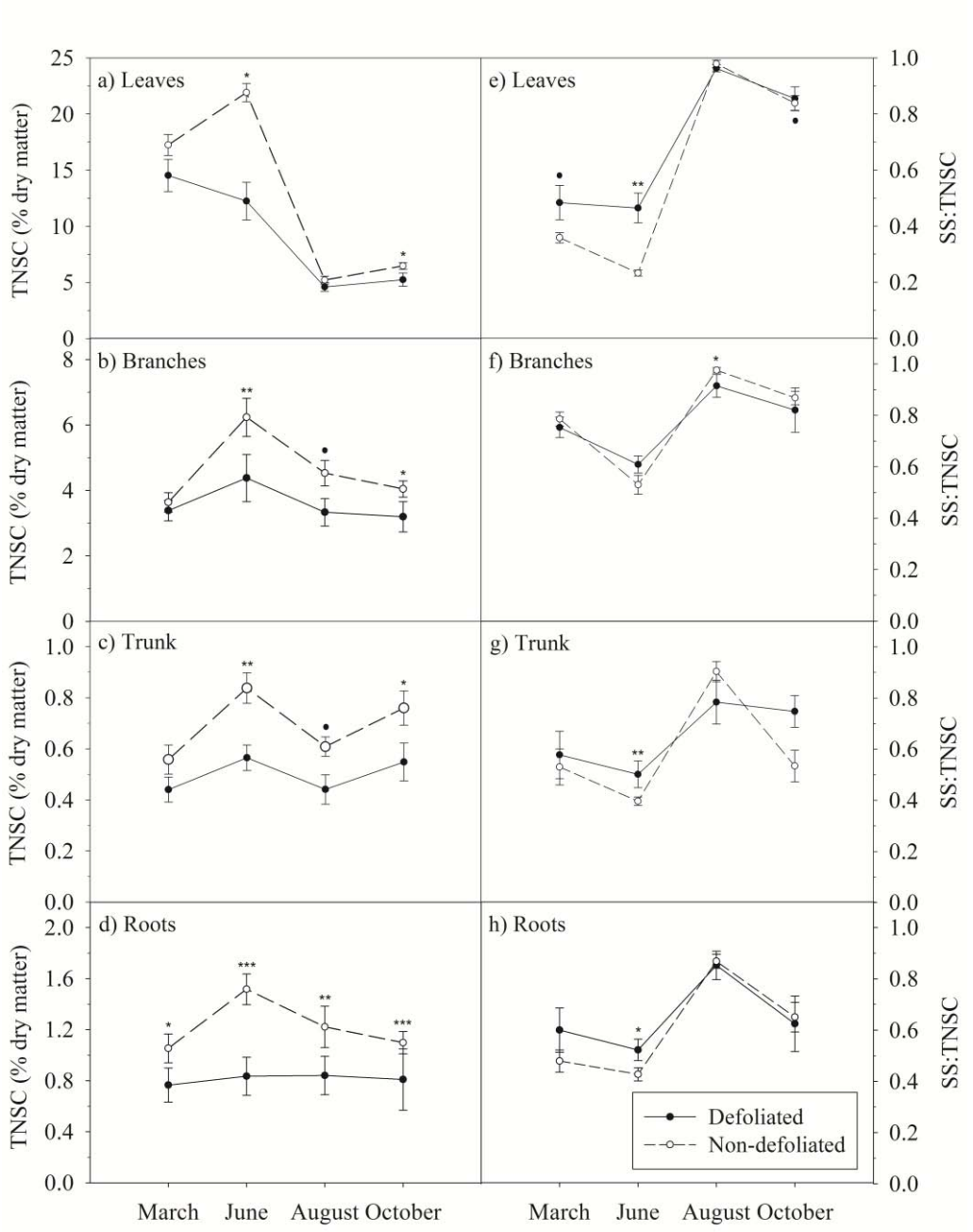

Figure 2. Seasonal variation in TNSCs and the ratio between soluble sugars and total non-structural carbohydrates (SS:TNSC) in the four studied organs. Error bars indicate ± 1 SE. The asterisks indicate significant differences between defoliation classes within a given sampling month (˙0.05 < *P* < 0.1; *0.01 < *P* < 0.05; **0.001 < *P* < 0.01; ***P < 0.001).

Table 1. Summary of the fitted linear mixed models with TNSC, the ratio between soluble sugars and total non-structural carbohydrates (SS:TNSC) and root starch as response variables.

Parameter	**log(TNSC)**	**SS:TNSC**	**sqrt(Starch)**
	R^2 **= 0.90**	R^2 **= 0.61**	R^2 **= 0.57**
Intercept	2.50 ± 0.19***	0.54 ± 0.06***	0.65 ± 0.13***
Branches	-1.31 ± 0.19***	0.27 ± 0.07***	ne
Trunk	-3.22 ± 0.19***	0.10 ± 0.07 (ns)	ne
Roots	-2.78 ± 0.19***	0.07 ± 0.07 (ns)	ne
June	-0.15 ± 0.19 (ns)	-0.08 ± 0.07(ns)	-0.02 ± 0.18(ns)
August	-1.17 ± 0.19***	0.41 ± 0.07***	-0.40 ± 0.18*
October	-1.28 ± 0.19***	0.37 ± 0.07***	-0.51 ± 0.18**
Non-defoliated	0.15 ± 0.17 (ns)	-0.10 ± 0.05•	0.21 ± 0.21
Non-infected	0.18 ± 0.20 (ns)	-0.09 ± 0.06 (ns)	-0.17 ± 0.16 (ns)
Branches:June	0.31 ± 0.19 (ns)	-0.13 ± 0.07•	ne
Trunk:June	0.31 ± 0.19 (ns)	-0.03 ± 0.07 (ns)	ne
Roots:June	0.21 ± 0.19 (ns)	0.01 ± 0.07(ns)	ne
Branches:August	1.23 ± 0.19***	-0.37 ± 0.08***	ne
Trunk:August	1.21 ± 0.19***	-0.26 ± 0.08***	ne
Roots:August	1.26 ± 0.19***	-0.23 ± 0.08**	ne
Branches:October	0.88 ± 0.19***	-0.35 ± 0.08***	ne
Trunk:October	1.26 ± 0.19***	-0.33 ± 0.08***	ne
Roots:October	0.90 ± 0.19***	-0.33 ± 0.08***	ne
Branches:Non-defoliated	0.05 ± 0.14 (ns)	0.10 ± 0.05•	ne
Trunk:Non-defoliated	0.05 ± 0.14 (ns)	0.02 ± 0.05 (ns)	ne
Roots:Non-defoliated	0.29 ± 0.14*	0.04 ± 0.05 (ns)	ne
Branches:Non-infected	-0.28 ± 0.16•	0.04 ± 0.06 (ns)	ne
Trunk:Non-infected	-0.36 ± 0.16*	0.03 ± 0.06 (ns)	ne
Roots:Non-infected	-0.39 ± 0.16*	0.03 ± 0.06 (ns)	ne
June:Non-defoliated	0.31 ± 0.14*	-0.07 ± 0.05 (ns)	0.28 ± 0.29 (ns)
August:Non-defoliated	0.14 ± 0.14 (ns)	0.11 ± 0.05*	0.04 ± 0.29 (ns)
October:Non-defoliated	0.27 ± 0.14 (ns)	0.01 ± 0.05 (ns)	0.47 ± 0.29 (ns)
June:Non-infected	0.04 ± 0.16 (ns)	0.05 ± 0.06 (ns)	0.15 ± 0.22 (ns)
August:Non-infected	-0.10 ± 0.16*	0.12 ± 0.06•	0.14 ± 0.22 (ns)
October:Non-infected	0.16 ± 0.16 (ns)	0.07 ± 0.06 (ns)	0.59 ± 0.22**
Non-defoliated:Non-infected	ne	ne	0 ± 0.24 (ns)
June:Non-defoliated:Non-infected	ne	ne	-0.22 ± 0.33 (ns)
August:Non-defoliated:Non-infected	ne	ne	-0.13 ± 0.33 (ns)
October:Non-defoliated:Non-infected	ne	ne	-0.72 ± 0.33*

For factors, the coefficients indicate the difference between each level of a given variable and its reference level. In models the reference organ was "Leaves" (except in root starch where the effect of organ is not evaluated in the model), the reference month was "March", the reference defoliation class was "Defoliated" and the reference infestation occurrence was "Infected". The values are the estimate ± SE. Abbreviations: ns, no significant differences; • $0.05 < P < 0.1$; * $0.01 < P < 0.05$; ** $0.001 < P < 0.01$; *** $P < 0.001$; ne, not evaluated in the model. Conditional R^2 values are given for each model.

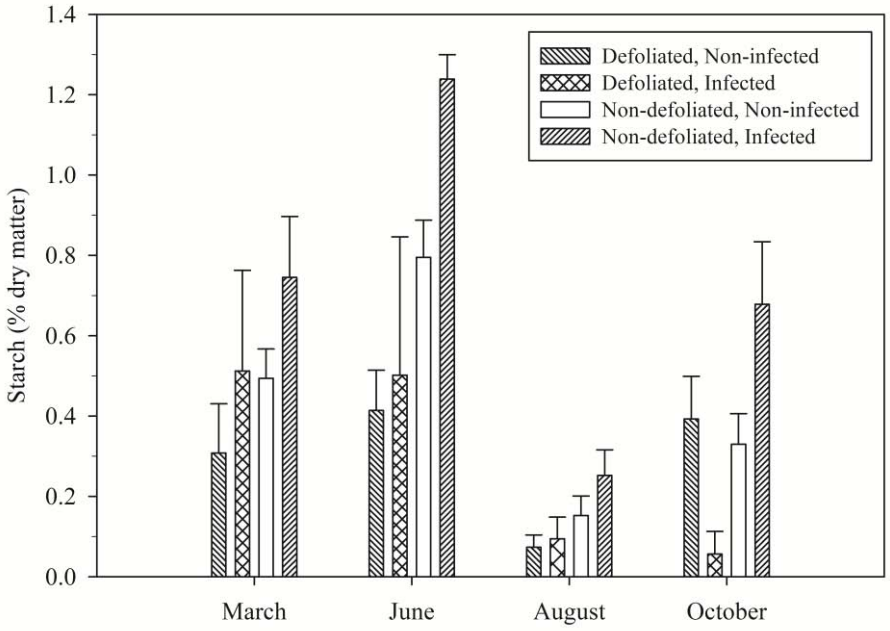

Figure 3. Seasonal changes in root starch concentration as a function of infection and defoliation classes. Error bars indicate ± 1 SE.

Vulnerability curves and hydraulic properties

Roots were more vulnerable to embolism than branches, reaching 50% PLC slightly below -2 MPa, compared with a value close to -3 MPa for branches (Figure 4). This effect was statistically significant (overall *P*-value for Organ = 0.0062 in a least significant means multiple comparison), although the difference was not significant for all the combinations of defoliation and infections classes (cf. Table 2). The vulnerability to embolism of branches was similar between defoliation classes (Figure 4b, Table 2). In roots, there was no difference between defoliation classes in P_{50}, but the slope of the vulnerability curve was steeper in defoliated trees (Table 2). This result implies that the roots of non-defoliated pines would begin to lose conductivity at higher (i.e., closer to zero) water potentials than those of defoliated individuals, but the latter would lose conductivity faster than non-defoliated pines as water potentials declines (Figure 4a). Infection did not affect vulnerability to xylem embolism (Table 2).

No differences in specific hydraulic conductivity (K_s) were found between roots and branches (Table 2), possibly due, at least in part, to the large variability in K_s observed for roots. Likewise, there were no significant differences in either K_S, K_L, or A_L:A_S between defoliated and non-defoliated pines (Table 2). However, we found lower branch K_L in infected trees (Table 2).

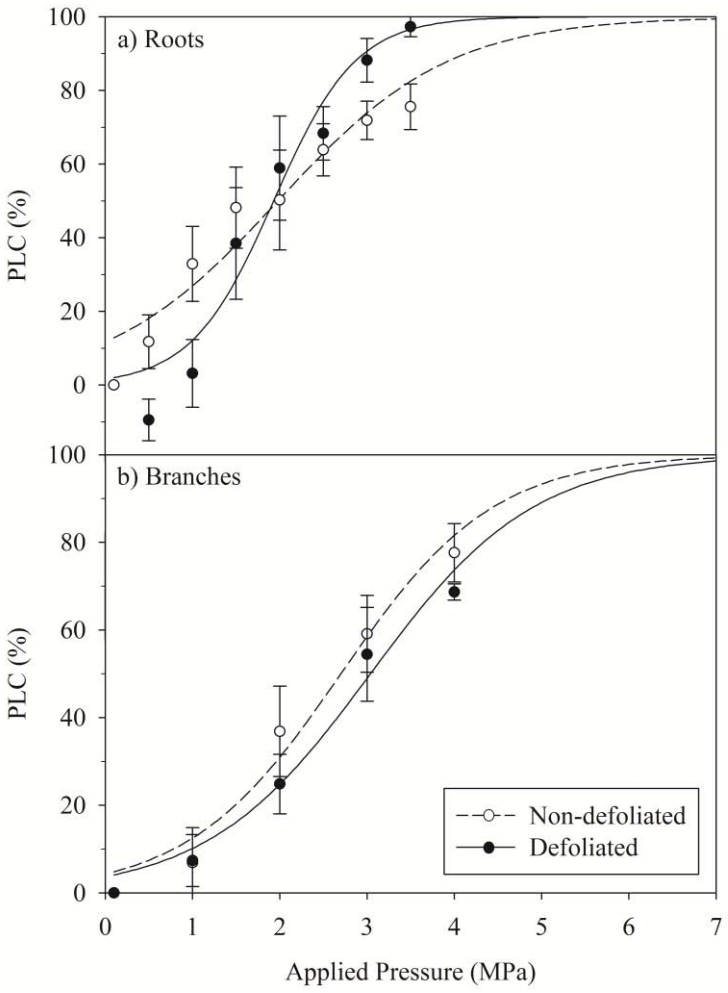

Figure 4. Vulnerability curves for roots (a) and branches (b) of defoliated and non-defoliated Scots pine trees, showing PLC as a function of applied pressure. Equation 1 was use to fit the curves. Error bars indicate ± 1 SE.

Table 2. Summary of the fitted models with the vulnerability-curves parameters (a and P_{50}), specific hydraulic conductivity (K_S), leaf specific conductivity (K_L) and leaf-to-sapwood area ratio (A_L:A_S) as response variables.

Parameter	**Parameter *a***	**P_{50}**	**log(K_S)**	**log(K_L)**	**log (A_L:A_S)**
	R^2 = 0.37	**R^2 = 0.40**	**R^2 = 0.10**	**R^2 = 0.36**	**R^2 = 0.11**
Intercept	-2.04 ± 1.38 (ns)	2.72 ± 0.42***	-8.70 ± 0.81***	-16.56 ± 0.75***	7.48 ± 0.64***
Roots	-1.80 ± 1.78 (ns)	-0.99 ± 0.55 (ns)	0.20 ± 1.04 (ns)	ne	ne
Non-defoliated	-0.12 ± 1.20 (ns)	-0.51 ± 0.37 (ns)	0.01 ± 0.70 (ns)	1.90 ± 1.30 (ns)	-0.73 ± 1.10 (ns)
Non-infected	0.36 ± 1.50 (ns)	0.41 ± 0.46 (ns)	1.12 ± 0.88 (ns)	2.50 ± 0.89*	-0.83 ± 0.75 (ns)
Roots:Non-defoliated	4.26 ± 1.74*	0.42 ± 0.54 (ns)	0.16 ± 1.02 (ns)	ne	ne
Roots:Non-infected	-2.74 ± 1.99 (ns)	-0.12 ± 0.61 (ns)	-0.67 ± 1.16 (ns)	ne	ne
Non-defoliated:Non-infected	ne	ne	ne	-2.71 ± 1.44$^{\bullet}$	1.29 ± 1.22 (ns)

In the models the reference organ was “Branches”, the reference defoliation class was “Defoliated” and the infestation occurrence was “Infected”. The values are the estimate ± SE. Abbreviations: ns, no significant differences; $^{\bullet}$ 0.05 < P < 0.1; * 0.01 < P < 0.05; *** P < 0.001; ne, not evaluated in the model. Conditional R^2 values are given for each model.

Water potentials and native embolism

Shoot water potentials measured in the morning, at the time of sampling for PLC measurements, increased from June to July (Figure 5b, Table 3), consistent with the rainfall events occurring in late June (Figure 1). Afterwards, water potentials declined sharply down to values around -2 MPa in August, coinciding with the driest part of the study period. These water potentials were usually between the corresponding predawn and midday shoot water potentials measured in simultaneous sampling campaigns in nearby Scots pine individuals (Figure 5c). We did not find any significant effect of defoliation or infection on water potential (Table 3).

Native PLC varied significantly among sampling dates, following the variation in shoot water potentials. Percentage loss of hydraulic conductivity was particularly low in July, with values around 20%, and it was highest in August, with average values around 65% (Figure 5a, Table 3). In August, six branches (four from non-defoliated, and two from defoliated pines) showed PLC values > 85%. Native embolism was not significantly different between defoliation and infection classes (Table 3), except for October when non-defoliated pines showed higher PLC (Figure 5b) (P = 0.048).

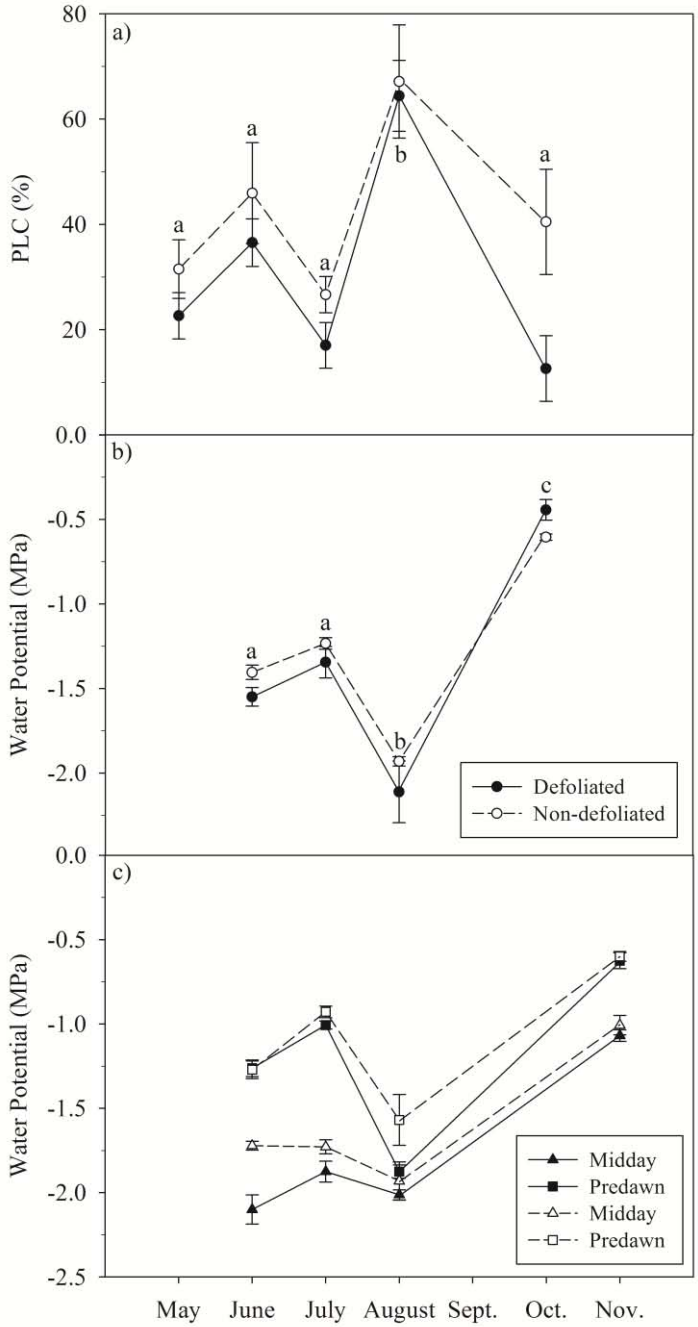

Figure 5. Seasonal variation in (a) native embolism expressed as PLC and (b) corresponding water potential, measured in the same branches, of defoliated and non-defoliated Scots pine trees. (c) Predawn and midday water potentials from nearby Scots pine trees from the same population measured on the same dates, where solid lines and symbols indicate defoliated trees and dashed lines and open symbols designate non-defoliated individuals. Error bars indicate ± 1 SE. Different letters indicate significant differences ($P < 0.05$) between sampling dates.

Table 3. Summary of the fitted linear mixed models with the percentage loss of conductivity (PLC) and the water potential as response variables.

Parameter	**PLC**	**Water Potential**
	R^2 = 0.45	**R^2 = 0.82**
Intercept	23.01 ± 10.98*	-1.57 ± 0.13***
June	10.95 ± 14.96 (ns)	ne
July	-9.95 ± 14.96 (ns)	-0.04 ± 0.19 (ns)
August	45.23 ± 14.96**	-0.69 ± 0.19***
October	-12.74 ± 15.00 (ns)	1.14 ± 0.19***
Non-defoliated	8.60 ± 10.47 (ns)	0.14 ± 0.13 (ns)
Non-infected	-0.52 ± 11.87 (ns)	0.02 ± 0.15 (ns)
June:Non-defoliated	0.25 ± 14.33 (ns)	ne
July:Non-defoliated	0.19 ± 14.33 (ns)	-0.07 ± 0.18 (ns)
August:Non-defoliated	-5.15 ± 14.33 (ns)	0.01 ± 0.18 (ns)
October:Non-defoliated	14.72 ± 14.64 (ns)	-0.30 ± 0.19 (ns)
June:Non-infected	4.42 ± 16.23 (ns)	ne
July:Non-infected	6.51 ± 16.23 (ns)	0.37 ± 0.21$^{\bullet}$
August:Non-infected	-5.16 ± 16.23 (ns)	0.20 ± 0.21 (ns)
October:Non-infected	9.13 ± 16.38 (ns)	-0.05 ± 0.21 (ns)

The reference month was “May” in PLC and “June” in Water Potential, the reference defoliation class was “Defoliated” and the reference infestation occurrence was “Infected”. The values are the estimate ± SE. Abbreviations: ns, no significant differences; $^{\bullet}$ 0.05 < *P* < 0.1; * 0.01 < *P* < 0.05; ** 0.001 < *P*< 0.01; *** P < 0.001; ne, not evaluated in the model. Conditional R^2 values are given for each model.

Basal area increment and sapwood depth

We found a marginally significant reduction of BAI associated with defoliation (*P* = 0.064) and this effect tended to be larger in infected trees as shown by the marginally significant (*P* = 0.083) interaction between defoliation and infection (Figure 6a).

Trunk sapwood depth showed patterns similar to those for BAI, but with significantly lower values for defoliated and infected individuals (Figure 6b). Finally, infected trees showed a significantly lower root sapwood depth compared to non-infected trees (*P* = 0.039), regardless of defoliation class, whereas defoliation had no significant effect on root sapwood depth (Figure 6c) (*P* = 0.89).

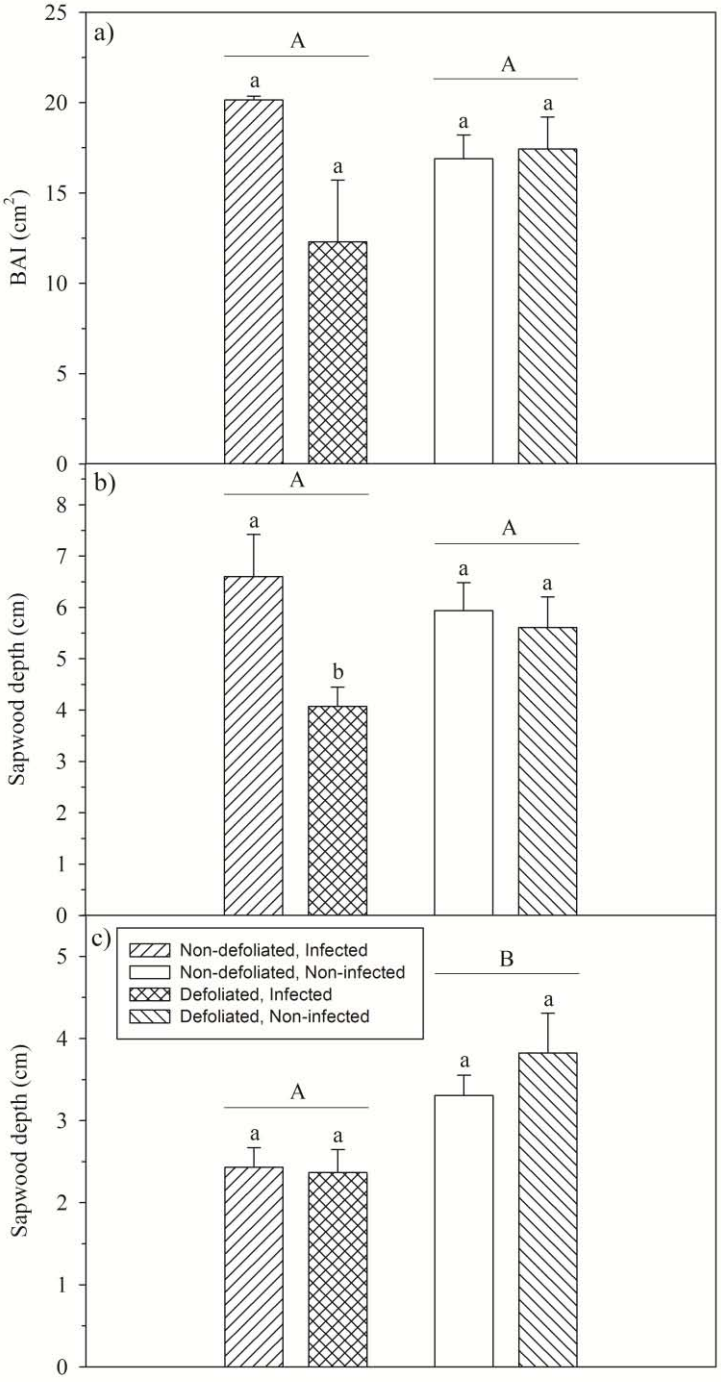

Figure 6. Basal area increment (BAI) (a), trunk sapwood depth (b) and root sapwood depth (c) as a function of infection and defoliation classes. Different uppercase letters indicate significant differences ($P < 0.05$) between infestation occurrence, and different lowercase letters indicate significant differences between defoliation classes within a given infection class. Note that the interaction between defoliation and infection in the BAI model was marginally significant ($0.05 < P < 0.1$). Error bars indicate ± 1 SE.

3.4. Discussion

Our results show that both high levels of embolism and low carbohydrate reserves occurred in the studied trees during a particularly dry summer. In addition, we show that defoliation was more associated with reduced carbohydrate reserves than with greater hydraulic impairment at the branch level. We also report that drought-induced defoliation and infection by a root rot fungus occur independently, but they both interact to determine the mode of physiological failure in Scots pine at the dry edge of its distribution. We note, however, that some of these results (particularly those regarding pathogen infection) should be interpreted with caution due to the low sample size.

Defoliation is associated with lower carbon availability, but not with higher hydraulic impairment at the branch level

We found no consistent differences between defoliated and non-defoliated pines in terms of their vulnerability to embolism according to P_{50} values. This is consistent with previous studies comparing Scots pine populations suffering different levels of drought-induced decline in the same area (Martínez-Vilalta et al. 2012b). Although we found steeper vulnerability curves for roots of defoliated pines, which would yield comparatively higher root PLC at water potentials lower than ca. -2 MPa (Figure 4a), these conditions only occur during exceptional droughts (Poyatos et al. 2013). In addition, branch-level leaf K_S and A_L:A_S were similar for defoliated and non-defoliated pines, in contrast to different values observed across Scots pine populations within the same study area (Martínez-Vilalta and Piñol 2002) and with the lower A_L:A_S reported at the tree level for defoliated pines (Poyatos et al. 2013). It should be emphasised, however, that our sampling design is representative at the branch level, but not necessarily at the whole crown level, as we were forced to sample living (as opposed to random) branches in heavily defoliated crowns.

It is also interesting to note that our results show a slightly higher branch vulnerability to embolism compared to the P_{50} of approximately -3.2 MPa reported previously for the same population (Martínez-Vilalta and Piñol 2002). This result may be related to some sort of filtering at the population level (i.e., preferential mortality of pines with higher resistance to embolism) or a by-product of the large variability in P_{50} observed across branches. But it is also possible that vulnerability to embolism may be increasing over time as a result of repeated droughts (i.e.,

cavitation fatigue; Hacke et al. 2001), as has been reported in the case of aspen die-off (Anderegg et al. 2013b).

The decline in PLC observed after a rainy period in July (Figure 5a) suggests some partial embolism reversal (e.g., McCulloh et al. 2011), but we cannot rule out the possibility that sampling artefacts may be causing an overestimation of this PLC recovery (e.g., Sperry 2013). Although our results imply that defoliation may be relatively effective in avoiding further increases in branch PLC, maximum PLC values were still within a range (~50-90%) associated with canopy dieback in several angiosperms (Anderegg et al. 2012b; Anderegg et al. 2013b; Hoffmann et al. 2011; Nardini et al. 2013) and gymnosperms (Klein et al. 2013; Plaut et al. 2012). Overall, these results also suggest that the steeper declines in whole-plant hydraulic conductance observed for defoliated pines during drought (Poyatos et al. 2013) may occur primarily belowground, as observed in other pine species prior to death (Plaut et al. 2013).

Defoliated pines showed consistently lower TNSC values than non-defoliated pines for most combinations of organ and season, as already observed in early autumn measurements of stem TNSC in other declining Scots pine populations (Galiano et al. 2011), including the study site (Poyatos et al. 2013). Interestingly, we did not observe increased TNSC in leaves of defoliated pines, despite their higher assimilation rates (Salmon et al. 2015). Total NSC decreased in all organs during drought, and most dramatically in leaves, tracking the seasonality of gas exchange (Poyatos et al. 2013).

The observed seasonal variation of the fraction of soluble sugars (SS:TNSC) (Figure 2) is consistent with starch concentration building up prior to bud-break and then decreasing during the summer period (Gruber et al. 2012; Hoch and Körner 2003). During August, the greater mobilisation of starch to soluble sugars could be attributed to several causes, including osmoregulation (Sala et al. 2012), the de novo synthesis of carbon-rich compounds into defence against root rot pathogens (Oliva et al. 2012), the energy-dependent process of embolism repair (Brodersen and McElrone 2013) and the growth of new tissue. The two latter processes are consistent with the reduction of native embolism after August, reaching pre-drought values in October (Figure 5a).

Despite the combination of drought and defoliation, our results did not show a complete depletion of TNSC in any of the organs studied (Figure 2), even in the tree that died during the monitoring period (data not shown). Values of trunk TNSC as low as 0.1% were measured in Scots pine 1 year prior to death in a nearby population (Galiano et al. 2011) while our trunk TNSC values

were always > 0.4%. Experimental studies on conifer saplings (Hartmann et al. 2013b), including pine species (Mitchell et al. 2013), have found evidence for drastic reductions in TNSC (especially starch) in stems and/or roots at mortality, without actually showing completely depleted carbohydrate storage. Phloem impairment may preclude the translocation of NSC and its availability for the maintenance of xylem transport or for the production of defence compounds (Hartmann et al. 2013a; Sala et al. 2010; Sevanto et al. 2014). A recent modelling analysis in the same study system predicts slow, but not disrupted, phloem transport under extreme drought (Mencuccini et al. 2015).

Root rot pathogens exacerbate hydraulic and carbon-related constraints at the tree level

We did not find a clear BAI reduction in *Onnia*-infected trees (Figure 6a), contrary to other studies reporting growth reductions caused by root rot pathogens from the *Armillaria* (Fr.) Staude (Cruickshank et al. 2011) and *Heterobasidion* Bref. genus (Oliva et al. 2012). Although the interaction between infection and defoliation was only marginally significant, the trend towards lower BAI in trees that were both defoliated and infected would be consistent with the reduced sapwood depth observed in these trees (Figure 6b). Hence, post-drought recovery of xylem specific hydraulic conductivity would be severely constrained in the long-term. Lower sapwood depth in the roots of infected trees (Figure 6c) could be the ultimate consequence of the decay progress, due to the reduction of tree growth caused by the formation of a reaction zone (Oliva et al. 2012). Infection-driven reductions in sapwood depth in roots (and in the trunk of infected, defoliated trees) may also result in lower tissue capacitance and a decreased ability to buffer short-term variations in water potential under drought (McCulloh et al. 2014).

Even though *Onnia* infection did not affect the vulnerability to embolism, it was associated with reduced K_L, particularly in defoliated pines (Table 2). Hence, infection by a root rot pathogen likely exacerbated hydraulic constraints through effects on growth and sapwood depth but also more directly through its impact on hydraulic conductivity.

Our results show a complex picture of the root rot infection effects on NSC pools. We did not find any evidence for consistent reductions in TNSC across tree organs associated with *Onnia* infection. However, for non-defoliated pines, infection appeared to drive starch accumulation in roots, rather than depletion, possibly as a response to increased sink strength in the roots associated to higher C demand (de novo synthesis of defence compounds; Oliva et al. 2014). Presumably, defoliated pines were so severely carbon-limited that this starch sink in the roots

could not be maintained, and they ended the year with extremely low levels of starch in roots (Figure 3). These findings are in line with a recently proposed framework which postulates that the net effect of the infection by a necrotrophic pathogen, such as *Onnia*, is strongly dependent on tree C availability and the timing of drought events (Oliva et al. 2014).

A complex pathway to mortality

In this final section we synthesise our current understanding on the process of drought-induced mortality in the study area, from the perspective of the comparison of coexisting defoliated and healthy individuals, using the information gathered here and in other studies conducted at the same site (Figure 7). Drought-induced defoliation is associated with drier microenvironments (Vilà-Cabrera et al. 2013) and with steeper reductions in whole-plant hydraulic conductance during seasonal drought (Poyatos et al. 2013). Hydraulic constraints may be related to higher vulnerability to embolism in roots (steeper vulnerability curves) and can be magnified by cavitation fatigue following repeated droughts. Defoliation and prolonged periods of near complete stomatal closure both contribute to reduce NSC in defoliated trees (Poyatos et al. 2013). Defoliated trees appear to enter a death spiral in which reduced C assimilation constrains radial growth (Hereş et al. 2012) and crown development (Poyatos et al. 2013). Root rot fungi may further damage hydraulic function through direct effects on sapwood depth and cumulative growth reductions. Moreover, the demand for C-rich compounds for osmoregulation, hydraulic repair and defence against root rot infection may contribute to the depletion of C reserves in defoliated pines, possibly increasing the minimum C threshold for tree survival and hence accelerating tree mortality (Oliva et al. 2014). It remains to be established whether the framework outlined in Figure 7, which has been developed for only one species in a given region, can be applied to other species and study systems. Overall, our study reflects the intertwined nature of physiological mechanisms leading to drought-induced mortality (McDowell 2011) and the inherent difficulty of isolating their contribution under field conditions.

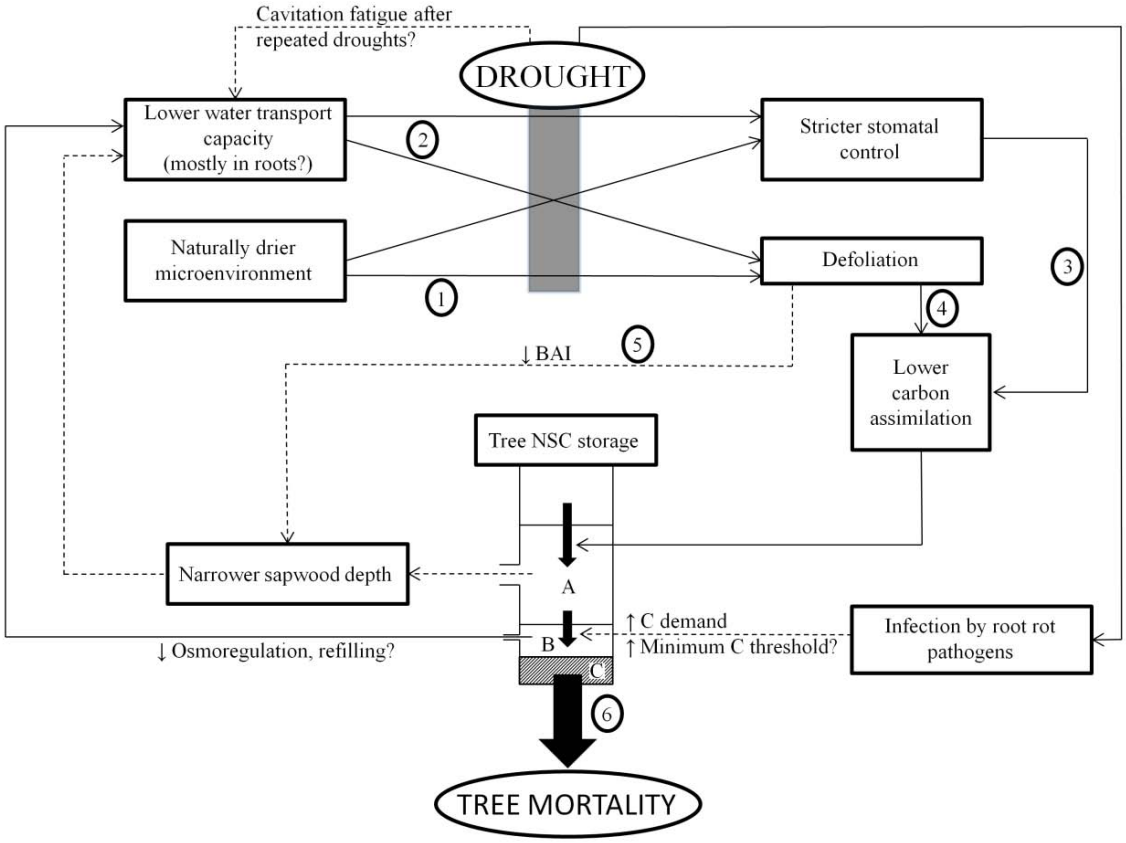

Figure 7. Schematic diagram of the processes associated with drought-induced mortality in Scots pine at our study site in Prades. Different numbers depict studies where the relationship has been reported: 1) Vilà-Cabrera et al. (2013), Poyatos et al. (2013), 2) Poyatos et al. (2013), 3) Poyatos et al. (2013), 4) Hereş et al. (2013), 5) Hereş et al. (2012) and 6) Galiano et al. (2011). Only Galiano et al. 2011 refers to a study conducted in a nearby population. Arrows indicate relationship between mechanisms. Dashed lines depict the relationships examined in this study. Question marks identify consequences for which the evidence is still weak. Letters inside "Tree NSC storage" compartment indicate different levels of NSC: A) high levels (tree survives), B) medium levels (tree survives), and C) low levels (tree dies).

Acknowledgements

We thank L. Galiano and T. Rosas for assistance in field sampling and carbohydrate analysis. We also thank all the staff from the Poblet Forest Natural Reserve for allowing us to carry out research at the "Barranc del Tillar" and for their logistic support in the field. The comments by Rick Meinzer and two anonymous reviewers greatly improved the manuscript. The study was supported by a Juan de la Cierva postdoctoral fellowship through the Spanish Ministry of Economy and Competitiveness awarded to R.P. (competitive grants CGL2010-16373, CSD2008-0004), and a FPU doctoral fellowship through the Spanish Ministry of Education, Culture and Sport awarded to D.A. (AP2010-4573).

Chapter 4

Roots hydraulic constraints during drought-induced decline in Scots pine[1]

Aguadé, D., Poyatos, R. and Martínez-Vilalta, J.

[1]In preparation

Abstract

Drought-induced tree die-off episodes have been observed in all vegetated continents and have become an important concern to humanity mainly because of the interdependence between forests and the atmosphere. Although notorious advances in the last years have been reported, there is still a lack of knowledge of the ecophysiological mechanisms involved in drought-induced tree mortality. However, while the role of non-structural carbohydrates is unclear, the dysfunction of hydraulic failure seems to be ubiquitous. Furthermore, roots have arisen as the most vulnerable organs to embolism. Linear variable displacement transducers (LVDTs) have been widely used to study changes in xylem radius and to estimate tree water status and the partition of hydraulic resistances along the plant.

In this paper we measured sap flow, leaf water potentials and stem pressure differences in apparently healthy (non-defoliated) and defoliated pines in a declining Scots pine (*Pinus sylvestris* L.) population in the NE Iberian Peninsula in 2012. Tree below-crown hydraulic resistance (R_{bc}) was estimated from the relationship between leaf-specific sap flow rates and stem pressure difference measured by LVDTs.

R_{bc} played an important role with increasing drought, but in this case, non-defoliated pines suffered higher constraints on water transport in the root zone under drought conditions. The percent contribution of below-crown to whole-tree hydraulic resistance also increased in summer. The nule association between defoliation and R_{bc} were more related to components of the hydraulic pathway, rather than root xylem. Our results are consistent with a predominant role of carbon depletion in driving Scots pine drought-induced mortality, but it is urged more research to understand how drought-driven changes in differenct components of below-ground hydraulics affect tree survival under extreme drought.

Keywords: drought-induced decline, LVDT, sap flow, stem diameter variations, root hydraulic resistance

4.1. Introduction

Drought is a major driver of the composition, function and dynamics of forests worldwide (Allen et al. 2015). Anthropogenic global warming has exacerbated drought conditions in the last decades (Trenberth et al. 2014) and drought-induced tree die-off may be increasing as a result (Allen et al. 2010). Drought-induced forest mortality episodes can potentially cause severe changes in ecosystem structure and function (Anderegg et al. 2013a), and substantial research efforts are being dedicated to understand the mechanisms behind drought-induced tree mortality (McDowell et al. 2008; McDowell 2011; Sala et al. 2010) and to improve our capacity to predict die-off events (Anderegg et al. 2012a). Hydraulic failure and carbon starvation have been identified as two physiological mechanisms potentially involved in drought-induced tree mortality (McDowell et al. 2008; McDowell 2011), but no consensus has been yet achieved on the relative importance of these two mechanisms and their interaction in triggering tree death (Hartmann et al. 2015). While the dysfunction of hydraulic transport by xylem embolism appears to be ubiquitous during drought-induced tree mortality (e.g., Anderegg and Anderegg 2013; Anderegg et al. 2012b; Galvez et al. 2013), the role of non-structural carbohydrate (NSC) dynamics is still unclear, as NSC have been reported to increase (e.g., O'Brien et al. 2015; Piper 2011; Piper and Fajardo 2016) or decrease (e.g., Duan et al. 2014; Galiano et al. 2011; Garcia-Forner et al. 2016b; Hartmann et al. 2013a) in different plant organs during drought-induced mortality.

Plant hydraulic traits are important factors determining the vulnerability to drought-induced tree decline and mortality (Anderegg et al. 2015a; Anderegg et al. 2016). However, it is still unclear which part of the plant's hydraulic pathway is more vulnerable to hydraulic failure during extreme drought (Anderegg et al. 2014; Bartlett et al. 2016). Although most of the studies on tree hydraulics during drought-induced mortality have focused on the mechanisms occurring within aboveground tissues (e.g., Anderegg et al. 2015a), belowground organs may have a strong influence on whole-tree hydraulic dynamics and tree survival during drought. For example, hydraulic impairment or even death of shallow roots has been suggested as an explanation of the shift to deeper soil water sources observed under extreme drought in *Pinus edulis* Engelm. (Grossiord et al. 2016). Similarly, extensive root embolism has recently been identified as the trigger of general physiological impairment prior to tree death in *Quercus ilex* L. and *Ulmus minor* Mill. (Rodríguez-Calcerrada et al. 2016).

Belowground hydraulic resistance is typically around half of whole-tree hydraulic resistance (Irvine and Grace 1997; Running 1980). In contrast, the belowground contribution may increase

during edaphic drought as a result of root embolism (Domec et al. 2009) because roots tend to be more vulnerable to embolism than stems (Hacke et al. 2000; Martínez-Vilalta et al. 2002). Increasing belowground resistance with drought can also be driven by reductions in the hydraulic conductance of the soil-root interface, for example following hydraulic isolation from the soil (Sperry et al. 2002), a process that has been suggested to occur in dying pines under extreme drought (Plaut et al. 2012).

Linear variable displacement transducers (LVDTs) measure microvariations in stem radius non-invasively. This technique has been widely used to study changes in xylem radius (Irvine and Grace 1997). Due to the elastic characteristics of the xylem, diurnal dynamics of radial shrinkage and swelling occur as a result of tension changes experienced by xylem water (Irvine and Grace 1997). These dynamics are related to changes in tree water status during the course of a day (Simonneau et al. 1993). The study of these xylem radius microvariations using the LVDT technique can be used to estimate the partition of hydraulic resistances along the plant's hydraulic pathway, and has been used to obtain continuous measurements of xylem water potential (Offenthaler et al. 2001; Ueda and Shibata 2001). Assuming steady-state conditions, LVDT measurements can be combined with whole-tree sap flow and leaf water potential measurements to estimate the hydraulic conductance of different components of the pant's hydraulic pathway (Martínez-Vilalta et al. 2007). Although these measurements have been used to estimate belowground resistance and its percent contribution to whole-tree hydraulic resistance (e.g., Martínez-Vilalta et al. 2007), to our knowledge there is no previous study of how these variables change during drought-induced tree decline.

Scots pine (*Pinus sylvestris* L.) is undergoing drought-induced decline in many sites throughout the southern and dry limit of its distribution (Bigler et al. 2006; Martínez-Vilalta and Piñol 2002; Vertui and Tagliaferro 1998), and it is often replaced by more competitive *Quercus* species (Galiano et al. 2010; Rigling et al. 2013). In Scots pine, hydraulic adjustment to increasing drought conditions along climatic gradients occurs mostly through reductions of leaf area relative to conductive sapwood area (Martínez-Vilalta et al. 2009; Poyatos et al. 2007). Within a site, however, crown defoliation has been postulated as an inevitable consequence of drought rather than as an effective strategy to avoid water stress, and is associated to increased mortality risk during subsequent droughts (Poyatos et al. 2013). Defoliation and low levels of NSC have been related to Scots pine decline (Aguadé et al. 2015; Galiano et al. 2011; Poyatos et al. 2013), but the physiological differences between defoliated and non-defoliated pines coexisting at the same sites have not been completely elucidated yet. Defoliated pines show the steepest declines of

whole-plant hydraulic conductance with drought and tend to have lower predawn leaf water potentials (Poyatos et al. 2013; Salmon et al. 2015), which suggest differences in the belowground system of defoliated and healthy pines. While roots tend to be more vulnerable to embolism than branches in this species and roots of defoliated trees are slightly more vulnerable than those of healthy individuals (Aguadé et al. 2015), it remains unclear how these differences will scale-up to whole-tree hydraulic resistance dynamics.

In this study, we monitored sap flow, xylem radius variations and leaf water potentials in Scots pine trees from a mountain Mediterranean forest where episodes of drought-induced decline have been reported since the 1990's (Hereş et al. 2012; Martínez-Vilalta and Piñol 2002). Our main objective was to estimate the below-crown hydraulic resistance (R_{bc}) and its contribution to whole-tree hydraulic resistance and explore their seasonal dynamics in a declining Scots pine population at the dry-edge of its distribution. We hypothesised that (1) R_{bc} will increase in summer in all trees studied due to the higher vulnerability to embolism of roots, (2) the summer increase in R_{bc} will be more acute in defoliated pines, and (3) $\%R_{bc}$ will increase in summer in both defoliated and non-defoliated pines due to greater contribution of roots relative to leaves to hydraulic resistance during acute drought.

4.2. Materials and methods

Study site

Measurements were conducted in Tillar Valley within the Poblet Forest Natural Reserve (Prades Mountains, northeast Iberian Peninsula). The climate is Mediterranean, with a mean annual rainfall of 664 mm (spring and autumn being the rainiest seasons and with a marked summer dry period), and moderately warm temperatures (11.3°C on average) (Poyatos et al. 2013). The soils are mostly xerochrepts with fractured schist and clay loam texture, although outcrops of granitic sandy soils are also present (Hereter and Sánchez 1999).

The forest studied (41°19'58.05''N, 1°0'52.26''E; 1015 m asl) consists of a mixed holm oak (*Quercus ilex* L.) - Scots pine stand with a predominantly northern aspect and with a very shallow and unstable soil due to the high stoniness and steep slopes (35° on average). The canopy is dominated by pines whereas oaks dominate the understorey; see Poyatos et al. (2013) for further details on stand characteristics. As a consequence of several drought-induced mortality episodes since the 1990s (Hereş et al. 2012; Martínez-Vilalta and Piñol 2002), Scots pine average standing

mortality and crown defoliation are currently 12% and 52%, respectively. However, in some parts of the forest, standing mortality is > 20% and cumulative mortality is as high as 50% in the last 20 years (J. Martínez-Vilalta, unpublished). The Scots pine population studied is more than 150 years old and has remained largely unmanaged for the past 30 years (Hereş et al. 2012). No major insect infestation episode was detected that could explain the forest decline in the area (Mariano Rojo, Catalan Forest Service, pers com.).

Experimental design

Between 2010 and 2013, several physiological variables were measured in defoliated and non-defoliated Scots pine trees (Aguadé et al. 2015; Pereira Blanco et al. 2014; Poyatos et al. 2013; Salmon et al. 2015), together with continuous monitoring of meteorological and soil moisture conditions (cf. Poyatos et al. 2013, for full details on the measurements of environmental variables). Here, we use the complete set of monitored trees to show the general pattern in the seasonal dynamics of sap flow for defoliated and non-defoliated trees, but we then focus on a subset of four defoliated and four non-defoliated co-occurring Scots pine trees in which sap flow, xylem radius variations and leaf water potentials were measured between August 2011 and November 2012 (Table 1). In order to minimise unwanted variation, all trees had a similar diameter at breast height (DBH) without differences between defoliation classes ($P > 0.05$; data not shown) (Table 1). Defoliation was visually estimated relative to a completely healthy tree in the same population. A tree was considered as non-defoliated if the percentage of green needles was >= 80% and defoliated if the percentage of green needles was <= 50%.

Table 1. Main characteristics of the trees studied. Defoliation class (D, defoliated; ND, non-defoliated), diameter at breast height (DBH), height (h), basal area (A_b), sapwood area (A_s), maximum leaf area (A_L), leaf-to-sapwood area ratio (A_L:A_S). The subset of trees with measurements of xylem radius variations are marked with an asterisk (*).

Tree	Class	Green leaves (%)	DBH (cm)	h (m)	A_b (cm^2)	A_s (cm^2)	A_L (m^2)	A_L:A_S (m^2 cm^{-2})
364	D	40	40.1	11.5	1262.9	430.0	19.53	0.045
542*	D	45	42.6	14.5	1425.3	496.0	19.46	0.039
544*	D	45	28.4	16.1	633.5	174.2	8.53	0.049
693	D	35	42.8	11.7	1438.7	501.4	10.47	0.021
699*	D	40	45.7	15.7	1640.3	583.3	15.23	0.026
704	D	50	48.0	11.2	1809.6	652.1	16.64	0.026
706	D	50	38.8	14.6	1182.4	397.3	20.89	0.053
707	D	45	24.9	11.5	487.0	114.7	6.69	0.058
714	D	50	40.9	14.9	1313.8	450.7	16.52	0.037
748*	D	40	37.8	11.9	1122.2	372.8	22.25	0.060
561*	ND	80	35.5	16.1	989.8	319.0	17.06	0.097
562*	ND	80	38.3	18.0	1152.1	385.0	37.24	0.097
572*	ND	100	44.7	17.3	1569.3	554.5	45.99	0.083
711	ND	90	46.5	15.2	1698.2	606.8	32.91	0.054
712	ND	80	59.4	14.4	2771.2	1042.8	93.33	0.089
713	ND	80	26.7	8.2	559.9	144.3	19.94	0.138
715	ND	100	45.8	14.1	1647.5	586.2	37.02	0.063
716	ND	80	43.8	14.9	1506.7	529.0	31.63	0.060
717	ND	100	41.7	15.2	1365.7	471.7	25.84	0.055
725*	ND	100	41.0	14.4	1320.3	453.3	23.03	0.051

Measurement of sap flow

Measurements of sap flow density were conducted throughout the study period at 15-min intervals using constant heat dissipation sensors (Granier 1985). The sensors consisted of a pair of 2 cm long stainless steel needles, each of them containing a copper-constantan thermocouple in the middle. These probes were inserted radially at breast height into the xylem after removing the bark, and covered with a reflective material to avoid solar radiation. Two sensors (north- and south-facing side of the trunk) were placed in each tree and averaged to account for azimuthal variation of sap flow within the trunk. Measurements made using single-point sensors were integrated to the entire xylem depth using measured radial profiles of sap flow by measuring it at six depths in the xylem using the heat field deformation (HFD) method (Nadezhdina et al. 2006) in three trees, during at least seven days per tree. This sap flow per unit sapwood area was also expressed on a leaf area basis (J_L) after estimation of tree leaf area using site-specific allometries

for Scots pine and accounting for seasonal variations of leaf area. More detailed information about sap flow measurements, the scaling to the tree level and temporal aggregation can be found in Poyatos et al. (2013).

Water potential measurements

Predawn (Ψ_{PD}; just before sunrise, 03:00-05:00 h, solar time) and midday (Ψ_{MD}; 11:00-13:00 h, solar time) leaf water potentials were measured once per month in June, July, August and November in 2012. On each sampling time, a sun-exposed twig from each tree was excised using a pruning pole and stored immediately inside a plastic bag with a moist paper towel to avoid water loss until measurement time, typically within 2 hours of sampling. Leaf water potentials were measured using a pressure chamber (PMS Instruments, Corvallis, OR, USA).

Measurement of xylem radius variations

Xylem radius variations were measured throughout the study period using point dendrometers consisting of linear variable displacement transducers (LVDTs; DG 2.5 Solartron Metrology, West Sussex, UK). LVDTs were mounted on metal frames following the design by Sevanto et al. (2005b) with some modifications. Briefly, the frame was held around the bole, just below the living tree crown, by two metal plates that were screwed ca. 20 cm above the measuring point. The frame was made of aluminium, except for the two rods parallel to the direction of the measured radius changes, which were made of Invar, a nickel-iron alloy with a low thermal expansion coefficient. Each frame held two LVDT sensors, placed ca. 30 mm apart from each other, one measured over bark radius changes (not used here) and the other one measured xylem radius changes (i.e., the sensor measuring tip was in contact with the xylem, since bark, phloem and cambium were removed before the installation). LVDTs measurements were taken every 30 s and the averages stored every 15 min in a datalogger (CR1000, Campbell Scientific Inc., Logan, US). Since natural expansion and contraction of the metal frame and sapwood occurs due to changes in air temperature, frame and sapwood temperatures were measured using thermocouples. We used these temperatures to account for thermal expansion of the frame and the sapwood using the linear expansion coefficients for the Invar rods (1.2×10^{-6} K^{-1}) and for Scots pine wood (7.9×10^{-6} K^{-1}, Sevanto et al. 2005a).

Estimation of stem water potential

We used within-day xylem radius variations to estimate changes in below-crown stem water potential. We first calculated the difference between the maximum stem radius within a day, which corresponds to the minimum shrinkage, and the instantaneous measurements of the xylem radius. This below-crown xylem radius difference (Δr_{bc}) quantifies the instantaneous shrinkage compared to maximum swelling conditions within a day, when stem water content is assumed to be in equilibrium with soil water potential.

We then used Δr_{bc} to calculate the corresponding water pressure difference (ΔP_{bc}), by dividing Δr_{bc} by the sapwood radius (r_{bc}), and multiplying it by the radial modulus of elasticity of wood (E_r), following the equation (Irvine and Grace 1997):

$$\Delta P_{\mathrm{bc}} = E_r \frac{\Delta r_{\mathrm{bc}}}{r_{bc}} \qquad \text{Equation 1}$$

We can assume that the osmotic potential in xylem sap is very low and unlikely to change over time, and therefore water pressure in the xylem can be used to estimate xylem water potential (Irvine and Grace 1997). ΔP_{bc} is thus equivalent to the difference between water potential at the LVDT location (under the living crown) and the soil, assuming that the xylem water potential under conditions of maximum swelling was in equilibrium with the soil.

We did not measure E_r for the trees in our study. A literature survey showed that values of E_r for Scots pine are variable across trees and populations, with values ranging between 0.03 and 7.89 GPa (Irvine and Grace 1997; Mencuccini et al. 1997; Perämäki et al. 2001). We applied a value of E_r (0.18 GPa) so that the maximum percentage of below-crown resistance to whole tree hydraulic resistance ($\%R_{bc}$) (observed during summer) was 100%. We can justify this assumption on the grounds that, under extreme drought conditions, it is expected that most of the hydraulic resistance is found belowground (Domec et al. 2009; Sperry et al. 2002). While this assumption should not affect the relative values of $\%R_{bc}$ over time or between trees, the absolute $\%R_{bc}$ values reported here are subject to high uncertainty and have to be considered with caution.

Sapwood radius was measured below the living crown, at each LVDT location. We extracted a core with a Pressler borer, put the core in paper bags and stored them in a portable cooler. Samples were then coloured with bromocresol green (Kutscha and Sachs 1962) in the laboratory to distinguish between sapwood and heartwood and measure their length.

Below-crown hydraulic resistance

We used the maximum daily values of sap flow ($J_{L,max}$) and stem pressure difference ($\Delta P_{bc,max}$) to calculate the below-crown hydraulic resistance (R_{bc}):

$$R_{bc} = \frac{\Delta P_{bc,max}}{J_{L,max}} \qquad \text{Equation 2}$$

The percent contribution of below-crown resistance to whole-tree hydraulic resistance ($\%R_{bc}$) was calculated by comparing the water pressure difference (ΔP_{bc}) measured with LVDTs and the leaf water potential difference ($\Delta\psi$; ψ_{MD} minus ψ_{PD}) when both measurements were taken on the same day (Irvine and Grace 1997):

$$\%R_{bc} = \frac{\Delta P_{bc}}{\Delta\psi} 100 \qquad \text{Equation 3}$$

We assumed that pines reached equilibrium with the soil during night and, as a consequence, ψ_{PD} is an estimate of soil water potential (Irvine et al. 2004), that corresponded to the maximum stem radius within a day.

Data analysis

The analyses of ΔP_{bc}, R_{bc}, and J_L relied on having reliable data of both sap flow and xylem radius variations measured simultaneously. However, due to technical problems mostly related to power failures due to the remote location of the sampling site, we had to select periods with good quality data for the analyses. We selected representative periods within three different seasons of year 2012 showing contrasted characteristics of soil water content: winter (from day 53 to day 78), spring (days 145 to 164) and summer (days 224 to day 248). Note that for these periods we did not always have usable data from the four trees per defoliation class.

Linear mixed-effects models were fitted to test for statistical differences between defoliation classes (defoliated or non-defoliated) and season (winter, spring or summer) on the response of R_{bc}, $\%R_{bc}$, ψ_{PD}, ψ_{MD} and $\Delta\psi$. Measurements of ψ in June and August were considered as spring and summer seasons, respectively. Winter measurements of ψ were not available and, thus, models for $\%R_{bc}$ and ψ did not include a winter season. To test the effects of vapour pressure deficit (VPD), soil water content (SWC) and defoliation class on ΔP_{bc} and $\%R_{bc}$ we fitted similar linear mixed-effects models including a quadratic term in the case of the relationships with VPD or log-transforming SWC, in order to account for nonlinear responses. In all mixed models, tree identity

was included as a random factor. R_{bc} and ΔP_{bc} were log-transformed and $\%R_{bc}$ square root transformed to achieve normality prior to all analyses. In all cases, we started by fitting the most complex, biologically plausible model and then this model was compared with all the alternative and simpler models resulting from different combinations of explanatory variables. We selected the simplest model from all those models that were within 2 AICc units of the best-fitting one, which were considered equivalents in terms of fit. All statistical analyses were carried out using the R Statistical software version 3.3.1 (R Core Team, 2016), using the "lme" function to fit mixed-effects models, and the "dredge" function ("MuMIn" package) to compare models.

4.3. Results

Seasonal course of sap flow for the complete set of trees

The patterns of sap flow per unit leaf area (J_L) measured in all defoliated and non-defoliated Scots pine trees from our whole study population (Figure 1) were higher in defoliated trees relative to non-defoliated ones throughout the study period, especially in late spring and early summer. With the beginning of summer drought, J_L strongly decreased in both defoliated and non-defoliated pines, though this response was more acute in the former. Winter, spring and summer periods selected in Figure 1 are representative of different values of J_L and environmental conditions in year 2012.

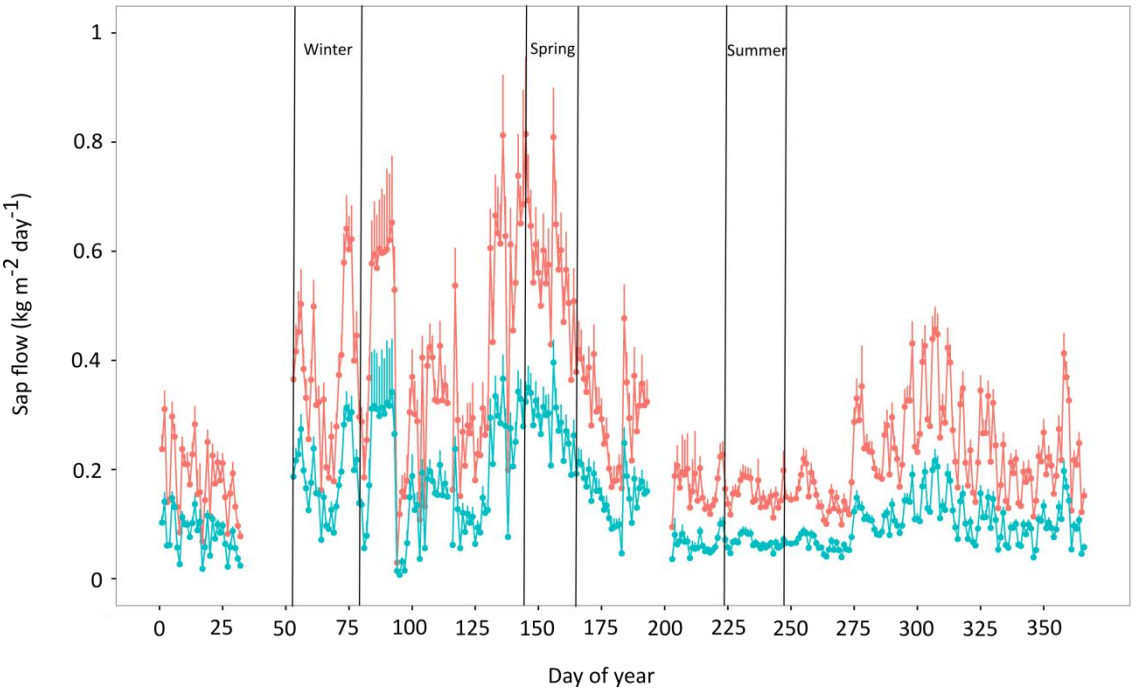

Figure 1. Seasonal course of daily-averaged sap flow per unit leaf area (J_L) over year 2012 in defoliated (red) and non-defoliated (blue) Scots pine trees. Error bars indicate + 1SE. Periods selected for the present paper, representative of different seasons, are indicated by vertical bars.

Seasonal courses of sap flow, leaf water potentials and stem pressure difference of the target trees

In Figure 2 we show the measurements of J_L and stem pressure difference (ΔP_{bc}) for the four defoliated and four non-defoliated Scots pines with available data for the selected winter, spring and summer periods (see Materials and Methods section). Throughout these seasons, climatic conditions were typical of the Mediterranean climate, with highest evaporative demands (maximum VPD of 3.86 kPa) and lowest soil water contents (minimum SWC of 0.08 m^3 m^{-3}) during summer (Figure 2). J_L for these trees followed the same patterns as the full set of measured trees (Figure 2), with higher J_L in defoliated trees over all periods, and an acute reduction of J_L in both defoliation classes in summer (Figure 2).

The temporal dynamics of ΔP_{bc} generally followed the course of J_L, and ΔP_{bc} was higher in defoliated pines over winter and spring (Figure 2). However, both defoliated and non-defoliated Scots pines showed similar ΔP_{bc} values in summer (Figure 2). Within periods, we sometimes observed different responses of J_L and ΔP_{bc} to variations in VPD and SWC. For example, in winter, J_L seemed to be comparatively more responsive than ΔP_{bc} to VPD increases from DOY 68 to DOY

73, especially in defoliated pines. In spring, J_L appeared to decline, tracking the variation in SWC, while ΔP_{bc} showed an increasing trend with time.

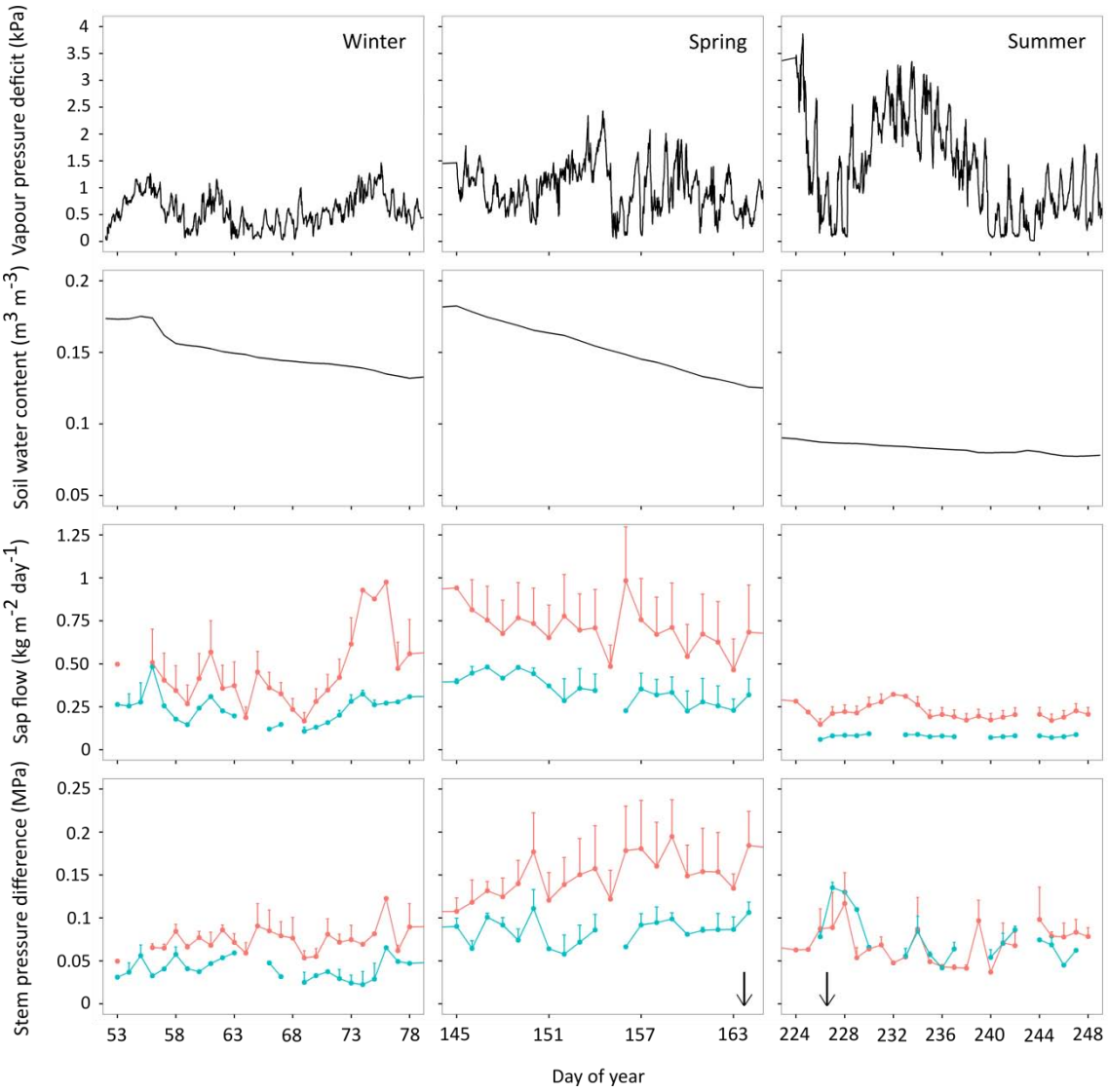

Figure 2. Seasonal course of daily vapour pressure deficit (VPD) and soil water content (SWC), and daily-averaged sap flow per unit leaf area (J_L) and stem pressure difference (ΔP_{bc}) in defoliated (red) and non-defoliated (blue) Scots pine trees for three seasons studied in 2012. Error bars indicate + 1SE. Arrows in the lower panel indicate sampling dates of leaf water potentials.

Ψ_{PD} measurements of the four defoliated and non-defoliated Scots pines showed similar values between defoliation classes, but significant differences between seasons, with lower values in summer (Figure 3, Table 1). In contrast, Ψ_{MD} showed differences between defoliation classes, with lower values for defoliated trees, but no season effect (Figure 3, Table 1). On the other hand, the interaction between season and defoliation was significant for $\Delta\psi$, indicating that the water potential difference was highest for defoliated trees in spring, and similarly low for all the other combinations of season and defoliation class (Figure 3, Table 1).

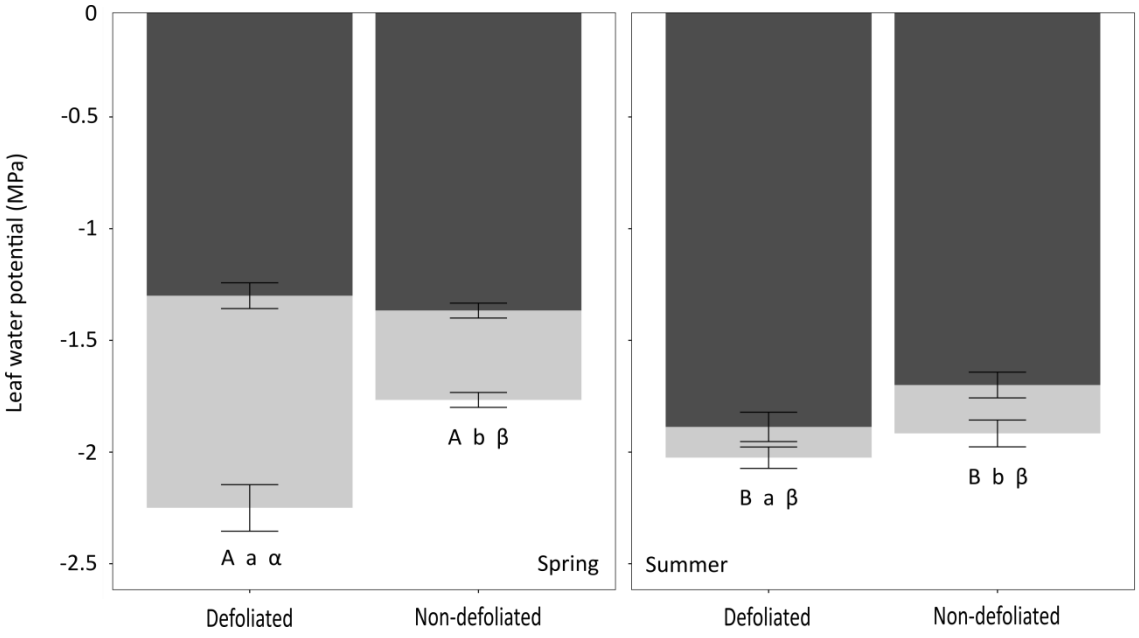

Figure 3. Daily averages of predawn (ψ_{PD}; dark grey) and midday (ψ_{MD}; light grey) leaf water potential measurements in defoliated and non-defoliated Scots pine trees in spring and summer 2012. Different uppercase letters indicate significant differences ($P < 0.05$) between predawn measurements, different lowercase letters indicate significant differences between midday measurements and different Greek letters indicate significant differences in the water potential difference between predawn and midday ($\Delta\psi$) across defoliation classes and seasons. Error bars indicate ± 1SE.

Table 1. Summary of the fitted linear mixed models with predawn (ψ_{PD}), midday (ψ_{MD}) leaf water potentials and their difference ($\Delta\psi$) as response variables.

Parameter	**ψ_{PD}**	**ψ_{MD}**	**$\Delta\psi$**
	R^2 = 0.82	**R^2 = 0.50**	**R^2 = 0.87**
Intercept	-1.33 ± 0.05***	-2.14 ± 0.06***	-0.95 ± 0.08***
Non-defoliated	ni	0.30 ± 0.09*	0.55 ± 0.12**
Summer	-0.48 ± 0.07***	ni	0.81 ± 0.11***
Non-defoliated:Summer	ni	ni	-0.63 ± 0.17*

For factors, the coefficients indicate the difference between each level of a given variable and the corresponding reference level ("Defoliated" for defoliation class and "spring" for season). The values are the coefficient estimates ± 1SE. Abbreviations: *0.01 < *P* < 0.05; **0.001 < *P* < 0.01; ****P* < 0.001; ni, not included in the model. Conditional R^2 values are given for each model.

Seasonal course of below-crown hydraulic resistance and its percent contribution to whole-tree hydraulic resistance

Below-crown hydraulic resistance (R_{bc}) increased from winter to summer for both defoliation classes (Figure 4, Table 2). Although defoliated and non-defoliated Scots pine trees presented similar levels of R_{bc} in winter and spring, the summer increase in R_{bc} was comparatively larger for non-defoliated Scots pine trees (Figure 4, Table 2). Despite this difference in the seasonal changes in R_{bc} with defoliation class, we did not find any significant difference in R_{bc} between defoliation classes within any of the three study periods ($P > 0.05$) (Figure 4, Table 2).

The percent contribution of below-crown hydraulic resistance to whole-tree hydraulic resistance (%R_{bc}) increased in summer for both defoliated and non-defoliated Scots pine trees relative to spring (Figure 4, Table 2). Within seasons, the response of %R_{bc} was similar between defoliation classes (Figure 4, Table 2), though non-defoliated pines tended to show a greater increase in %R_{bc} in summer (not significant).

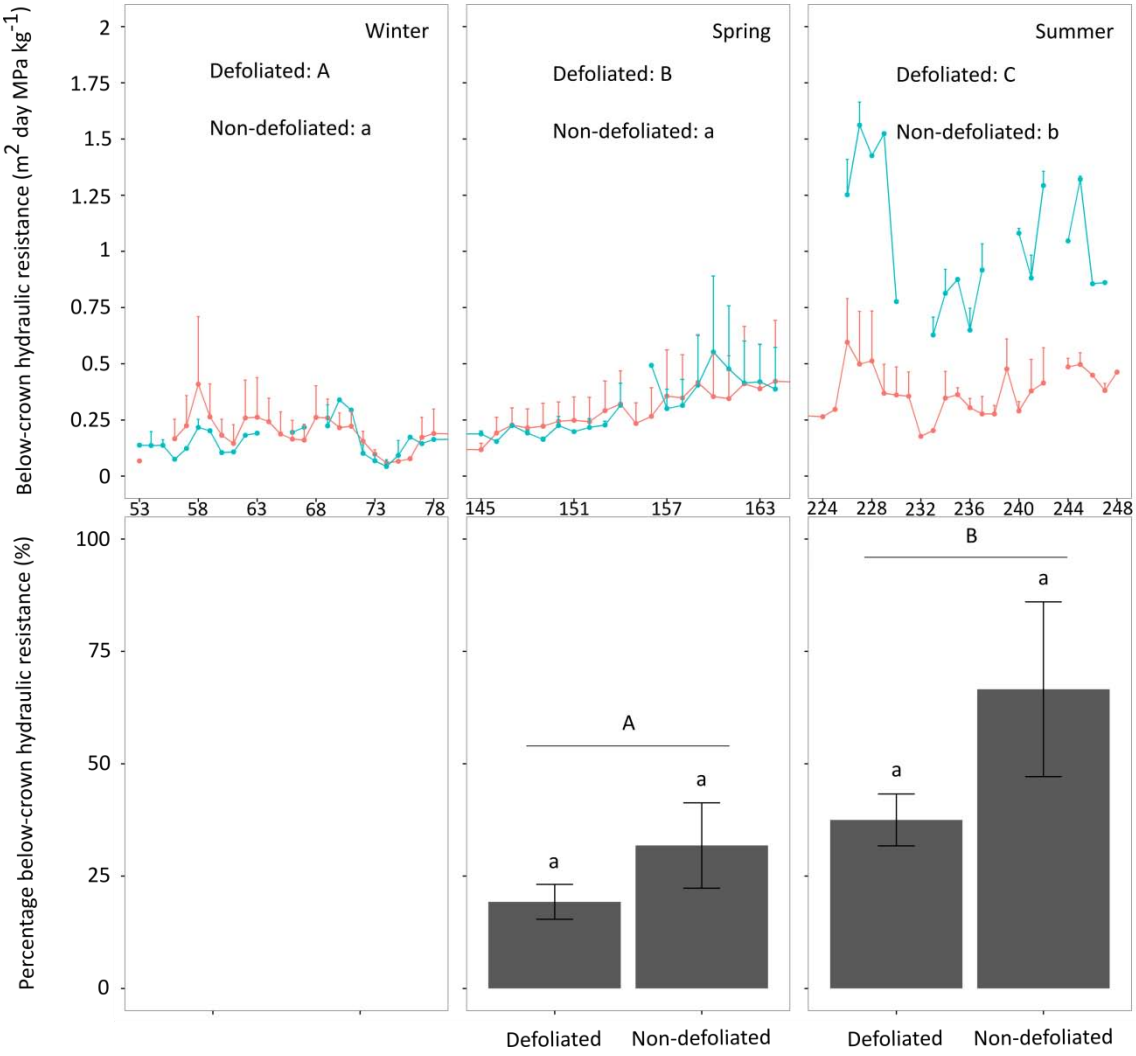

Figure 4. Upper panels: seasonal course of daily averages of below-crown hydraulic resistance (R_{bc}) in defoliated (red) and non-defoliated (blue) Scots pine trees over the three seasons studied in 2012. Different letters indicate significant differences ($P < 0.05$) between seasons within a given defoliation class. Error bars indicate + 1SE. Lower panels: percent contribution of below-crown resistance to whole-tree hydraulic resistance (%R_{bc}). Different uppercase letters indicate significant differences ($P < 0.05$) between seasons, and different lowercase letters indicate significant differences between defoliation classes within a given season. Error bars indicate ± 1SE. Note that we did not measure leaf water potentials in winter, so we could not estimate %R_{bc} for this season.

Table 2. Summary of the fitted linear mixed models with below-crown hydraulic resistance (R_{bc}) and the percent contribution of below-crown hydraulic resistance to whole-tree hydraulic resistance (%R_{bc}) as response variables.

Parameter	**log(R_{bc})**	**sqrt(%R_{bc})**
	R^2 = 0.87	**R^2 = 0.84**
Intercept	-1.62 ± 0.41***	4.21 ± 0.55**
Non-defoliated	-0.41 ± 0.59 (ns)	1.56 ± 0.78 (ns)
Spring	0.33 ± 0.09***	
Summer	1.28 ± 0.09***	2.1 ± 0.56*
Non-defoliated:Spring	-0.04 ± 0.14 (ns)	ni
Non-defoliated:Summer	0.60 ± 0.14***	ni

For factors, the coefficients indicate the difference between each level of a given variable and its reference level ("Defoliated" for defoliation class and "winter" for season, except for %R_{bc} where the reference season was "spring"). The values are the coefficient estimates ± 1SE. Abbreviations: ns, no significant differences; **0.001 < P < 0.01; ***P < 0.001; ni, not included in the model. Conditional R^2 values are given for each model.

Responses of stem pressure difference and below-crown hydraulic resistance to vapour pressure deficit and soil water content

We did not find any significant differences (P > 0.05) between defoliated and non-defoliated Scots pine trees in the response of ΔP_{bc} to VPD, with both defoliation classes showing similar parabolic response (Figure 5, see Table S1 available in Supplementary Material 3). On the contrary, ΔP_{bc} of defoliated and non-defoliated Scots pine trees responded differently to SWC (Figure 5, see Table S1 available in Supplementary Material 3), with a greater sensitivity of ΔP_{bc} to SWC in defoliated pines, thus having larger reduction of ΔP_{bc} with decreasing SWC than non-defoliated trees. This is consistent with the strongest decline of $\Delta\psi$ in defoliated pines between spring and summer (Figure 3).

R_{bc} of defoliated and non-defoliated pines increased as summer drought progressed (with increasing VPD and depletion of soil water, more clearly for the latter), and these responses were significantly different in defoliated and non-defoliated Scots pine trees (Figure 5, see Table S1 available in Supplementary Material 3). R_{bc} in non-defoliated pines was more sensitive to the depletion of soil water content, leading to higher R_{bc} at low levels of SWC, compared to defoliated Scots pines (Figure 5, see Table S1 available in Supplementary Material 3).

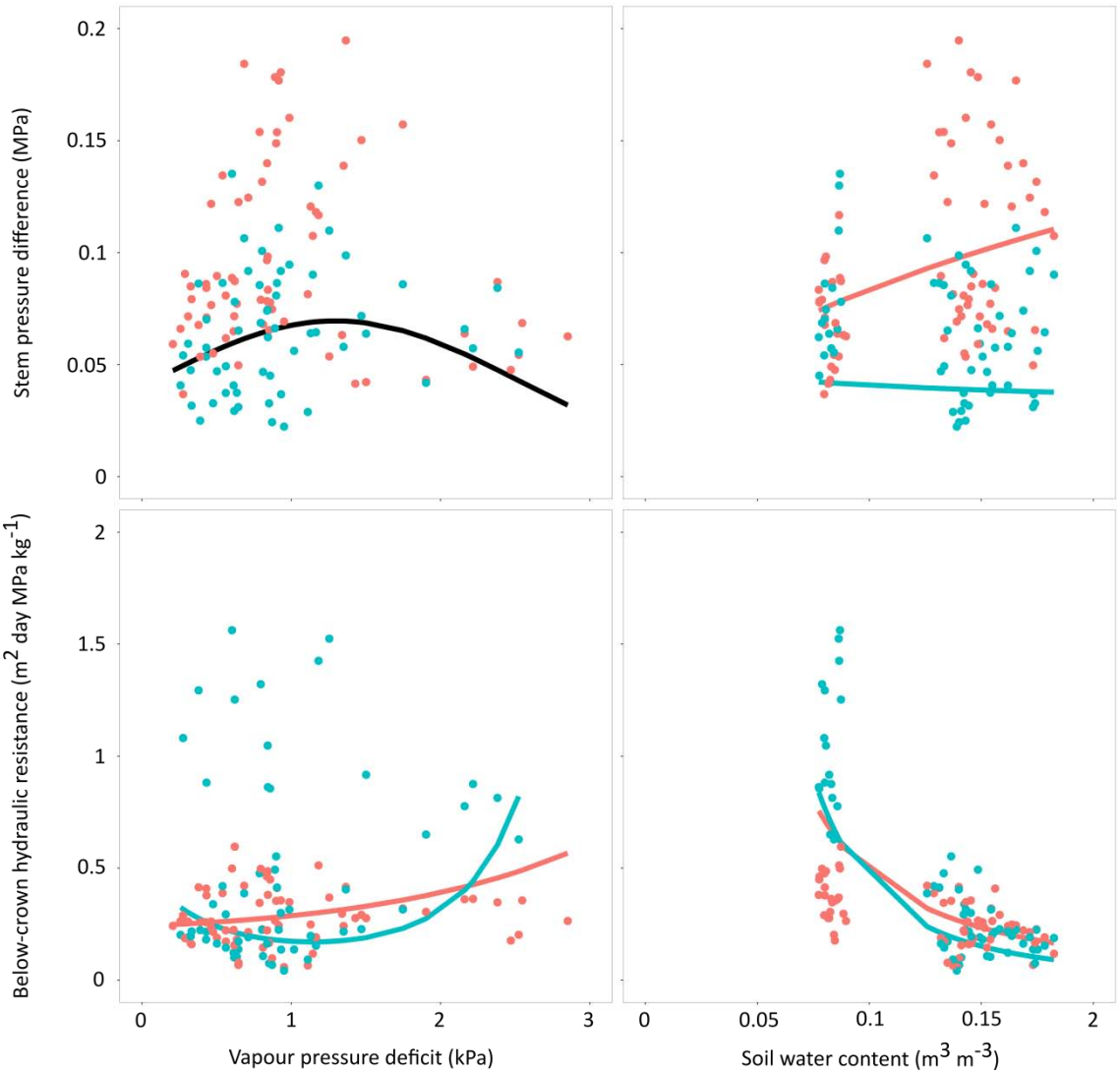

Figure 5. Responses of stem pressure difference (ΔP_{bc}) and below-crown hydraulic resistance (R_{bc}) to vapour pressure deficit (VPD) and soil water content (SWC) in seasons studied in 2012. Daily averages for defoliated (red) and non-defoliated (blue) Scots pine trees are shown. Standard errors are not displayed to ensure clarity. Regression lines depict the models shown in Table S1.

4.4. Discussion

Our study area experienced the second driest growing season since 1951 (133.9 mm of rainfall in May-October 2012), which followed the driest growing season on record (Poyatos et al. 2013). Drought conditions during summer 2012 were enhanced by occasionally high values of VPD (Figure 2; see also Salmon et al. 2015). In terms of the overall sap flow responses in the studied Scots pine population, defoliated Scots pine trees showed a more pronounced sap flow decrease in summer, concomitant with soil water depletion (Figure 1) and consistent with the patterns observed in the previous two years (Poyatos et al. 2013). The target trees in this study also behaved similarly (Figure 2). For these trees, the seasonality of leaf water potential measurements (Figure 3) was largely consistent with that reported in previous years within the same population (Poyatos el al. 2013), with only slight differences. Here we found lower values of ψ_{MD} in defoliated pines in spring and summer, and both defoliation classes presented homeostasis in ψ_{MD} between seasons. In contrast, ψ_{PD} measurements showed a similar decrease from spring to summer, for both defoliation classes, tracking the depletion in soil water content. We did not detect differences in ψ_{PD} between defoliation classes within seasons, and albeit these differences were indeed observed in other periods, they were small in magnitude (Poyatos et al. 2013).

Drought increases below-crown hydraulic resistance and its contribution to whole-tree resistance

As hypothesised, below-crown hydraulic resistance (R_{bc}) increased in both defoliated and non-defoliated Scots pine trees as drought progressed (Figure 4). In our study, R_{bc} includes the whole trunk, the root system and the rhizosphere, but we can assume that the trunk will probably contribute little to variations in hydraulic resistance of this below-crown component, compared to the roots and the rhizosphere (Domec et al. 2009; Johnson et al. 2016; McCulloh et al. 2014). We observed increases in R_{bc} with declining soil water content, which were especially strong under very dry conditions (Figure 5), consistent with the decrease in root hydraulic conductance observed in *Pinus taeda* L. (Domec et al. 2009). We also found that R_{bc} tended to increase with VPD, in contrast with the increase of below-ground conductance (i.e., decrease in resistance) with increasing evaporative demand reported for a mesic Scots pine population (Martínez-Vilalta et al. 2007). This discrepancy may be associated to the fact that in the present study periods with high VPD were associated with low soil water content, and may reflect the fact that different mechanisms may be causing the variation in below-ground (or below-crown, in our case)

hydraulic conductance. For example, in the study by Martínez-Vilalta et al. (2007), soil water conditions were probably not limiting and roots did not experience much decline in hydraulic conductance.

We also showed that the percentage contribution of below-crown to whole-tree hydraulic resistance (%R_{bc}) increases with severe drought in Scots pine (Figure 4). Although the absolute values of %R_{bc} should be taken with caution because of the use of approximated values for the radial modulus of elasticity (see Materials and Methods), our results imply that constraints on below-ground water transport increase with drought comparatively more than aboveground limitations. Taken together, the observed patterns in R_{bc} and %R_{bc} highlight the dynamic nature of belowground hydraulics in forests experiencing drought-induced decline processes.

One possible factor contributing to the increase in R_{bc} could be the role of the rhizosphere, the narrow soil layer that is in tight contact with the roots. This layer influences tree water uptake through soil texture itself (Bristow et al. 1984) and determines the water potential gradient between soil and roots during soil water depletion (Newman 1969; Sperry et al. 2002). Increased resistance of the soil-root interface have been reported in pines under extreme drought, and has been associated with lower ψ_{PD} compared to ψ_{MD} (Plaut et al. 2012), with reduced sap flow responses to precipitation pulses (Plaut et al. 2013) or with higher ψ_{PD} compared to soil ψ (Pangle et al. 2015). In our study, ψ_{PD} measurements were always less negative than ψ_{MD}, but Scots pine sap flow recovered only partially after autumn rains (Figure 1; see also Poyatos et al. 2013). These results do not provide clear evidence for hydraulic isolation and suggest that in our case other constrains, involving for example fine root mortality (Bauerle et al. 2008; Espeleta et al. 2009), may underlie the changes in R_{bc} during drought.

Defoliation is not associated with drought-driven increases in below-crown hydraulic resistance

Our results do not support the hypothesis that defoliated trees would show stronger increases in R_{bc} during drought. On the contrary, non-defoliated trees showed larger increases in R_{bc} between spring and summer (Figure 4). These results are not entirely consistent with the differences in root vulnerability to embolism between defoliation classes reported in Aguadé et al. (2015). In that study, defoliated trees showed a significantly steeper decline of root hydraulic conductance with decreasing water potentials, but, at high ψ (> - 2MPa), roots of non-defoliated trees tended to show higher percent loss of conductivity (PLC). Assuming that ψ_{PD} represents root

water potential, the estimated variation in root PLC between spring (Non-defoliated, ψ_{PD}= -1.4 MPa, PLC = ~38 %; defoliated, ψ_{PD}= -1.3 MPa, PLC = ~36 %) and summer (Non-defoliated, ψ_{PD}= -1.7 MPa, PLC = ~40 %; defoliated, ψ_{PD}= -1.9 MPa, PLC = ~42 %) is at odds with the R_{bc} dynamics observed in Figure 4 of the present study. While the root embolism vulnerability curves suggest that PLC differences between defoliated and non-defoliated trees tend to decrease as ψ_{PD} tends to – 2 MPa, R_{bc} shows a significantly higher spring to summer increase in non-defoliated trees (Figure 4).

These differences in R_{bc} dynamics could be related to changes in below-ground components of the hydraulic pathway, other than root xylem. For example, soil water content at the study site was measured only at some locations, and hence these measurements did not reflect local soil water availability for each tree. During summer tree-level sap flow of defoliated trees is 60-70% of that of non-defoliated trees (Poyatos et al. 2013, see Table S2 available in Supplementary Material 3 Section). Higher tree transpiration of non-defoliated trees implies more intense soil water depletion, which could lead to locally reduced soil moisture and increased hydraulic resistances in the soil and the rhizosphere. Aquaporins, the integral membrane proteins conducting water in and out of the cells (Maurel et al. 2008) could have also played a role in modifying extra-xilematic components of root hydraulic conductance (Aroca et al. 2012; Vandeleur et al. 2009). Upregulation of aquaporin activity has been reported to occur during extreme drought (Johnson et al. 2014) and it may have contributed to minimise the summer increase in R_{bc} of defoliated pines. Although there is evidence that defoliation may be related to increased aquaporin expression in leaves and roots (Liu et al. 2014), it is unclear whether aquaporin-mediated reductions in root hydraulic resistance may explain differences in R_{bc} dynamics between defoliation classes under drought.

Below-ground hydraulic constraints in the context of the whole-plant physiology in declining Scots pine

We did not find evidence for increased impairment of below-ground water transport in defoliated Scots pine under drought conditions. Increased R_{bc} during drought was not associated to defoliation and cannot explain the larger declines in whole-plant hydraulic conductance of defoliated pines during drought (Poyatos et al. 2013). Minimising drought-driven increases in R_{bc} may have contributed to the higher gas exchange rates observed in defoliated pines during summer (Salmon et al. 2015). Likewise, we observed near-constant values of ΔP_{bc} with varying soil

water content in non-defoliated pines (Figure 5), which is consistent with their more isohydric behaviour compared to defoliated pines (Salmon et al. 2015), which also showed a more variable ΔP_{bc} with varying soil water content (Figure 5). Overall, our results are largely consistent with a predominant role of carbon limitations in driving Scots pine drought-induced mortality (Aguadé et al. 2015; Galiano et al. 2011; Garcia-Forner et al. 2016b; Salmon et al. 2015). Defoliation promotes tree-level water saving during drought, but at the expense of reduced tree-level assimilation (Poyatos et al. 2013).

The fact that higher tree-level hydraulic sensitivity in defoliated pines is not explained by differences in below-ground hydraulics (Aguadé et al. 2015, this study) does not imply that below-ground processes are irrelevant during the mortality processes. At longer time scales it has been shown that, at least for saplings, increased below-ground biomass allocation enhances Scots pine survival (Garcia-Forner et al. 2016). What seems clear is that the need to maintain adequate NSC levels for a proper hydraulic and metabolic functioning of the plant (Dietze et al. 2014; Sala and Mencuccini 2014) appears to dominate the physiological response of defoliated pines (Salmon et al. 2015), as prioritising carbon acquisition at the expense of water loss seems to promote survival under extreme drought in this species (Garcia-Forner et al. 2016).

Implications for the physiological mechanisms of drought-induced tree mortality

We still know very little about the role of below-ground hydraulics on drought-induced tree mortality mechanisms, which mostly reflects the difficulty in measuring the relevant processes involved. Our study contributes to this topic by providing continuous, albeit indirect, estimates of below-crown hydraulic conductance during extreme drought in a Scots pine population suffering drought-induced decline. We did not find direct evidence of extensive root hydraulic impairment (Rodríguez-Calcerrada et al. 2016) associated with defoliation (and hence with increasing mortality risk). On the contrary, our results suggest a buffering of below-ground hydraulic constraints during summer drought in defoliated trees, which may be associated with lower tree-level water use and hence higher (local) water availability. Our measurements, however, integrate root and rhizosphere responses to drought. More detailed measurements would be needed to understand how drought-driven changes in different components of below-ground hydraulics, including as the dynamics of shallow and deep roots (Grossiord et al. 2016; Johnson et al. 2014) and soil-root interfaces, affect tree survival under extreme drought.

Chapter 5

Comparative drought responses of *Quercus ilex* L. and *Pinus sylvestris* L. in a montane forest undergoing a vegetation shift[1]

Aguadé, D., Poyatos, R., Rosas, T. and Martínez-Vilalta, J.

[1]Published in *Forests* (DOI: 10.3390/f6082505)

Abstract

Different functional and structural strategies to cope with water shortage exist both within and across plant communities. The current trend towards increasing drought in many regions could drive some species to their physiological limits of drought tolerance, potentially leading to mortality episodes and vegetation shifts. In this paper, we study the drought responses of holm oak (*Quercus ilex* L.) and Scots pine (*Pinus sylvestris* L.) in a montane Mediterranean forest where the former species is replacing the latter in association with recent episodes of drought-induced mortality. Our aim was to compare the physiological responses to variations in soil water content (SWC) and vapor pressure deficit (VPD) of the two species when living together in a mixed stand or separately in pure stands, where the canopies of both species are completely exposed to high radiation and VPD.

Scots pine showed typical isohydric behavior, with greater losses of stomatal conductance with declining SWC and greater reductions of stored non-structural carbohydrates during drought, consistent with carbon starvation being an important factor in the mortality of this species. On the other hand, holm oak trees showed a more anisohydric behavior, experiencing more negative water potentials and higher levels of xylem embolism under extreme drought, presumably putting them at higher risk of hydraulic failure. In addition, our results show relatively small changes in the physiological responses of holm oak in mixed vs. pure stands, suggesting that the current replacement of Scots pine by holm oak will continue.

Keywords: drought response, global change, holm oak, leaf conductance, non-structural carbohydrates, stomatal conductance, Scots pine, water potential

5.1. Introduction

Plants have different functional strategies to cope with drought and seasonal variations in water availability, including physiological (e.g., stomatal control) and structural acclimation (e.g., leaf area loss) (Chaves et al. 2002). However, ongoing climate change can potentially drive plants to their physiological limits of climate tolerance (Allen et al. 2010). The impacts of climate change on vegetation are likely to vary regionally and will result from a combination of stress factors, including elevated temperatures (Williams et al. 2012), reduction of rainfall (Dore 2005), and shifts in wildfire regimes (Grulke et al. 2008). Furthermore, the consequences of these new conditions will be modulated by biotic factors and direct human impacts on forests (e.g., management) (Linares et al. 2009; Zhang et al. 2015).

Different ways of classifying plant drought responses have been postulated. For instance, plants have been classified as drought-avoiders (i.e., species with deep roots) or drought-tolerant (i.e., species with high xylem embolism resistance) depending on the water potentials they experience (Chaves et al. 2002). A related classification differentiates between isohydric and anisohydric species depending on their degree of stomatal regulation in response to drought (Jones 1998; Tardieu and Simonneau 1998). From a hydraulic perspective, the isohydric strategy (which could be related to the aforementioned drought-avoiders) is characterised by an early stomatal closure during drought to limit water losses and prevent a drastic reduction of leaf water potential (McDowell et al. 2008). These plants have been hypothesised to be prone to suffer carbon starvation during a prolonged drought, since they cannot maintain assimilation and may not be able to meet sustained carbon demands (e.g., respiration) (McDowell et al. 2008). On the other hand, anisohydric species (related to the aforementioned drought-tolerant species) would show less strict stomatal control and more negative water potential during drought. It has been hypothesised that these plants would be more likely to suffer extensive embolism and, ultimately, hydraulic failure during an intense drought (McDowell et al. 2008).

In many ways, the dichotomy between iso-/anisohydric strategies underlies our current conceptual framework to explain plant responses to extreme drought. However, this dichotomy is controversial. First of all, plants do not necessarily fall into either category, but rather stomatal regulation lies within a spectrum of stomatal sensitivity to water potential (Klein 2014). Hence, there is a wide range of stomatal responses to drought and these physiological responses are generally coordinated with the tree's hydraulic architecture (Martínez-Vilalta et al. 2014). Furthermore, iso-/anisohydric behavior may vary within species as a function of environmental

conditions (Domec and Johnson 2012). In addition, the link between stomatal regulation and leaf water potential is likely to be more complex that previously realised, both because of the need to account for differences in the hydraulic properties of plants (e.g., the vulnerability to xylem embolism) (Martínez-Vilalta et al. 2014) and because of the different mechanisms of stomatal closure across species (Brodribb et al. 2014). A further complication in the study of plant responses to severe drought arises because water stress is triggered by both a reduction in soil moisture and an increase of the evaporative demand (vapour pressure deficit; VPD), and stomata regulation responds to both of them (Gollan et al. 1985). Despite the important role of the soil compartment in drought-induced decline (Bréda et al. 1993; Hartmann et al. 2013a), atmospheric dryness is also important in explaining drought-induced mortality processes (Eamus et al. 2013).

Water-limited woodlands frequently host coexisting species with contrasting drought responses (Quero et al. 2011). However, extreme and/or chronic drought events outside of the historic range experienced by the local community can affect species differentially, potentially altering competitive relationships and causing vegetation shifts (Allen and Breshears 1998; Galiano et al. 2010; McDowell et al. 2008) (however, see Lloret et al. 2012). However, most of our knowledge on species-specific drought-responses and physiological thresholds is based on studies on potted plants or small trees under experimental conditions (Anderegg et al. 2012b; Filella et al. 1998), which may not represent the true responses of mature forest trees. On the other hand, drought conditions experienced by a tree within a forest depend on its exposure to the atmosphere, which may change dramatically during a die-off event (i.e., an understorey tree may suddenly be exposed to much higher radiation and VPD). In general, species whose leaves are more exposed to the atmosphere would respond differently to VPD than those in the understorey, especially under drought conditions (Holmgren et al. 2012). For an understorey species to become dominant in the canopy as a result of a drought event, it is required that the formerly dominant species dies off but also that the species initially in the understorey is able to cope with new, more exposed, conditions.

Scots pine (*Pinus sylvestris* L.) and holm oak (*Quercus ilex* L.) coexist in montane Mediterranean forests, where the latter species frequently grows in the understorey of a pine canopy. However, these two species have different geographical distributions and contrasted physiological strategies to cope with drought (Martin-StPaul et al. 2013; Poyatos et al. 2007). Scots pine is distributed from Siberia to the Mediterranean basin, with the Iberian Peninsula being the southwestern limit of its range. On the contrary, holm oak is restricted to the Mediterranean basin. When studied separately, both species are considered relatively isohydric, since they close

stomata at moderately high water potentials. This is particularly true for Scots pine, which has been shown to reduce stomatal conductance and sap flow, as well as leaf area, dramatically during dry periods (Irvine et al. 1998; Poyatos et al. 2013). Consistent with this behaviour, low levels of carbohydrate reserves during drought have been associated with increased mortality risks in this species (Aguadé et al. 2015; Galiano et al. 2011), in agreement with the carbon starvation hypothesis (McDowell et al. 2008). Although holm oak tends to operate at lower (more negative) water potentials than Scots pine, it appears relatively isohydric compared to many of the species with which it coexists (Barbeta et al. 2012; Martínez-Vilalta et al. 2003) and carbohydrate reductions associated with drought-induced mortality have also been documented in this species (Galiano et al. 2012). Scots pine and holm oak species coexist in some forests of the northern Iberian Peninsula, where both of them have suffered drought-related die-off episodes in recent years (Martínez-Vilalta and Piñol 2002; Ogaya et al. 2015). However, where the two species coexist mortality seems to preferentially affect Scots pine, which has led to the hypothesis that holm oak may end up replacing Scots pine as the canopy-dominant species (Galiano et al. 2010; Vilà-Cabrera et al. 2013). It remains to be established, however, whether holm oak individuals that formerly occupied the understorey will be able to cope with increased drought conditions as they become more exposed to high radiation and VPD.

In this study, we compare the physiological responses of coexisting Scots pine and holm oak trees to two major components of drought: vapour pressure deficit (VPD) and soil water content (SWC), both in pure and mixed stands, in an area where Scots pine has been affected by drought-induced mortality (Aguadé et al. 2015; Martínez-Vilalta and Piñol 2002; Poyatos et al. 2013) and where this species is being replaced by holm oak as the canopy-dominant species (Vilà-Cabrera et al. 2013). An important aspect of this study is that, unlike much previous work comparing conifers with angiosperms, it compares species with the same leaf habit. We hypothesise that (1) Scots pine would close stomata at higher (closer to zero) water potentials than holm oak and, therefore, it would experience lower losses of xylem hydraulic conductivity and greater reductions of NSC concentrations during drought, and (2) holm oak would suffer higher water stress in pure stands than in mixed ones, limiting the capacity of holm oak to become the canopy-dominant species in the long term.

5.2. Materials and Methods

Study site

Measurements were conducted at the Poblet Forest Natural Reserve (Prades Mountains, NE Iberian Peninsula). The climate is typically Mediterranean, with a mean annual precipitation of 664 mm (spring and autumn being the rainiest seasons, and with a marked summer dry period), and moderately warm temperatures (11.3°C on average) (Poyatos et al. 2013).

Most of the studied Scots pine (*Pinus sylvestris* L.) and holm oak (*Q. ilex* ssp. *ilex* L.) trees are located in the Tillar Valley (41°19'N, 1°00' E; 990–1090 m asl) on NW- or NE-facing hillsides with very shallow and unstable soil due to the high stoniness and steep slopes (35° on average). The soils are mostly Xerochrepts with fractured schist and clay loam texture, although outcrops of granitic sandy soils are also present. The canopy-dominant tree species at this site is Scots pine, while the understorey is mainly dominated by holm oak trees. Phenologically, both species show similar behavior in the Tillar Valley. In Scots pine, stem radial growth starts in mid-April and finishes in June (with maximum growth rates throughout May) (R. Poyatos, unpublished). Moreover, leaf flushing starts in May and leaf expansion finishes in June in Scots pine (R. Poyatos, unpublished) and in holm oak (Ogaya and Peñelas 2004). Holm oak in the Prades Mountains does not normally present leaf flushing during autumn (Ogaya and Peñelas 2004).

The study area has been affected by severe droughts since the 1990s and drought-induced mortality of Scots pine has been reported (Hereş et al. 2012; Martínez-Vilalta and Piñol 2002). Scots pine average standing mortality and crown defoliation in Tillar Valley are currently 12% and 15%, respectively. In some parts of the forest standing mortality is > 20% and cumulative mortality is as high as 50% since the year 2000 (J. Martínez-Vilalta, unpublished). In addition, Scots pine recruitment is extremely low and, as a result, holm oak is replacing Scots pine as the canopy-dominant species in many parts of the valley (Vilà-Cabrera et al. 2013).

Sampling scheme

Three different stand types were sampled in the Tillar valley: 1) a pure stand where holm oak is the canopy dominant species; 2) a mixed stand where both species grow together (Scots pine generally dominating the canopy and holm oak dominating the undergrowth but also constituting the main canopy where Scots pine mortality patches occur), and 3) a pure Scots pine stand

located at a more elevated and wetter location without any symptoms of drought-induced mortality. All measurements were carried out on mature trees, and all trees of the same species had a similar height and diameter at breast height (DBH) to minimise unwanted variation (Table 1). The holm oak pure stand was < 50 m from the mixed stand (both at 1015 m asl) and the Scots pine pure stand was ca. 800 m up the valley (1065 m asl). Soil depth was ~40 cm on average in mixed and pure holm oak stands and deeper (~74 cm) in the pure Scots pine stand. The main stand characteristics are summarised in Table 1. Seasonal dynamics of predawn (ψ_{PD}) and midday (ψ_{MD}) leaf water potentials, whole-tree leaf-specific hydraulic conductance ($K_{S\text{-}L}$), stomatal conductance ($G_{s,md}$), and percentage loss of xylem embolism (PLC) were measured or estimated on trees from all stand types. These measurements, in combination with a continuous monitoring of the main meteorological variables and soil moisture, were carried out from 2010 until 2013 (see Figure S1 available in Supplementary Material 4 Section), and included an exceptionally intense drought in 2011 (Poyatos et al. 2013). Volumetric soil water content (SWC) was measured in the upper 30 cm of soil at each stand using several (n = 3–6) frequency domain reflectometers (CS616, Campbell Scientific Inc., Logan, UT, USA; cf. Poyatos et al. 2013). Meteorological variables, including VPD estimates, were measured in the mixed stand (cf. Poyatos et al. 2013 for additional details) and were assumed to be representative of above-canopy atmospheric conditions for all the stands.

Table 1. Main characteristics (mean ± SE) of the three stands studied in the Tillar valley.

Variable	Holm oak Pure	Mixed	Scots pine Pure
Stand level			
Stem density (stems·ha^{-1})			
Scots pine	65 (66% def.)	257 (41% def.)	428
Holm oak	5262	2913	285
Other	87	242	326
TOTAL	5414	3412	1039
DBH (cm)			
Scots pine	23.60 ± 7.66	27.70 ± 3.08	32.30 ± 1.38
Holm oak	8.76 ± 0.30	8.40 ± 0.40	5.89 ± 0.85
Basal area (m^2 ha^{-1})			
Scots pine	3.44 (96% def.)	23.79 (52% def.)	41.75
Holm oak	40.63	24.86	0.99
Other	0.48	2.9	1.65
TOTAL	44.55	51.55	44.39
Leaf area index (m^2 m^{-2})			
Scots pine	nm	0.58	0.91
Holm oak	4.59	2.69	nm
TOTAL	4.59	3.27	1.02
Measured trees			
A_L:A_S (m^2 cm^{-2})			
Scots pine	nm	0.076 ± 0.008	0.067 ± 0.004
Holm oak	0.167 ± 0.001	0.139 ± 0.008	nm
DBH (cm)			
Scots pine	nm	38.60 ± 1.81	39.90 ± 0.89
Holm oak	12.61 ± 1.03	16.21 ± 1.58	nm
Height (m)			
Scots pine	nm	14.24 ± 0.78	18.3 ± 0.62
Holm oak	~5	~5	nm

DBH, diameter at breast height; A_L:A_S, leaf-to-sapwood area ratio at the tree level; nm, not measured; def., percentage of defoliated pines of total Scots pine stem density and basal area is indicated in brackets.

Non-structural carbohydrates (NSC) measurements on Scots pine were conducted in 2012 on trees from the mixed and pure stands at Tillar Valley (cf. below for specific methods).

The dynamics of NSC in holm oaks were studied, also in 2012, in a nearby area (Torners Valley; 41°21′ N, 1°2′ E; 990 m asl) within less than 3 km of the sampling area at the Tillar valley. Average DBH for these holm oak trees was 19.02 ± 1.99 cm. The two valleys sampled in this study have similar substrate and soil characteristics, but they differ in aspect and vegetation cover. The south-facing orientation at Torners is associated with a lower-statured forest dominated by holm

oaks, and accompanied by other drought-tolerant species such as *Phillyrea latifolia* L. and *Arbutus unedo* L. Holm oaks from this valley, like Scots pine in Tillar Valley, have also experienced some episodes of drought-induced decline (Ogaya et al. 2015). Although some of the sampled trees are part of a long-term drought simulation study (Ogaya and Peñelas 2004), here we only considered trees sampled outside the experimental area or in the control stands.

Only non-defoliated Scots pine and holm oak trees were chosen for this study. All studied variables and the years of each measurement are summarised in Table 2. The detailed methodologies used to measure each variable are described in Poyatos et al. (2013), Rosas et al. (2013), and Aguadé et al. (2015) and are summarised in the following sections. The trees included in this study partially overlap with those included in the previous references, although we also include unpublished measurements for pure stands of Scots pine and for holm oak trees in the Tillar Valley.

Water potential measurements

Predawn (ψ_{PD}, MPa; just before sunrise, 03:00 h–05:00 h, solar time) and midday (ψ_{MD}, MPa; 11:00 h–13:00 h, solar time) leaf water potentials were measured monthly in 12 Scots pine and nine holm oak trees from Tillar Valley, from June to November in different years (Table 2). On each sampling time, a sun-exposed twig from each tree was excised using a pruning pole and stored immediately inside a plastic bag with a moist paper towel to avoid water loss until measurement time, typically within 2 h of sampling. Leaf water potentials were measured using a pressure chamber (PMS Instruments, Corvallis, OR, USA).

We also calculated the water potential difference ($\Delta\psi$) between predawn and midday measurements in each tree, as an indicator of the driving force for transpiration.

Table 2. Main variables reported in this study.

Species	Valley	Stand type	ψ	G_s	$K_{S\text{-}L}$	NSC	PLC
Scots pine	Tillar	Mixed	8 [2010–2012] [1]	11 [2010–2013] [1]	8 [2010–2012] [1]	10 [2012] [2]	8 [2010–2012] [4]
Holm oak	Tillar	Mixed	5 [2010–2011] [4]	10 [2010–2013] [4]	5 [2010–2011] [4]		5 [2010–2011] [4]
Scots pine	Tillar	Pure	4 [2010–2011] [4]	10 [2010–2011] [4]	4 [2010–2011] [4]	10 [2012] [2]	4 [2010–2011] [4]
Holm oak	Tillar	Pure	4 [2010–2011] [4]	10 [2010–2011] [4]	4 [2010–2011] [4]		4 [2010–2011] [4]
Holm oak	Torners	Pure				19 [2012] [3]	

ψ, water potential; $G_{s,md}$, stomatal conductance; $K_{S\text{-}L}$, whole-tree leaf-specific conductance; NSC, non-structural carbohydrates; PLC, percentage loss of hydraulic conductivity due to xylem embolism. Number of trees sampled for each variable and years of measurements (in brackets) are provided for each combination of species, valley and stand type. Exponent numbers indicate references where data were gathered from: [1],(Poyatos et al. 2013); [2],(Aguadé et al. 2015); [3],(Rosas et al. 2013); [4], this study.

Sap flow and canopy stomatal conductance

Continuous measurements (at 15-min intervals) of sap flow density were conducted since the end of April 2010 and throughout the study period (Table 2) on 11 Scots pine and 10 holm oak trees from the mixed stand and 10 trees of both species from the pure stand (Table 2) in Tillar Valley using constant heat dissipation sensors. The sensors consisted of a pair of stainless steel needles, each of them containing a copper-constantan thermocouple at the middle. These probes were inserted radially at breast height into the xylem after removing the bark, and covered with a reflective material to avoid solar radiation. Two sensors (on the north- and south-facing sides of the trunk) with two cm long needles were placed in each Scots pine tree, and only one sensor with one cm long needles (north-facing side) were placed in holm oak trees due to their smaller diameters. Since sap flow is not uniform throughout the xylem, sap flow measurements made using single-point sensors installed in the outer sapwood were integrated to the entire xylem depth using measured radial profiles of sap flow. We obtained these radial profiles by measuring the sap flow at six depths in the xylem using the heat field deformation (HFD) method in three Scots pine and Holm oak trees, over at least seven days per tree. This sap flow per unit of sapwood area was also expressed on a leaf area basis after calculation of tree leaf area using site-specific allometries for Scots pine (Poyatos et al. 2013) and holm oak (Ogaya 2003) and accounting for seasonal variations of leaf area for each species (Ogaya and Peñelas 2004; Poyatos et al. 2013). More information about this experimental design, measurements, and scaling of sap flow to the tree level can be found in Poyatos et al. (2013).

Midday canopy stomatal conductance ($G_{s,md}$, mm s^{-1}) was calculated for all trees with sap flow sensors (Table 2), using midday (averaged between 11:00 h. and 14:00 h, thus minimising capacitance effects) measurements of sap flow per unit leaf area ($J_{L,md}$, kg m^{-2} s^{-1}) and the simplified Penman–Monteith equation for aerodynamically rough canopies:

$$G_{s,md} = \frac{\gamma \cdot \lambda \cdot J_{\mathrm{L,md}}}{\rho \cdot c_{\mathrm{P}} \cdot \mathrm{VPD}_{\mathrm{md}}} \qquad \text{Equation 1}$$

Here γ is the psychrometric constant (kPa K^{-1}), λ is the latent heat of vaporisation of water (J kg^{-1}), ρ is the air density (kg m^{-3}), c_p is the specific heat air at constant pressure (J kg^{-1} K^{-1}), and VPD_{md} is the midday vapour pressure deficit (kPa). Measurements obtained under conditions where $VPD_{md} < 0.1$ kPa were filtered out (Phillips and Oren 1998).

Whole-tree leaf-specific hydraulic conductance

We also used $J_{L,md}$ and ψ measurements to calculate whole-tree leaf-specific hydraulic conductance ($k_{S\text{-}L}$, kg m^{-2} MPa^{-1} s^{-1}), assuming that trees had reached equilibrium with the soil during the night, and that ψ_{PD} represents an estimate of soil water potential (Irvine et al. 2004). The following equation was used:

$$k_{S-L} = \frac{J_{L,md}}{\psi_{PD} - \psi_{MD}} \qquad \text{Equation 2}$$

In our analysis of $k_{S\text{-}L}$ responses to SWC and VPD we only considered $k_{S\text{-}L}$ values estimated for the spring and summer seasons (drought progression; cf. Figure S1 available in Supplementary Material 4 Section), as autumn values were shown not to recover even after substantial rainfall and despite relatively high SWC (Poyatos et al. 2013).

Percentage loss of hydraulic conductivity

An estimate of the percentage loss of conductivity (PLC) due to xylem embolism was calculated in those Scots pine and holm oak trees for which leaf water potentials had been measured (Table 2), using the following function (Pammenter and Van Der Willigen 1998):

$$PLC = \frac{100}{1+\exp\left(a(P-P_{50})\right)} \qquad \text{Equation 3}$$

In this equation, PLC is the percentage loss of hydraulic conductivity, P the applied pressure, P_{50} the pressure causing 50% PLC, and a is related to the slope of the vulnerability curve. P_{50} and a values were obtained from vulnerability curves established on roots and branches using the dehydration (holm oak; Martínez-Vilalta et al. 2002) and air-injection methods (Scots pine; Aguadé et al. 2015) for individuals from the same populations studied here. Values of P to estimate PLC were obtained from measured water potentials (ψ_{MD} for branch PLC and ψ_{PD} for root PLC). All sampling methods and vulnerability curve measurements are detailed in Aguadé et al. (2015) and Martínez-Vilalta et al. (2002). Since there is controversy regarding the best method for establishing vulnerability curves, particularly for species with long vessels such as holm oak, we also estimated PLC using the vulnerability curve coefficients (a and P_{50}) estimated in another study comparing several methods to establish vulnerability curves in holm oak (Martin-StPaul et al. 2014), which obtained higher embolism resistance than the study cited above (Martínez-Vilalta et al. 2002) that was conducted at our study site.

Non-structural carbohydrates

Twenty non-defoliated Scots pine trees (10 from mixed and 10 from pure stands) from the Tillar Valley and 19 holm oak trees from the Torners valley (Table 2) were selected for NSC measurements. Holm oak trees from the mixed stand were not sampled for NSC measurements. In this study we only consider measurements taken before the onset of the summer drought (June) and at the peak of the dry period (August). For Scots pine, we sampled leaves, branches, and roots and for holm oak we sampled leaves, branches, and lignotuber (Table 1). Scots pine roots and holm oak lignotuber were considered "belowground organs" in all analyses and stands of NSC data. Field and laboratory methods were identical in all cases; more detailed information of sampling design and NSC analyses can be found in Aguadé et al. (2015) and Rosas et al. (2013). Total non-structural carbohydrates (TNSC) were considered as including free sugars (glucose and fructose), sucrose and starch and were analysed following the procedures described by Hoch et al. (2002) with some minor variations (Galiano et al. 2011). Determination of soluble sugars (glucose, fructose, and sucrose) was carried out by an extraction of 12–14 mg of sample powder with 1.6 ml distilled water; after centrifugation, an aliquot of the extract was used for the determination of soluble sugars by enzymatic conversion of fructose and sucrose into glucose (invertase from *Saccharomyces cerevisae* Meyen ex E.C. Hansen, Sigma-Aldrich, Madrid, Spain) and glucose hexokinase (GHK assay reagent, I4504 and G3293, Sigma-Aldrich, Madrid, Spain). Another aliquot was incubated with an amyloglucosidase from *Aspergillus niger* van Tieghem at 50°C overnight, to break down all NSC (starch included) to glucose and then determined photometrically. Starch was calculated as total NSC minus low-molecular-weight sugars. All NSC values are expressed as percent dry matter.

In order to focus on the summer changes of NSC and starch during drought we only considered the differences of the concentrations between August and June in this study. This difference was calculated in two ways: as the absolute change ($\Delta NSC_{Aug\text{-}Jun}$ and $\Delta Starch_{Aug\text{-}Jun}$) or as the change relative to the initial (June) concentration ($\Delta NSC_{Aug\text{-}Jun,rel}$ and $\Delta Starch_{Aug\text{-}Jun,rel}$). These variables are likely to reflect both drought- and phenology-driven changes in NSC, but phenological effects are likely to be minimised because shoot and stem radial growth is already complete by the end of June (see Study site Section).

Data analysis

We used the R Statistical Software version 3.0.2 (R Core Team, 2013) for all statistical analyses. We performed linear mixed-effects models to test the differences between species (Scots pine and holm oak) and stand types (mixed or pure) in physiological response variables (ψ_{MD}, ψ_{PD}, $\Delta\psi$, $K_{S\text{-}L}$, PLC) to either SWC or VPD. For each physiological variable, separate models were fitted for SWC and VPD responses. Tree identity was included in all models as a random factor. PLC was log-transformed to achieve normality prior to all analyses. SWC was also log-transformed in some models (ψ_{MD}, ψ_{PD} and PLC) to better capture the functional relationship with the response variable. VPD was log-transformed in the PLC model for the same reason. To better represent the relationship between $\Delta\psi$ and SWC, we used a quadratic function. Linear mixed models were also used to assess differences in summer NSC variation as a function of species, organ (leaves, branches, and belowground) and stand type (as fixed effects). As before, tree identity was included as a random factor. Four models were fitted, one for each NSC-related variable ($\Delta NSC_{Aug\text{-}Jun}$, $\Delta Starch_{Aug\text{-}Jun}$, $\Delta NSC_{Aug\text{-}Jun,\ rel}$, and $\Delta Starch_{Aug\text{-}Jun,\ rel}$).

In all cases, we started by fitting the most complex, biologically plausible model (including all three-order interactions for ψ_{MD}, ψ_{PD}, $\Delta\psi$, $K_{S\text{-}L}$, and PLC models; and species x organ, and organ x stand type in models of NSC-related variables) using the "lme" function. This model was compared with all the simpler, alternative models resulting from different combinations of explanatory variables (multimodel inference) using the "dredge" function ("MuMIn" package). The corrected Akaike information criterion (AICc) was used to select the best fitting model. Models within 2 AICc units of the best fitting model (lowest AICc) were considered equivalent in terms of fit and the simplest one (i.e., that with a lower number of fitted coefficients) was selected. The R^2 of the best-fitting model was calculated by using the "r.squaredGLMM" function.

In order to analyse the nonlinear responses of $G_{s,md}$ to VPD and SWC, we first filtered out the values of $G_{s,md}$ measured under low radiation (solar radiation < 200 W m^{-2}). As the corresponding bivariate relationships still showed a large scatter, indicating situations in which $G_{s,md}$ was co-limited by VPD and SWC, we used separate quantile regressions (95th percentile) between $G_{s,md}$ and log-transformed VPD and SWC to characterise the upper boundary of the relationships. Quantile regressions were fitted using the "rq" function ("quantreg" package). Differences across species and stand types were examined by plotting the 95% confidence intervals around the regression lines and comparing 95% confidence intervals of the obtained parameters (see Table S1 available in Supplementary Material 4 Section).

5.3. Results

Leaf water potential

The range of SWC differed across stands, with the pure Scots pine stand reaching the highest values, and the mixed stand the lowest ones (Figure 1). Both ψ_{PD} and ψ_{MD} reached more negative values with reductions of SWC and with increasing VPD, whereas $\Delta\psi$ peaked at intermediate SWC values and was unrelated to VPD (Figures 1 and 2). The response of ψ_{PD}, ψ_{MD}, and $\Delta\psi$ to SWC varied between stand types and between species within each stand type (Figure 1, see Table S2 available in Supplementary Material 4 Section). Holm oak trees achieved more negative water potentials and higher $\Delta\psi$ during water stress in both stand types, but particularly so in pure stands.

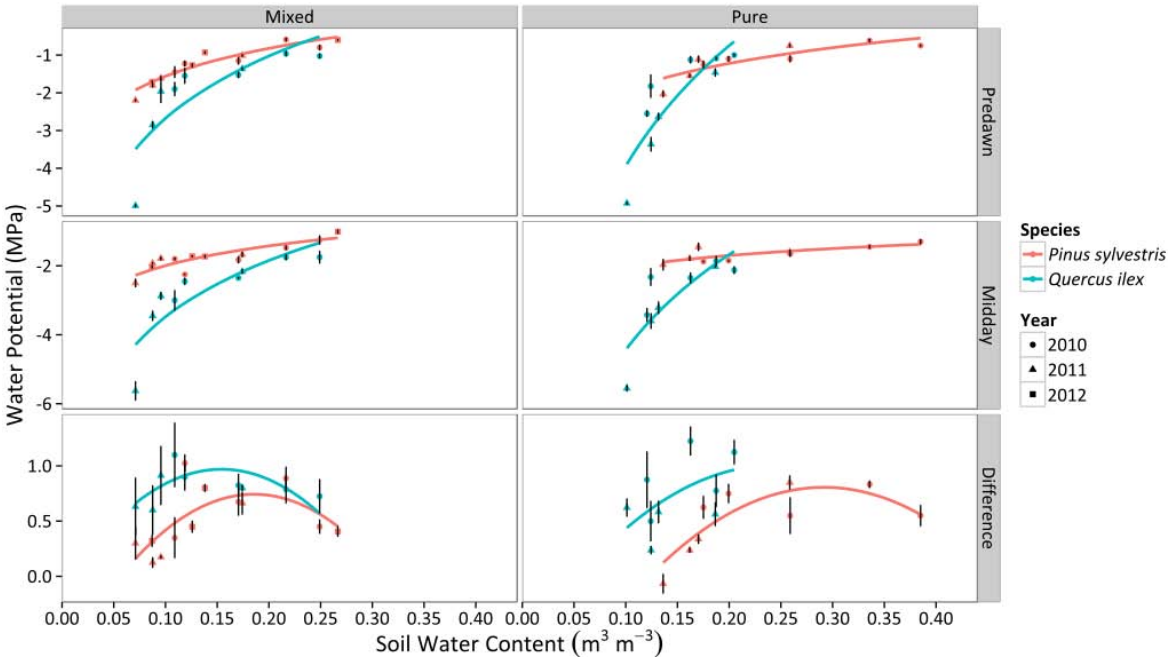

Figure 1. Responses of ψ_{PD}, ψ_{MD}, and $\Delta\psi$ to daytime averages of SWC in two different stand types throughout three consecutive years. Average values for Scots pine and holm oak trees for a given sampling are shown. Error bars indicate ±1 SE. The regressions for the different combinations of species and stand type according to best-fitting models are also depicted (cf. Table S2 available in Supplementary Material 4 Section).

Regarding the relationship between ψ and VPD, no statistical difference was found between mixed and pure stands, but there were statistical differences between species (Figure 2, see Table S2 available in Supplementary Material 4 Section), with stronger reduction of ψ_{PD} and ψ_{MD} with VPD in *Q. ilex*. The variation of ψ_{MD} with declining ψ_{PD} confirmed that Scots pine trees presented a more isohydric behavior (i.e., shallower slope of the linear relationship between ψ_{PD} and ψ_{MD}) than holm oak trees (Figure 3). Interestingly, the slope of the relationship between ψ_{PD} and ψ_{MD} (σ) was very close to 1 in holm oak, suggesting an anisohydric behavior.

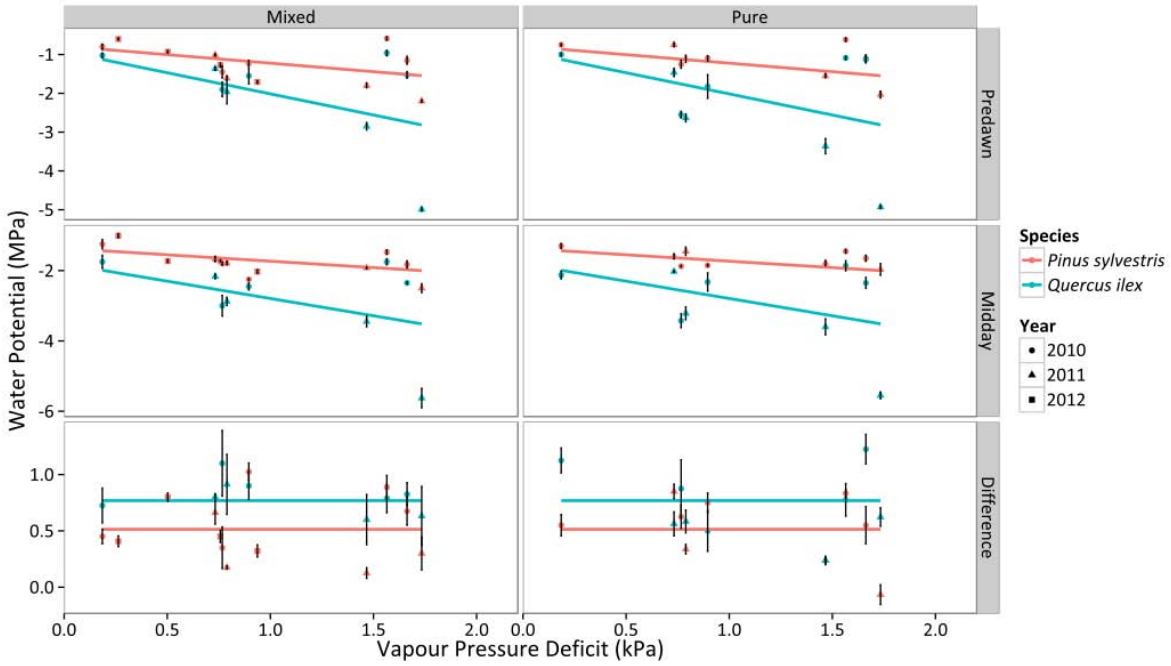

Figure 2. Responses of ψ_{PD}, ψ_{MD}, and Δψ to daytime averages of VPD in two different stand types throughout three consecutive years. Average values for Scots pine and holm oak trees for a given sampling period are shown. Error bars indicate ±1 SE. The regressions for the different combinations of species and stand type according to best-fitting models are also depicted (cf. see Table S2 available in Supplementary Material 4 Section).

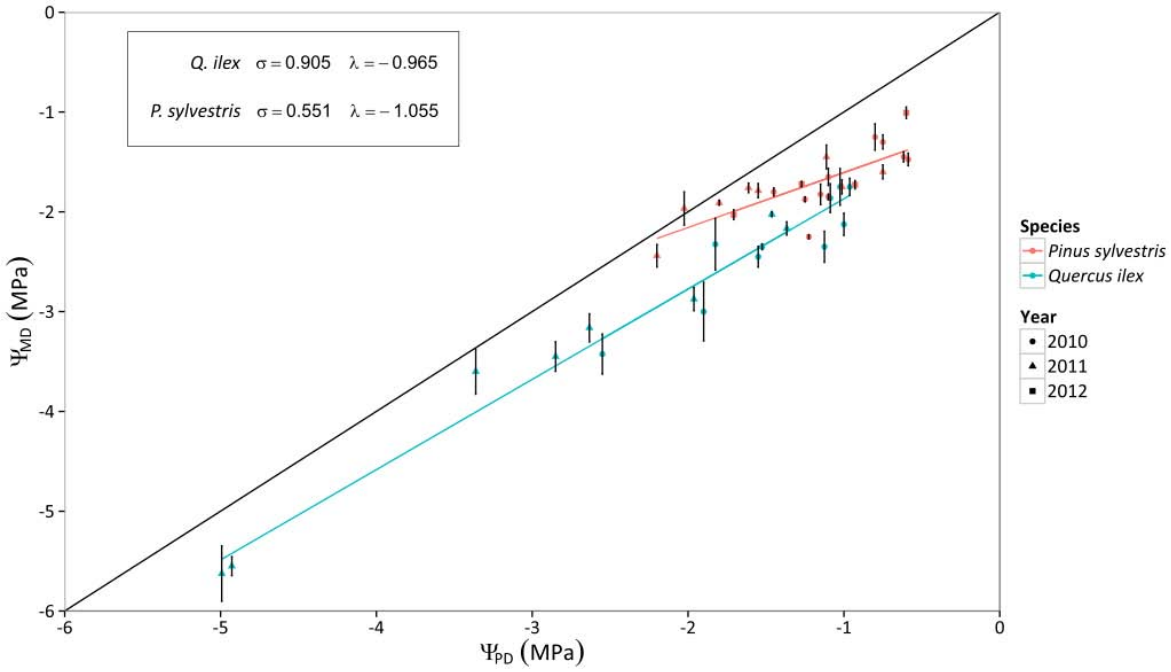

Figure 3. Relationship between predawn leaf water potential (ψ_{PD}) and midday leaf water potential (ψ_{MD}) throughout three years of measurements for Scots pine and holm oak trees. Error bars indicate ±1 SE. The 1:1 line is also depicted. Linear regression lines are also depicted for each species. The intercept (λ) and the slope (σ) of the relationship are shown in the insert.

Canopy stomatal conductance

Canopy stomatal conductance ($G_{s,md}$) increased with soil moisture in both species and stand types (Figure 4). For lower values of SWC, holm oak had higher values of $G_{s,md}$ than Scots pine. However, Scots pine experienced a faster increase of $G_{s,md}$ and achieved more elevated conductances (per unit leaf area) under well-watered conditions (Figure 4), which could be attributed to the lower A_L:A_S reported in Scots pine (Table 1). In addition, the slope of the relationship was steeper in pure than mixed stands for both species (see Table S1 available in Supplementary Material 4 Section). $G_{s,md}$ steeply decreased with increasing VPD in the two species, with Scots pine showing higher values overall in both mixed and pure stands (Figure 5). Although the slope of the relationship with VPD was similar between species in the mixed stand, the slope was steeper for Scots pine in the pure stand, resulting in significant differences between species in this latter stand type (Figure 5, see Table S1 available in Supplementary Material 4 Section).

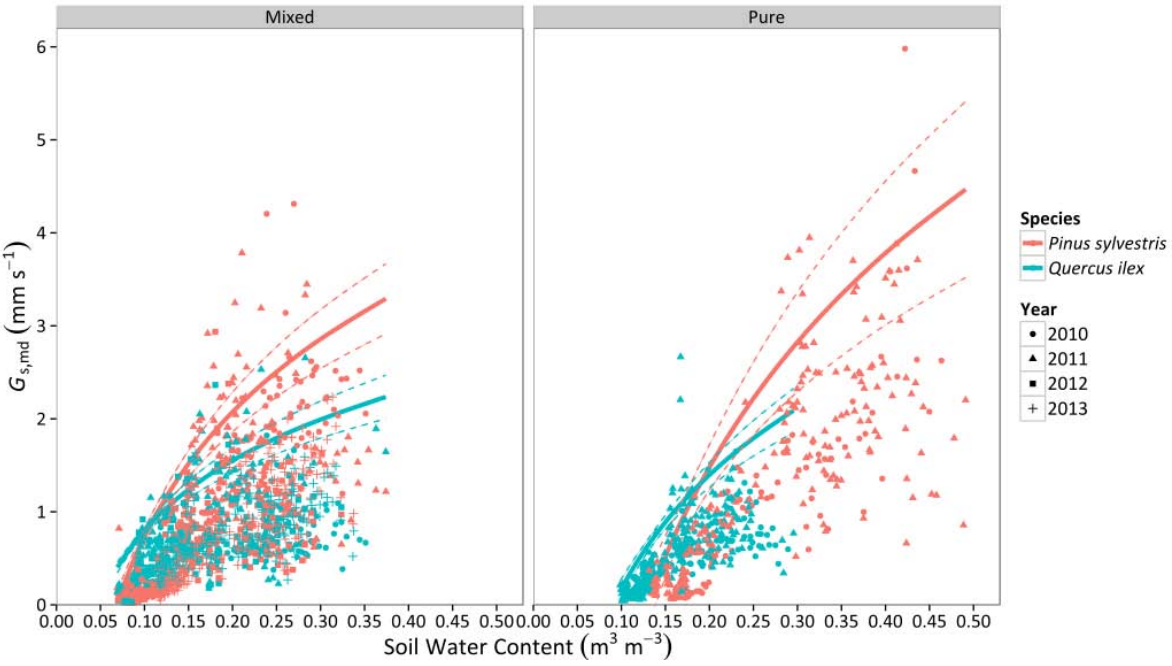

Figure 4. Responses of midday canopy stomatal conductance ($G_{s,md}$) to daytime averages of SWC in two different stand types throughout four consecutive years. Average values for Scots pine and holm oak trees are shown. Standard errors of individual measurements are not displayed to improve clarity. Solid lines represent the quantile regression fit of the 95th percentile and dashed lines are the 95% confidence intervals of the quantile regression.

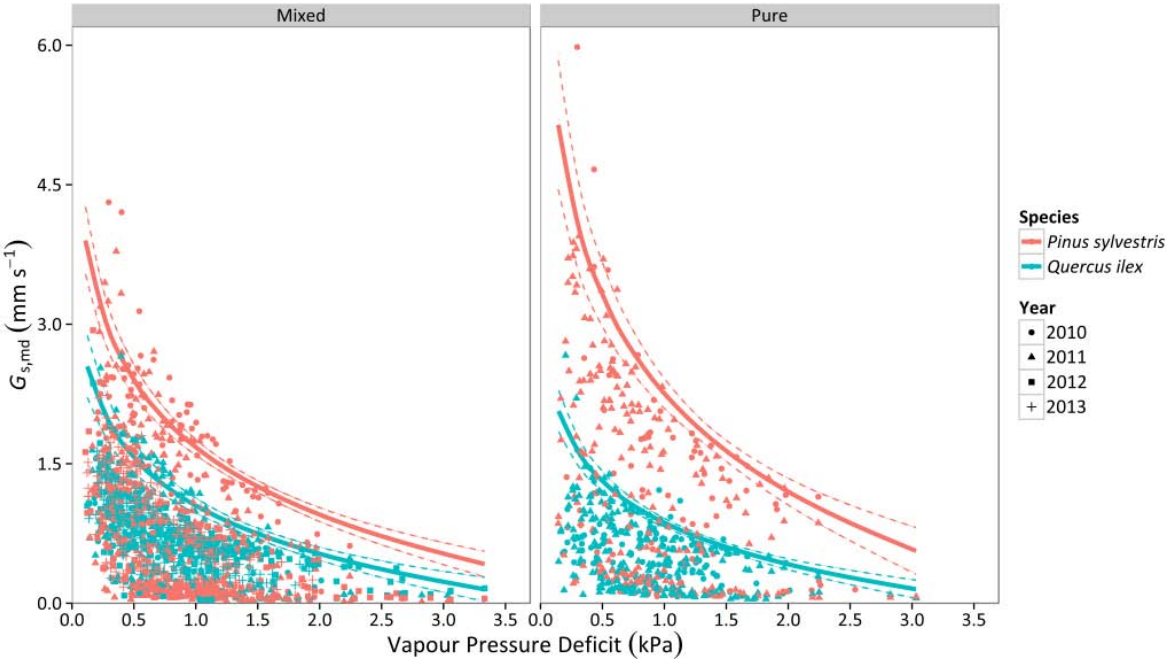

Figure 5. Responses of midday canopy stomatal conductance ($G_{s,md}$) to daytime averages of VPD in two different stand types throughout four consecutive years. Average values for Scots pine and holm oak trees are shown. Standard errors of individual measurements are not displayed to improve clarity. Solid lines represent the quantile regression fit of the 95th percentile and dashed lines are the 95% confidence intervals of the quantile regression.

Whole-tree leaf-specific conductance

Whole-tree leaf-specific conductance ($k_{S\text{-}L}$) increased linearly with increasing SWC in holm oak and Scsots pine, with a similar slope in both species (Figure 6, see Table S3 available in Supplementary Material 4 Section). Scots pine tended to have a significantly higher intercept in the mixed stand, whereas the opposite happened in the pure stands, where holm oak trees presented higher levels of $k_{S\text{-}L}$ than Scots pine for a given SWC value (Figure 6, see Table S3 available in Supplementary Material 4 Section). We did not find a significant effect of VPD on $k_{S\text{-}L}$. Lower $k_{S\text{-}L}$ values in pure compared to mixed stands were detected in both SWC and VPD models (Figures 6 and 7, see Table S3 available in Supplementary Material 4 Section).

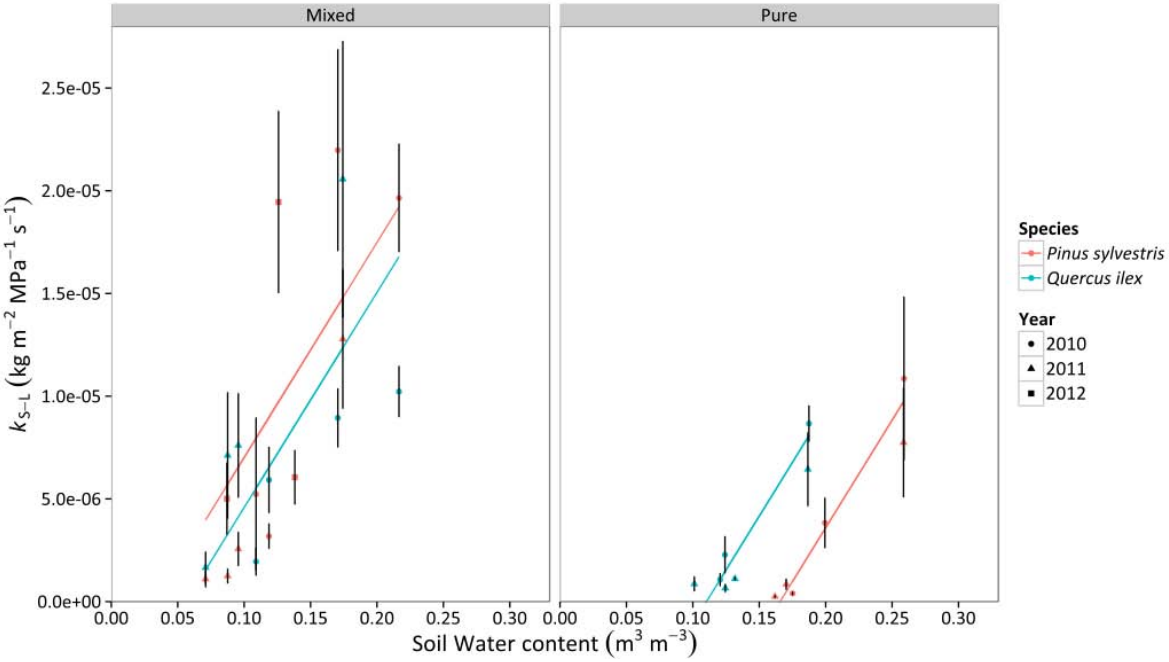

Figure 6. Responses of whole-tree leaf-specific conductance ($k_{S\text{-}L}$) to daytime averages of SWC in two different stand types throughout three consecutive years. Average values for Scots pine and holm oak trees are shown. Error bars indicate ±1 SE. The regressions for the different combinations of species and stand type according to best-fitting models are also depicted (cf. Table S3 available in Supplementary Material 4 Section).

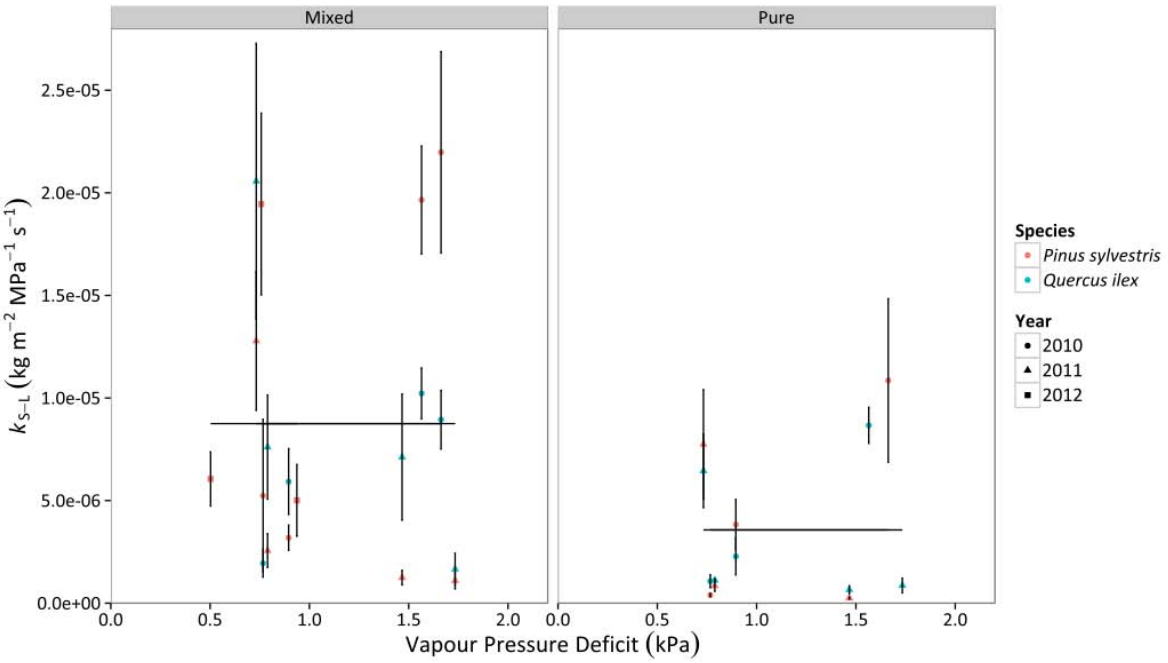

Figure 7. Responses of whole-tree leaf-specific conductance (k_{S-L}) to daytime averages of VPD in two different stand types throughout three consecutive years. Average values for Scots pine and holm oak trees are shown. Error bars indicate ±1 SE. The regressions for the different combinations of species and stand type according to best-fitting models are also depicted (cf. Table S3 available in Supplementary Material 4 Section).

Percentage loss of hydraulic conductivity

We observed an increase of the percentage loss of conductivity (PLC) with declining SWC in branches and belowground organs for mixed and pure stands of both species (Figure 8). Holm oak trees presented significantly higher levels of PLC at any given SWC (Figure 8, see Table S4 available in Supplementary Material 4 Section), reaching ~100% PLC in both stands at extremely dry conditions. In contrast, PLC in Scots pine only reached 50% in branches and 60% in roots in the mixed stand and there were slightly lower PLC values in the pure stand (Figure 8). Holm oak experienced a faster increase of PLC with declining SWC in all combinations of organ and stand type, except for roots in the mixed stand (Figure 8, see Table S4 available in Supplementary Material 4 Section). On the other hand, PLC increased with increasing values of VPD (Figure 9), with significantly higher PLC in holm oak trees in all organs and stand types (Figure 9, see Table S4 available in Supplementary Material 4 Section). However, we only observed statistically different values between stand types in branches, with lower values and shallower slopes in pure stands (see Table S4 available in Supplementary Material 4 Section). Results were qualitatively similar if the vulnerability curves obtained by Martin-StPaul et al. (2014) were used to estimate PLC for

holm oak. However, absolute PLC values were predicted to be much lower than those estimated using the vulnerability curves obtained previously for our study site, except for extremely low SWC and high VPD values (Figures 8 and 9).

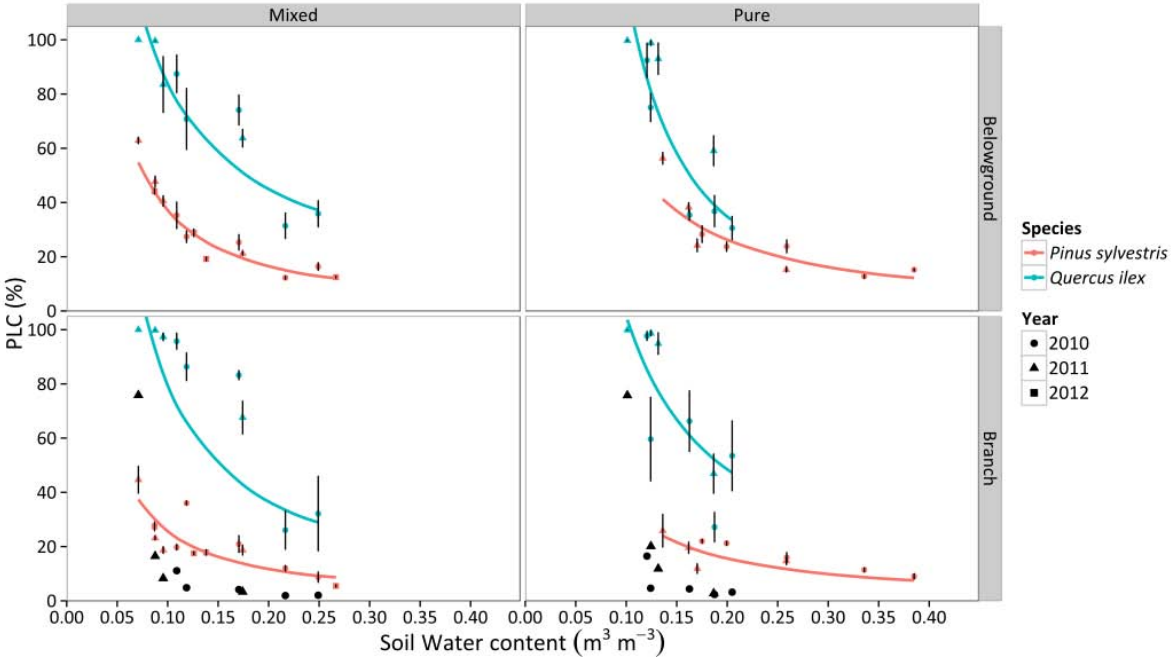

Figure 8. Responses of percentage loss of hydraulic conductivity (PLC) to daytime averages of SWC in two different stand types throughout three consecutive years. Average values for Scots pine and holm oak trees are shown. Error bars indicate ± 1 SE. The regressions for the different combinations of species and stand type according to best-fitting models are also depicted (cf. Table S4 available in Supplementary Material 4 Section). Black symbols represent the PLC values obtained following the vulnerability curves from Martin-StPaul et al. (2014) for holm oak.

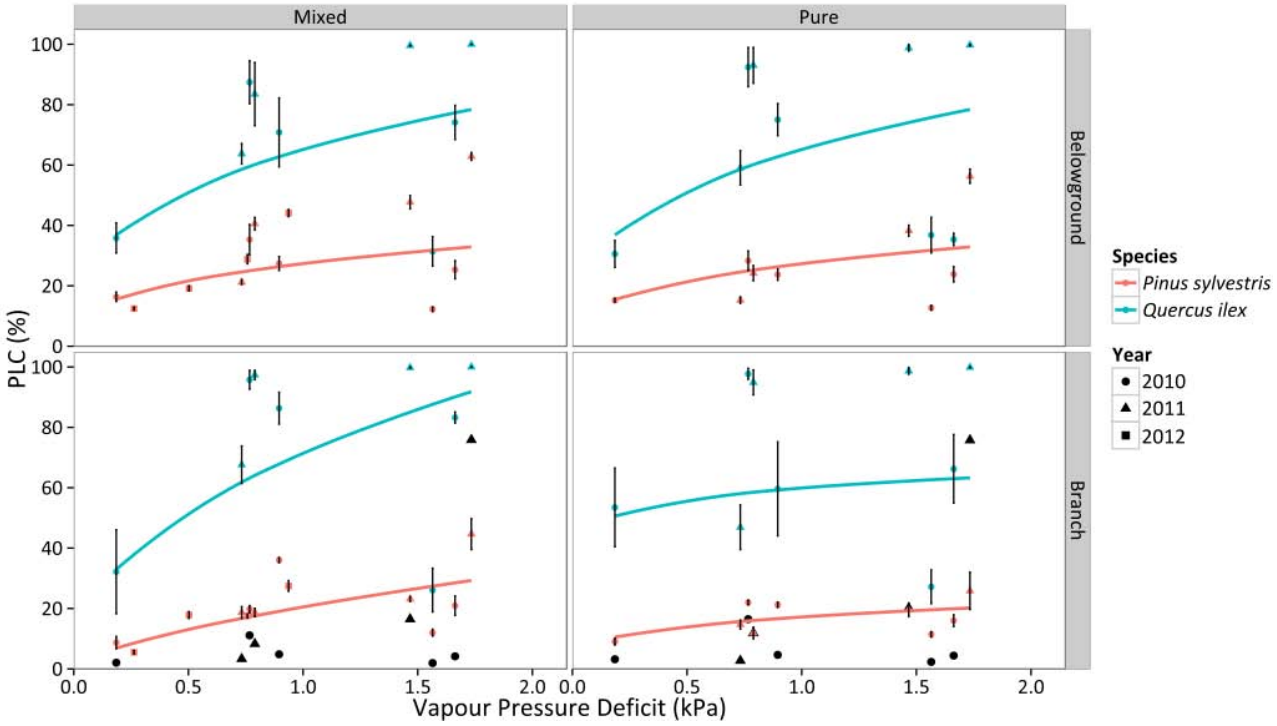

Figure 9. Responses of percentage loss of conductivity (PLC) to daytime averages of VPD in two different stand types throughout three consecutive years. Average values for Scots pine and holm oak trees are shown. Error bars indicate ±1 SE. The regressions for the different combinations of species and stand type according to best-fitting models are also depicted (cf. Table S4 available in Supplementary Material 4 Section). Black symbols represent the PLC values obtained following the vulnerability curves from Martin-StPaul et al. (2014) for holm oak.

Non-structural carbohydrates and starch

At the peak of the drought season (August) NSC concentration reached 4.81, 4.64, and 1.02% dry matter in Scots pine leaves, branches, and roots, respectively, in the pure stand. In the mixed stand these minimum values were 5.21, 4.52, and 1.22% dry matter in Scots pine leaves, branches, and roots, respectively. Finally, NSC concentrations were 4.36, 4.25, and 14.09% in holm oak leaves, branches, and lignotuber, respectively, in the pure oak stand (see also Aguadé et al. (2015) and Rosas et al. (2013).

NSC and starch declined between June and August in most combinations of species, organ, and stand type, as shown by negative $\Delta NSC_{Aug\text{-}Jun,rel}$ and $\Delta Starch_{Aug\text{-}Jun,rel}$ values (Figure 10), except for belowground organs and branches in holm oak; albeit these positive $\Delta NSC_{Aug\text{-}Jun,rel}$ corresponded to non-significant increases in the absolute values (see Figure S2 available in Supplementary Material 4 Section). Relative NSC and starch reductions ($\Delta NSC_{Aug\text{-}Jun,rel}$ and $\Delta Starch_{Aug\text{-}Jun,rel}$, respectively) were higher in leaves in both species (Figure 10, see Table S5

available in Supplementary Material 4 Section). No differences between stands were detected for Scots pine (the only species measured in both stand types) (Figure 10, see Table S5 available in Supplementary Material 4 Section). Holm oak showed a significantly lower relative reduction of NSC and starch across all organs (Figure 10, see Table S5 available in Supplementary Material 4 Section). Qualitatively similar results were obtained when absolute rather than relative differences in NSC and starch were analysed ($\Delta NSC_{Aug\text{-}Jun}$ and $\Delta Starch_{Aug\text{-}Jun}$, respectively), although in this case the interaction between organ and species was significant and the lower reductions experienced by holm oak trees were only significant in some organs (see Figure S2, Table S5 available in Supplementary Material 4 Section).

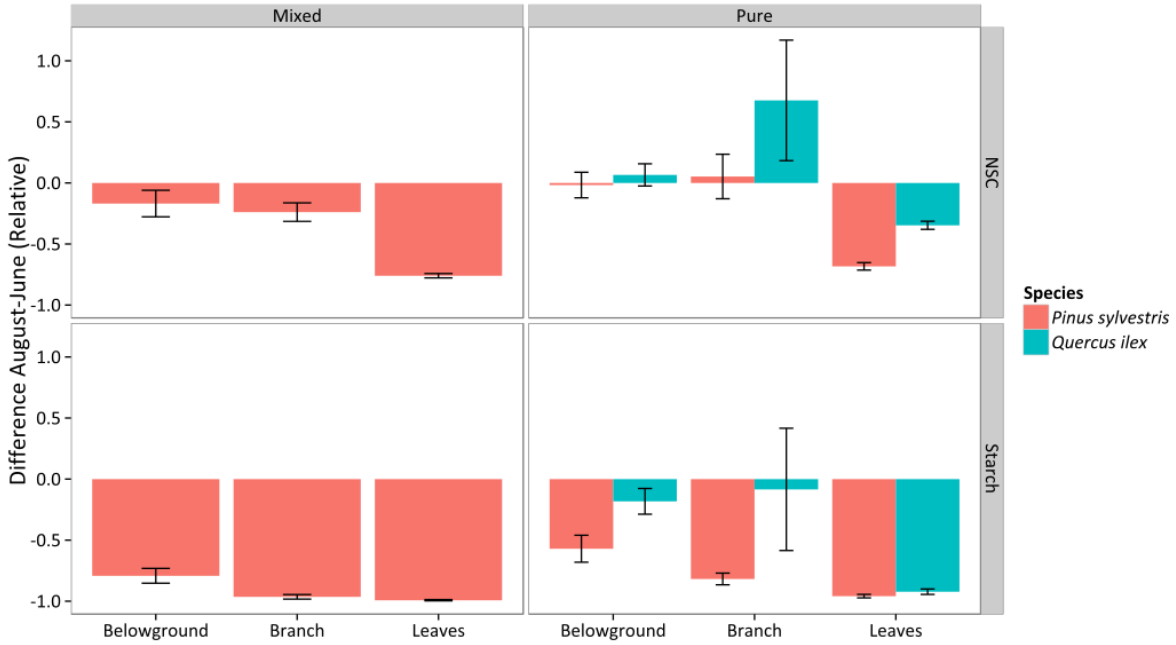

Figure 10. Relative difference between August and June in measured total non-structural carbohydrates ($\Delta NSC_{Aug\text{-}Jun,rel}$, upper panels) and starch ($\Delta Starch_{Aug\text{-}Jun,rel}$, bottom panels). Values are given for different organs, stand types (columns), and species. Average values for Scots pine and holm oak trees are shown. Error bars indicate ±1 SE.

5.4. Discussion

Overall, our results show that Scots pine and holm oak have contrasting physiological responses to extreme drought in terms of hydraulics, stomatal regulation, and carbohydrate dynamics. These differences may also be affected by species-specific phenological patterns, but the similar phenology of the two studied species in the study area and the fact that several consecutive summer droughts were monitored, including one of the driest summers on record, makes us confident that the broad differences we observe between species can be safely attributed to drought effects. Our results are generally consistent with carbon starvation and hydraulic failure being the main physiological mechanisms associated with drought-induced mortality in Scots pine and holm oak, respectively. Furthermore, we report changes in the physiological responses to drought of these two species depending on whether they coexist in the same stand or they grow in pure stands. However, these changes appear to be relatively small and, in the case of holm oak, they are unlikely to limit its ability to persist under more exposed conditions and maintain viable populations in the study area unless climatic conditions become substantially drier.

Contrasting hydraulic strategies in Scots pine and holm oak

Scots pine and holm oak displayed very different ranges of ψ, with holm oak reaching more negative values (Figure 1). Minimum values of ψ were representative of extreme drought conditions for both species. For example, ψ_{MD} for Scots pine (~−2.5 MPa) were in the lowest end of ψ_{MD} reported across Europe (Martínez-Vilalta et al. 2009) and ψ_{PD} values were lower than those observed in other drought-exposed populations (Zweifel et al. 2007). Likewise, holm oak reached values of ψ_{PD} and ψ_{MD} (~−5MPa and ~−6 MPa, respectively) that are among the most negative ones ever recorded for this species (Baquedano and Castillo 2007; Martínez-Vilalta et al. 2003).

Both ψ_{PD} and ψ_{MD} were better correlated with SWC than with VPD in both species, showing that SWC measured in the upper 30 cm of soil was tightly associated to the whole-tree water status. This is consistent with other studies in pines that have shown that (1) a strong relationship between transpiration and soil moisture is also found at a depth of 0–25 cm (Duursma et al. 2008) and (2) even if water can be extracted from deep layers, the topsoil layers, where most roots are located, have a larger influence on the rate of water uptake (Warren et al. 2005). Compared to

Scots pine, holm oak showed lower ψ_{PD} and a steeper decline of this variable with decreasing SWC. If we assume that ψ_{PD} is in equilibrium with SWC around roots (Irvine et al. 2004), these results would suggest that Scots pine roots have access to wetter soil pockets. This result contradicts the evidence showing that holm oak trees tend to be particularly deep rooted and reach deeper (and presumably wetter) soil layers than pines (Canadell et al. 1996); and authors' personal observations in the study area, as also shown in other pine-oak ecosystems, where higher ψ_{PD} values were found for oak trees compared to co-occurring pines (Kolb and Stone 2000). Hence, we may question whether ψ_{PD} is truly in equilibrium with soil water potential in our system, since we would expect the lowest ψ_{PD} measurements in the relatively shallow rooted Scots pine. One possible reason for this disequilibrium could be nocturnal sap flow (Donovan et al. 2003), which has been demonstrated in holm oak trees in our study site (Barbeta et al. 2012). However, Scots pine at our site also show some nocturnal sap flow during nights with high VPD (R. Poyatos, unpublished), making it an unlikely explanation for the differential ψ_{PD} patterns across species. Alternatively, hydraulic isolation from the surrounding soil has been hypothesised to explain relatively high (close to zero) water potentials in pines under extreme drought (Plaut et al. 2012). Other processes not studied here, such as hydraulic redistribution (Nardini et al. 2014), could also contribute to explain the observed discrepancy between ψ_{PD} values and rooting depth across species. Clearly, these mechanisms merit further investigation, as they are critical to understanding the drought responses of coexisting species.

Scots pine showed a more isohydric behavior than holm oak trees. If we interpret the relationship between ψ_{PD} and ψ_{MD} (Figure 3) following the theoretical framework recently presented by Martínez-Vilalta et al. (2014), holm oak would be classified as strictly anisohydric and Scots pine as partially isohydric. Indeed, when SWC diminished and VPD increased during drought, $G_{s,md}$ was more strongly reduced in Scots pine than in holm oak trees (Figures 4, 5). As a result, and also considering that vulnerability to embolism was similar across species, Scots pine generally kept belowground and branch PLC below 50%, whereas holm oak trees presented much higher embolism levels in both branch and belowground organs under conditions of low SWC and high VPD (Figures 8, 9). Our PLC values were estimated from xylem vulnerability curves obtained using appropriate methods for each species—air injection for Scots pine and bench dehydration for holm oak (Cochard et al. 2013; Martin-StPaul et al. 2014). However, none of these methods is free of potential artifacts (Torres-Ruiz et al. 2014), and estimated branch P_{50} values for holm oak in the study site (−2 MPa; Martínez-Vilalta et al. 2002) are low compared to the range of values reported in other studies (between −3.8 and −6.6 MPa; Martin-StPaul et al. 2013; Martin-StPaul et

al. 2014; Peguero-Pina et al. 2014; Urli et al. 2015). If we use the vulnerability curves recently reported for a climatically similar holm oak population (−4.70 MPa; Martin-StPaul et al. 2014) to estimate branch PLC, holm oak would keep PLC below ~20% except for the drought period in 2011, when PLC reached ~80% (Figure 8). This would imply that under normal summer drought conditions, branch PLC would be similar or lower in holm oak compared to Scots pine (Figure 8) and the comparatively higher risk of hydraulic failure in holm oak would be only apparent under extreme drought.

Interestingly, both Scots pine and holm oak trees exhibited similar rates of decline in $k_{S\text{-}L}$ under drought conditions, despite having different stomatal responses and different responses of xylem PLC to SWC. Whole-tree leaf-specific conductance linearly decreased with declining SWC for both species (Figure 6), and showed no relationship with VPD (Figure 7). At the lowest SWC measured in the mixed stand (ca. 0.07 $m^3\ m^{-3}$), holm oak showed close to 100% xylem PLC (in both roots and branches) and a similar ca. 90% reduction in $k_{S\text{-}L}$ compared to its maximum value. In contrast, at similarly low SWC values, co-occurring Scots pine showed a 30–40% xylem PLC but a 75% reduction in $k_{S\text{-}L}$. These discrepancies between organ-specific xylem PLC and losses at the whole-tree level ($k_{S\text{-}L}$) with SWC in Scots pine could be explained by a higher contribution of needle PLC, as needles have been shown to be more vulnerable than stems or roots in measurements taken on this species in the same study area (Salmon et al. 2015). The anisohydric behavior of holm oak observed here is at odds with the general view considering this species as isohydric (Martin-StPaul et al. 2013), even in studies conducted in a nearby valley in the same study area (Martínez-Vilalta et al. 2003; Martínez-Vilalta et al. 2002). Importantly, the iso-/anisohydric dichotomy does not account for differences in vulnerability to xylem embolism (Martínez-Vilalta et al. 2014), nor for leaf traits involved in turgor regulation (Meinzer et al. 2014). Given the current methodological controversy on the measurement of vulnerability to xylem embolism (e.g., Martin-StPaul et al. 2014; Torres-Ruiz et al. 2014) we cannot be sure that the extremely high PLC values estimated here are real. However, several notes are in order: (1) extremely high (~80%) PLC is also predicted by more conservative vulnerability estimates under extreme drought (Figures 8 and 9); (2) extremely high PLC in the xylem is consistent with measured seasonal reductions in $k_{S\text{-}L}$ (Figure 6); (3) the relationship between ψ_{PD} and ψ_{MD} for this species (Figure 3) suggests a similar sensitivity of stomata and plant hydraulic conductance to declining water potential (cf. Martínez-Vilalta et al. 2014); and (4) the water potentials measured here are much lower than those known to induce stomatal closure (Limousin et al. 2009) and even leaf turgor loss in this species (Peguero-Pina et al. 2014).

Implications for the mechanisms of drought-induced mortality in the two study species

Our results are broadly consistent with the hydraulic framework proposed by McDowell et al. (2008) and with recent experimental work by Pangle et al. (2015). The more isohydric behavior in Scots pine, in terms of maintaining relatively high water potentials, was associated with greater reductions of stomatal conductance as soil water availability declined (Figure 4), and is consistent with a greater relative reduction in NSC during drought, compared to holm oak (Figure 10) and with the low absolute levels of NSC concentration at the peak of summer drought (August). Similar NSC dynamics in responses to drought were found in a study comparing a conifer and a broadleaved species (Mitchell et al. 2013). NSC reserves are known to become even more depleted in Scots pine affected by crown defoliation following chronic drought stress and they have been directly associated with drought-induced decline and mortality in the study population (Aguadé et al. 2015). In comparison, its more anisohydric strategy likely allows holm oak to maintain higher assimilation rates under drought and minimise NSC reductions (see also Rosas et al. 2013), but puts this species under higher risk of hydraulic failure (Martínez-Vilalta et al. 2003). In fact, PLC values of ~80% reached by holm oak were close to the PLC value reported to cause irreversible damage in angiosperms (Urli et al. 2013). It is important to note here that NSC (including starch) concentrations in holm oak were measured in a drier area than the rest of the measurements reported in this study (see Methods) and, thus, summer NSC reductions may be overestimated in this species, providing further support to our interpretation. Finally, though we did not find a drastic depletion of NSC reserves in our holm oak population (Figure 10), severe drought episodes have also been associated with depleted NSC reserves in other holm oak populations (Galiano et al. 2012), highlighting the fact that different physiological mechanisms of drought-induced mortality may occur even within species.

Our study included an extraordinarily long drought period in 2011 (Poyatos et al. 2013). This drought event did not have immediate effects on landscape-scale mortality in Scots pine (at least no higher than an average summer drought) and, although holm oak trees in our main study sites were not visibly affected, a holm oak die-off event was observed in the drier, south-facing slopes of the Torners and Tillar valleys (Barbeta et al. 2015; Ogaya et al. 2015). This pattern and the extremely high PLC values reported in the branches and roots of this species during this extreme drought are consistent with the reduction of the relative use of groundwater by holm oak trees in the same study area in summer 2011 (Barbeta et al. 2015).

Comparison of mixed vs. *pure stands and implications for vegetation dynamics under climate change*

Our study allows for the comparison of physiological drought responses in two species involved in an ongoing drought-induced vegetation shift, including both mixed stands where the species coexist and pure stands where either species dominates the canopy. Species-specific values of ψ were affected by the SWC range in each stand, but also by stand type effects. The stomatal response of holm oak to SWC and VPD across stand types appeared to be less plastic than that of Scots pine. We also found differences in the species-specific relationships between PLC and drought drivers, especially SWC, between stand types (Figures 8, 9), but these differences did not translate into varying rates of decline in $k_{S\text{-}L}$ with SWC in either species. However, the stand type effect on the intercepts caused, in pure stands, holm oak to show higher $k_{S\text{-}L}$ values at a given SWC compared to Scots pine, whereas the opposite occurred in mixed stands. As a result, the SWC value at which $k_{S\text{-}L}$ reached a value of ~0 was lower in holm oak compared to Scots pine in pure stands, but the opposite appeared to be true in mixed stands (Figure 6). The higher PLC in holm oak mixed stand could explain the smaller $k_{S\text{-}L}$ for the same values of SWC of holm oak compared to Scots pine. Moreover, this threshold SWC tended to be lower in mixed compared to pure stands. However, holm oak trees showed similar water potentials and $G_{s,md}$ in mixed and pure stands. Altogether, these results suggest that holm oak in the study area (Tillar valley) is able to cope with current levels of summer drought even in pure stands where its canopy is totally exposed to solar radiation and high VPD values.

The previous results suggest that the ongoing replacement of Scots pine by holm oak trees in the study area (Vilà-Cabrera et al. 2013) will likely continue. It seems clear that holm oak can maintain a pure canopy under current climate conditions. However, the die-off observed for this species growing under somewhat drier conditions (south-facing slopes of the same Tillar or the nearby Torners valleys (Barbeta et al. 2015; Ogaya et al. 2015) also shows that if conditions become substantially drier, as predicted under climate change (IPCC 2014), other species may end up dominating the forest (Ogaya and Peñuelas 2007). Importantly, similar processes to those described here seem to be operating in other areas along the dry distribution limit of Scots pine (Galiano et al. 2010; Rigling et al. 2013). In determining what will be the consequences of these vegetation changes for the whole ecosystem (e.g., catchment level), carbon and water flux emerge as important research questions. Our results suggest that substantial differences in seasonal water fluxes are to be expected, as the more anisohydric holm oak maintains relatively

high transpiration rates for longer during seasonal drought. However, more research is needed to scale these results to yearly water and carbon fluxes under current and future climate conditions.

Acknowledgements

This work was funded by competitive grants CSD2008-0004, CGL2010-16373, and CGL2013-46808-R from the Spanish Ministry of Economy and Competitiveness, and an FPU doctoral fellowship through the Spanish Ministry of Education, Culture and Sport awarded to David Aguadé (AP2010-4573). The authors would like to thank Lucía Galiano for assistance in field sampling and carbohydrates analysis. We also thank all the staff from the Poblet Forest Natural Reserve for allowing us to carry out this research in these forests.

Chapter 6

General discussion and conclusions

This thesis studies the ecophysiological mechanisms underlying drought responses of plants and the corresponding mortality processes, focusing on Scots pine (*Pinus sylvestris* L.) as a model species. I tried to disentangle the consequences of stomatal behaviour on hydraulic dynamics and carbon uptake during drought periods. This thesis illustrates how the hypothesised mechanisms of "carbon starvation" and "hydraulic failure" play an important role during drought-induced decline, and how they are interconnected and enhanced by biotic agents. On the other hand, I also focused on the responses of holm oak (*Quercus ilex* L.) to drought, as the main candidate species to replace declining Scots pine trees in the study area.

An important strength of this thesis is the fact that all measurements were conducted under field conditions in a natural Scots pine population. The temporal scope was also relatively long for this type of studies, involving seasonal measurements throughout several years (2010 to 2012), which included contrasted conditions of soil water availability and atmospheric water demand and, therefore, different types and levels of drought. The fact that I also carried out simultaneous measurements in many plant organs allowed us to assess drought responses at the whole-tree level, which is a substantial step forward relative to many previous studies conducted at the organ level. In the following sections I summarise the main results of the thesis and provide some future prospects based on what has been learned from our study system.

Drought-induced responses in defoliated and non-defoliated Scots pine trees

An important characteristic of the Scots pine mortality process in our study area is that it is preceded by a long-term decline process that involves reduced growth and a progressive decline of the green foliage in the crown (Galiano et al. 2010; Galiano et al. 2011; Hereş et al. 2012). At the population level, apparently healthy trees coexist with individuals suffering different levels of leaf loss. Since more defoliated trees are more likely to die under future droughts, by comparing trees with different levels of leaf loss I was effectively comparing trees at different stages of drought-induced decline, which was the backbone of the experimental design of the thesis.

a) The study of carbon limitations in the field

Non-structural carbohydrates (NSC, including starch and soluble sugars) provide the main carbon reserves in trees. Therefore, periods in which carbon demand is higher than carbon uptake should result in reductions in total NSC (TNSC) (Dietze et al. 2014; Kozlowski 1992; Martínez-Vilalta et al. 2016). If TNSC levels fall below a given threshold, reserves may not be enough to

maintain vital plant functions, and therefore carbon starvation may occur, resulting in increased mortality risk (McDowell et al. 2008; McDowell 2011).However, our understanding of TNSC dynamics and their regulation, as well as its role during mortality, is still limited (Dietze et al. 2014). I studied the seasonal variation in TNSC in four organs (leaves, branches, stem and roots) and investigated whether defoliated and non-defoliated Scots pine trees showed different NSC dynamics.

In this thesis (Chapter 3), the largest stores of TNSC were found in leaves, consistent with the global patterns synthesised by Martínez-Vilalta et al. (2016), due to their great proportion of living tissues and an intrinsically higher metabolic activity. On the contrary, stems showed the smallest stores of TNSC. I also confirmed the high seasonality of NSC stores previously reported in other studies in the Mediterranean region (Palacio et al. 2007; Pratt et al. 2014; Rosas et al. 2013). Our results showed a clear conversion of starch into soluble sugars during the summer drought in all trees regardless of their defoliation level, consistent with the key role of soluble sugars in osmoregulation (Sala et al. 2012), defence against pathogens (Oliva et al. 2012) and, possibly, the maintenance of the hydraulic pathway (Brodersen and McElrone 2013). In addition, higher concentrations of TNSC in non-defoliated Scots pines were observed throughout the study period and across all organs. These results are consistent with concurrent studies suggesting an important role of carbon starvation in triggering drought-induced mortality in pines (Adams et al. 2013; Garcia-Forner et al. 2016b; Sevanto et al. 2014), but not necessarily in angiosperms (Anderegg et al. 2012b). Although we did not find complete depletion of TNSC in any defoliation class and in any organ, this result is difficult to interpret because the minimum NSC thresholds required for survival are unknown (Martínez-Vilalta et al. 2016; Sevanto et al. 2014).

b) The study of hydraulic failure

In the present thesis, different hydraulic mechanisms have been studied in order to disentangle their role in Scots pine drought-induced decline. The dysfunction of hydraulic transport by xylem embolism appears to be ubiquitous during drought-induced tree mortality (e.g., Anderegg and Anderegg 2013; Anderegg et al. 2012b; Galvez et al. 2013). In our case, different responses have been found when hydraulic mechanisms were studied in aboveground or belowground organs. When focusing on aboveground organs, defoliated pines showed a higher transport capacity and water use per unit leaf area, but they also showed a more sensitive stomatal behaviour, with a stronger decline of sap flow and hydraulic conductance with drought

stress (Chapter 2). Both defoliated and non-defoliated Scots pines showed high levels of native embolism (PLC) at the branch level under extreme drought (> 60%), consistent with PLC values reported to trigger drought-induced decline in the literature (e.g., Anderegg and Anderegg 2013; Sevanto et al. 2014). When focusing on belowground organs, root hydraulic resistance increased in both defoliation classes during water stress, but non-defoliated pines showed the greatest resistance at the peak of summer drought (Chapter 4). This results suggests that a hydraulic disconnection from the soil (North and Nobel 1997) may contribute in promoting drought resistance in Scots pine.

c) The role of biotic agents and the interactions between carbon and water economy under drought

Biotic agents can interact with the water and carbon economy of plants during drought, enhancing some of the effects reported in the previous paragraphs (Anderegg et al. 2015b; McDowell et al. 2008; Oliva et al. 2014). Insect pests seem not to play a minor role in triggering defoliation in our study population, as no evidences of bark beetle infestations were found before mortality started, contrary to other drought-induced mortality events (Bentz et al. 2010; Dobbertin et al. 2007). Root rot pathogens are likely more important in our case. Although mortality can occur regardless of their presence, they appear to enhance mortality risk in infected trees, by modifying both their water and carbon economy (Chapter 3).

This thesis highlights the importance of carbon-hydraulic interconnections in drought-induced mortality. Drought caused a reduction in hydraulic capacity and total NSC in both defoliated and non-defoliated trees, and these effects are likely to be intimately linked, reflecting similar likelihood of different plant failure modes under extreme stress (Mencuccini et al. 2015). However, the main differences between defoliated and non-defoliated trees involved NSC reserves, which suggest that in our case the mortality processes cannot be understood without accounting explicitly for the carbon economy. Given the potentially key role of NSC in Scots pine survival under drought, a better understanding of the translocation and storage of different NSC components, including lipids (which were not assessed in this thesis), and of minimum thresholds required for survival is required (Hartmann and Trumbore 2016; Martínez-Vilalta et al. 2016). Likewise, additional research is needed to better incorporate underground processes in the overall picture of drought-induced decline and mortality.

The future of Scots pine populations in Southern Europe

Drought-induced decline of Scots pine in Prades Mountains was first observed as a result of the droughts occurred in summer 1994 and 1998 (Martínez-Vilalta and Piñol 2002), and after that has continued to be observed during particularly dry years (Hereş et al. 2012). In this thesis I focused on the Scots pine population in the north-facing aspect of Tillar Valley, because at the beginning of the present thesis this valley was showing a particularly high percentage of dead Scots pine trees relative to other populations of this species in the Prades Mountains. This forest was dominated by Scots pine but also presented a thick understorey of holm oak that became the dominant canopy species at lower elevations and in areas where micro-environmental conditions were too dry for Scots pine. The recent episodes of drought-induced decline affecting Scots pine, together with the extremely low regeneration of this species, have resulted in a replacement by holm oak as the dominant canopy species in many areas within the study valley (Vilà-Cabrera et al. 2013). This process is not restricted to our study area but similar dynamics seem to be occurring in Scots pine forests in the Pyrenees (Galiano et al. 2010) and in the Alps (Rigling et al. 2013), and adds to a general change from conifer-dominated to broadleaf-dominated forests observed in many areas in Southern Europe (Vayreda et al. 2016).

Since holm oak has also experienced several episodes of mortality associated to drought in many areas, including drier populations in the Prades Mountains (Barbeta et al. 2015; Ogaya et al. 2015), an important question is to what degree the more exposed conditions experienced by oaks once they become the dominant canopy species (relative to understorey conditions) determine an increase in the susceptibility to future droughts. In order to address this question, in Chapter 5 I compared the general drought responses of pure and mixed populations of these two species in the study area. The results presented in this chapter showed that holm oak has a more anisohydric behaviour and relatively small changes in the physiological responses in mixed or pure oak stands, highlighting the ability of holm oak to substitute Scots pine trees in areas with higher pine mortality. On the contrary, Scots pine responses differed when studied in mixed or pure stands, probably due to the greater soil water availability in the pure stand located at a higher altitude. The capacity of holm oak to replace Scots pine will be increased even further by its capacity to resprout after drought (Lloret et al. 2004), albeit this capacity seems to be limited under increased drought frequency (Galiano et al. 2012).

Life goes on: anticipating and mitigating the ecosystem effects of drought-induced forest mortality

This thesis suggests new research questions related to the potential ecosystem changes following drought-induced forest mortality. I have shown that holm oak maintains higher transpiration rates during summer drought compared to Scots pine (Chapter 5), and hence we could expect higher evapotranspiration losses and decreased run-off at the catchment level if holm oak becomes the dominant species (Brantley et al. 2013). Published studies show either decreasing (Guardiola-Claramonte et al. 2011) or increasing (Bearup et al. 2014) runoff following forest mortality, because of the interplay of mortality-driven biotic and abiotic changes, including increased transpiration from regrowth vegetation and/or surviving trees (Ford et al. 2012), modified microclimate and enhanced soil evaporation or snow sublimation (Biederman et al. 2015). Nevertheless, most of these studies only deal with transient responses (Anderegg et al. 2013a) following pest-driven mortality, and do not address the long-term ecosystem consequences of vegetation shifts triggered by drought. Projections of evapotranspiration derived from process-based models, informed by ecophysiological data and applied to future climatic scenarios, could be used to predict the hydrological effects of drought-induced forest mortality (Anderegg et al. 2016).

Drought may be accelerating ecological succession and inevitably leading to the replacement of Scots pine by holm oak in the study area. While for holm oak functional acclimation and self-thinning processes may mitigate the fatal effects of drought in surviving trees (Barbeta et al. 2013), the conservation of Scots pine populations in the Tillar valley would probably need management actions to increase drought resistance. Thinning of Scots pine stands improves the water status of the remaining pines, reduces competition for water and enhances radial growth (Giuggiola et al. 2013; Giuggiola et al. 2015). I hypothesise that Scots pine prescribed thinning in the Tillar Valley could increase Scots pine survival and would promote the development of mixed Scots pine-holm oak stands. Furthermore, Scots pine individuals may still persist in more favourable microsites, because of increased soil water holding capacity and/or local adaptation to drought (Cavin and Jump 2016). Additional Research is needed to determine how generalisable our results are to wetter Scots pine populations under ongoing climate change, and what would be the associated impacts in terms of forest ecosystem services (Hanewinkel et al. 2013).

Graphic conclusions

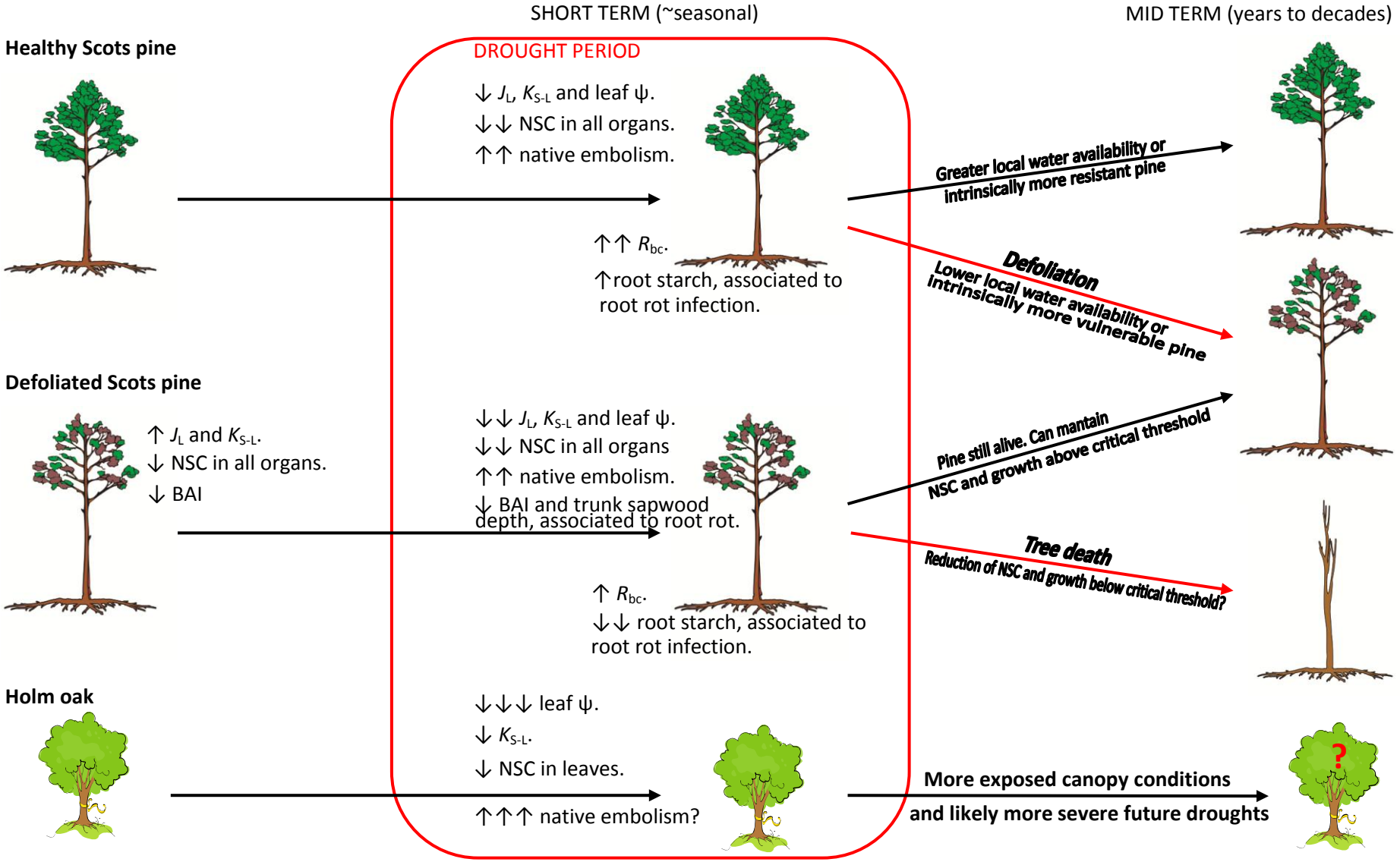

Schematic diagram of the main physiological responses in Scots pine and holm oak trees presented in this thesis, in relation to a healthy tree before the beginning of drought (↑, increase; ↓, decrease). Question marks identify processes for which the evidence is still weak. J_L; sap flow per unit leaf area; NSC, non-structural carbohydrates; BAI, basal area increment; ψ, water potential; K_{S-L}, whole-tree leaf-specific hydraulic conductance; R_{bc}, below-crown hydraulic resistance.

References

Abrams, M.D. 1990. Adaptations and responses to drought in *Quercus* species of North America. Tree Physiology. 7:227-238.

Achard, F., H.D. Eva, H.-J. Stibig, P. Mayaux, J. Gallego, T. Richards and J.-P. Malingreau 2002. Determination of deforestation rates of the world's humid tropical forests. science. 297:999-1002.

Adams, H.D., M.J. Germino, D.D. Breshears, G.A. Barron-Gafford, M. Guardiola-Claramonte, C.B. Zou and T.E. Huxman 2013. Nonstructural leaf carbohydrate dynamics of *Pinus edulis* during drought-induced tree mortality reveal role for carbon metabolism in mortality mechanism. New Phytologist. 197:1142-1151.

Adams, H.D., M. Guardiola-Claramonte, G.A. Barron-Gafford, J.C. Villegas, D.D. Breshears, C.B. Zou, P.A. Troch and T.E. Huxman 2009. Temperature sensitivity of drought-induced tree mortality portends increased regional die-off under global-change-type drought. Proceedings of the National Academy of Sciences. 106:7063-7066.

Addington, R.N., L.A. Donovan, R.J. Mitchell, J.M. Vose, S.D. Pecot, S.B. Jack, U.G. Hacke, J.S. Sperry and R. Oren 2006. Adjustments in hydraulic architecture of *Pinus palustris* maintain similar stomatal conductance in xeric and mesic habitats. Plant, Cell & Environment. 29:535-545.

Addington, R.N., R.J. Mitchell, R. Oren and L.A. Donovan 2004. Stomatal sensitivity to vapor pressure deficit and its relationship to hydraulic conductance in *Pinus palustris*. Tree Physiology. 24:561-569.

Aguadé, D., R. Poyatos, M. Gómez, J. Oliva and J. Martínez-Vilalta 2015. The role of defoliation and root rot pathogen infection in driving the mode of drought-related physiological decline in Scots pine (*Pinus sylvestris* L.). Tree Physiology

Alkama, R. and A. Cescatti 2016. Biophysical climate impacts of recent changes in global forest cover. Science. 351:600-604.

Allen, C.D. and D.D. Breshears 1998. Drought-induced shift of a forest-woodland ecotone: rapid landscape response to climate variation. Proceedings of the National Academy of Sciences. 95:14839-14842.

Allen, C.D., D.D. Breshears and N.G. McDowell 2015. On underestimation of global vulnerability to tree mortality and forest die-off from hotter drought in the Anthropocene. Ecosphere. 6:1-55.

Allen, C.D., A.K. Macalady, H. Chenchouni, D. Bachelet, N. McDowell, M. Vennetier, T. Kitzberger, A. Rigling, D.D. Breshears, E.H. Hogg, P. Gonzalez, R. Fensham, Z. Zhang, J. Castro, N. Demidova, J.-H. Lim, G. Allard, S.W. Running, A. Semmerci and N. Cobb 2010. A global overview of drought and heat-induced tree mortality reveals emerging climate change risks for forests. Forest Ecology and Management. 259:660-684.

Anderegg, W.R.L. and L.D.L. Anderegg 2013. Hydraulic and carbohydrate changes in experimental drought-induced mortality of saplings in two conifer species. Tree Physiology. 33:252-260.

Anderegg, W.R.L., L.D.L. Anderegg, J.A. Berry and C.B. Field 2014. Loss of whole-tree hydraulic conductance during severe drought and multi-year forest die-off. Oecologia. 175:11-23.

Anderegg, W.R.L., J.A. Berry and C.B. Field 2012a. Linking definitions, mechanisms, and modeling of drought-induced tree death. Trends in Plant Science. 17:693-700.

Anderegg, W.R.L., J.A. Berry, D.D. Smith, J.S. Sperry, L.D.L. Anderegg and C.B. Field 2012b. The roles of hydraulic and carbon stress in a widespread climate-induced forest die-off. Proceedings of the National Academy of Sciences. 109:233-237.

Anderegg, W.R.L., A. Flint, C.-y. Huang, L. Flint, J.A. Berry, F.W. Davis, J.S. Sperry and C.B. Field 2015a. Tree mortality predicted from drought-induced vascular damage. Nature Geoscience. 8:367-371.

Anderegg, W.R.L., J.A. Hicke, R.A. Fisher, C.D. Allen, J. Aukema, B. Bentz, S. Hood, J.W. Lichstein, A.K. Macalady and N. McDowell 2015b. Tree mortality from drought, insects, and their interactions in a changing climate. New Phytologist. 208:674-683.

Anderegg, W.R.L., J.M. Kane and L.D.L. Anderegg 2013a. Consequences of widespread tree mortality triggered by drought and temperature stress. Nature Climate Change. 3:30-36.

Anderegg, W.R.L., T. Klein, M. Bartlett, L. Sack, A.F.A. Pellegrini, B. Choat and S. Jansen 2016. Meta-analysis reveals that hydraulic traits explain cross-species patterns of drought-induced tree mortality across the globe. Proceedings of the National Academy of Sciences. 113:5024-5029.

Anderegg, W.R.L., L. Plavcová, L.D.L. Anderegg, U.G. Hacke, J.A. Berry and C.B. Field 2013b. Drought's legacy: multiyear hydraulic deterioration underlies widespread aspen forest die-off and portends increased future risk. Global Change Biology. 19:1188-1196.

Aroca, R., R. Porcel and J.M. Ruiz-Lozano 2012. Regulation of root water uptake under abiotic stress conditions. Journal of Experimental Botany. 63:43-57.

Baquedano, F.J. and F.J. Castillo 2007. Drought tolerance in the Mediterranean species *Quercus coccifera*, *Quercus ilex*, *Pinus halepensis*, and *Juniperus phoenicea*. Photosynthetica. 45:229-238.

Barba, J., J. Curiel Yuste, J. Martínez-Vilalta and F. Lloret 2013. Drought-induced tree species replacement is reflected in the spatial variability of soil respiration in a mixed Mediterranean forest. Forest Ecology and Management. 306:79-87.

Barbeta, A., M. Mejía-Chang, R. Ogaya, J. Voltas, T.E. Dawson and J. Peñuelas 2015. The combined effects of a long-term experimental drought and an extreme drought on the use of plant-water sources in a Mediterranean forest. Global Change Biology. 21:1213-1225.

Barbeta, A., R. Ogaya and J. Peñuelas 2012. Comparative study of diurnal and nocturnal sap flow of *Quercus ilex* and *Phillyrea latifolia* in a Mediterranean holm oak forest in Prades (Catalonia, NE Spain). Trees-Structure and Function. 26:1651-1659.

Barbeta, A., R. Ogaya and J. Peñuelas 2013. Dampening effects of long-term experimental drought on growth and mortality rates of a Holm oak forest. Global Change Biology. 19:3133-3144.

Bartlett, M.K., T. Klein, S. Jansen, B. Choat and L. Sack 2016. The correlations and sequence of plant stomatal, hydraulic, and wilting responses to drought. Proceedings of the National Academy of Sciences. 113:13098-13103.

Bates, B., Z.W. Kundzewicz, S. Wu and J. Palutikof 2008. Climate change and water: Technical paper VI. Intergovernmental Panel on Climate Change (IPCC).

Bauerle, T.L., J.H. Richards, D.R. Smart and D.M. Eissenstat 2008. Importance of internal hydraulic redistribution for prolonging the lifespan of roots in dry soil. Plant, Cell & Environment. 31:177-186.

Bealde, C.L., H. Talbot and P.G. Jarvis 1982. Canopy structure and leaf area index in a mature Scots pine forest. Forestry. 55:105-123.

Bearup, L.A., R.M. Maxwell, D.W. Clow and J.E. McCray 2014. Hydrological effects of forest transpiration loss in bark beetle-impacted watersheds. Nature Climate Change. 4:481-486.

Bentz, B.J., J. Régnière, C.J. Fettig, E.M. Hansen, J.L. Hayes, J.A. Hicke, R.G. Kelsey, J.F. Negrón and S.J. Seybold 2010. Climate change and bark beetles of the western United States and Canada: Direct and indirect effects. BioScience. 60:602-613.

Biederman, J.A., A.J. Somor, A.A. Harpold, E.D. Gutmann, D.D. Breshears, P.A. Troch, D.J. Gochis, R.L. Scott, A.J.H. Meddens and P.D. Brooks 2015. Recent tree die-off has little effect on streamflow in contrast to expected increases from historical studies. Water Resources Research. 51:9775-9789.

Bigler, C., O.U. Bräker, H. Bugmann, M. Dobbertin and A. Rigling 2006. Drought as an inciting mortality factor in Scots pine stands of the Valais, Switzerland. Ecosystems. 9:330-343.

Boisvenue, C. and S.W. Running 2006. Impacts of climate change on natural forest productivity-evidence since the middle of the 20th century. Global Change Biology. 12:862-882.

Bonan, G.B. 2008. Forests and climate change: forcings, feedbacks, and the climate benefits of forests. Science. 320:1444-1449.

Brantley, S., C.R. Ford and J.M. Vose 2013. Future species composition will affect forest water use after loss of eastern hemlock from southern Appalachian forests. Ecological Applications. 23:777-790.

Bréda, N., H. Cochard, E. Dreyer and A. Granier 1993. Water transfer in a mature oak stand (*Quercus petraea*): seasonal evolution and effects of a severe drought. Canadian Journal of Forest Research. 23:1136-1143.

Bréda, N., R. Huc, A. Granier and E. Dreyer 2006. Temperate forest trees and stands under severe drought: a review of ecophysiological responses, adaptation processes and long-term consequences. Annals of Forest Science. 63:625-644.

Breshears, D.D., L. López-Hoffman and L.J. Graumlich 2011. When ecosystem services crash: preparing for big, fast, patchy climate Change. AMBIO: A Journal of the Human Environment. 40:256-263.

Breshears, D.D., O.B. Myers, C.W. Meyer, F.J. Barnes, C.B. Zou, C.D. Allen, N.G. McDowell and W.T. Pockman 2009. Tree die-off in response to global change-type drought: mortality insights from a decade of plant water potential measurements. Frontiers in Ecology and the Environment. 7:185-189.

Bristow, K.L., G.S. Campbell and C. Calissendorff 1984. The effects of texture on the resistance to water movement within the rhizosphere. Soil Science Society of America Journal. 48:266-270.

Broadbent, E.N., G.P. Asner, M. Keller, D.E. Knapp, P.J.C. Oliveira and J.N. Silva 2008. Forest fragmentation and edge effects from deforestation and selective logging in the Brazilian Amazon. Biological Conservation. 141:1745-1757.

Brodersen, C.R. and A.J. McElrone 2013. Maintenance of xylem network transport capacity: a review of embolism repair in vascular plants. Frontiers in Plant Science. 4:1-11.

Brodribb, T.J., D.J.M.S. Bowman, S. Nichols, S. Delzon and R. Burlett 2010. Xylem function and growth rate interact to determine recovery rates after exposure to extreme water deficit. New Phytologist. 188:533-542.

Brodribb, T.J. and H. Cochard 2009. Hydraulic failure defines the recovery and point of death in water-stressed conifers. Plant Physiology. 149:575-584.

Brodribb, T.J., S.A.M. McAdam, G.J. Jordan and S.C.V. Martins 2014. Conifer species adapt to low-rainfall climates by following one of two divergent pathways. Proceedings of the National Academy of Sciences. 111:14489-14493.

Brooks, R.J., P.J. Schulte, B.J. Bond, R. Coulombe, J.C. Domec, T.M. Hinckley, N. McDowell and N. Phillips 2003. Does foliage on the same branch compete for the same water? Experiments on Douglas-fir trees. Trees-Structure and Function. 17:101-108.

Brunner, I., E.G. Pannatier, B. Frey, A. Rigling, W. Landolt, S. Zimmermann and M. Dobbertin 2009. Morphological and physiological responses of Scots pine fine roots to water supply in a dry climatic region in Switzerland. Tree Physiology. 29:541-550.

Cade, B.S. and B.R. Noon 2003. A gentle introduction to quantile regression for ecologists. Frontiers in Ecology and the Environment. 1:412-420.

Canadell, J., R.B. Jackson, J.B. Ehleringer, H.A. Mooney, O.E. Sala and E.D. Schulze 1996. Maximum rooting depth of vegetation types at the global scale. Oecologia. 108:583-595.

Carnicer, J., M. Coll, M. Ninyerola, X. Pons, G. Sánchez and J. Peñuelas 2011. Widespread crown condition decline, food web disruption, and amplified tree mortality with increased climate change-type drought. Proceedings of the National Academy of Sciences. 108:1474-1478.

Cavin, L. and A.S. Jump 2016. Highest drought sensitivity and lowest resistance to growth suppression are found in the range core of the tree *Fagus sylvatica* L. not the equatorial range edge. Global Change Biology. 23:362-379.

Chaves, M.M., J.S. Pereira, J. Maroco, M.L. Rodrigues, C.P.P. Ricardo, M.L. Osório, I. Carvalho, T. Faria and C. Pinheiro 2002. How plants cope with water stress in the field? Photosynthesis and growth. Annals of Botany. 89:907-916.

Choat, B., S. Jansen, T.J. Brodribb, H. Cochard, S. Delzon, R. Bhaskar, S.J. Bucci, T.S. Feild, S.M. Gleason, U.G. Hacke, A.L. Jacobsen, F. Lens, H. Maherali, J. Martínez-Vilalta, S. Mayr, M. Mencuccini, P.J. Mitchell, A. Nardini, J. Pittermann, R.B. Pratt, J.S. Sperry, M. Westoby, I.J. Wright and A.E. Zanne 2012a. Global convergence in the vulnerability of forests to drought. Nature. 491:752-755.

Choat, B., S. Jansen, T.J. Brodribb, H. Cochard, S. Delzon, R. Bhaskar, S.J. Bucci, T.S. Feild, S.M. Gleason, U.G. Hacke, A.L. Jacobsen, F. Lens, H. Maherali, J. Martínez-Vilalta, S. Mayr, M. Mencuccini, P.J. Mitchell, A. Nardini, J. Pittermann, R.B. Pratt, J.S. Sperry, M. Westoby, I.J. Wright and A.E. Zanne 2012b. Global convergence in the vulnerability of forests to drought. Nature. 491:752-755.

Cinnirella, S., F. Magnani, A. Saracino and M. Borghetti 2002. Response of a mature *Pinus laricio* plantation to a three-year restriction of water supply: structural and functional acclimation to drought. Tree physiology. 22:21-30.

Cochard, H., E. Badel, S. Herbette, S. Delzon, B. Choat and S. Jansen 2013. Methods for measuring plant vulnerability to cavitation: a critical review. Journal of Experimental Botany. 64:4779-4791.

Cochard, H., P. Cruiziat and M.T. Tyree 1992. Use of Positive Pressures to Establish Vulnerability Curves. Further Support for the Air-Seeding Hypothesis and Implications for Pressure-Volume Analysis. Plant Physiology. 100:205-209.

Creese, C., A.M. Benscoter and H. Maherali 2011. Xylem function and climate adaptation in *Pinus*. American journal of botany. 98:1437-1445.

Critchfield, W.B. and E.L. Little 1966. Geographic distribution of the pines of the world. US Dept. of Agriculture, Forest Service.

Croise, L., F. Lieutier, H. Cochard and E. Dreyer 2001. Effects of drought stress and high density stem inoculations with *Leptographium wingfieldii* on hydraulic properties of young Scots pine trees. Tree physiology. 21:427-436.

Cruickshank, M.G., D.J. Morrison and A. Lalumière 2011. Site, plot, and individual tree yield reduction of interior Douglas-fir associated with non-lethal infection by *Armillaria* root disease in southern British Columbia. Forest Ecology and Management. 261:297-307.

Delucia, E.H., H. Maherali and E.V. Carey 2000. Climate-driven changes in biomass allocation in pines. Global Change Biology. 6:587-593.

Delzon, S. and H. Cochard 2014. Recent advances in tree hydraulics highlight the ecological significance of the hydraulic safety margin. New Phytologist. 203:355-358.

Desprez-Loustau, M.L., B. Marçais, L.M. Nageleisen, D. Piou and A. Vannini 2006. Interactive effects of drought and pathogens in forest trees. Annals of Forest Science. 63:597-612.

Dietze, M.C., A. Sala, M.S. Carbone, C.I. Czimczik, J.A. Mantooth, A.D. Richardson and R. Vargas 2014. Nonstructural carbon in woody plants. Annual Review of Plant Biology. 65:667-687.

Do, F. and A. Rocheteau 2002. Influence of natural temperature gradients on measurements of xylem sap flow with thermal dissipation probes. 1. Field observations and possible remedies. Tree Physiology. 22:641-648.

Dobbertin, M., B. Eilmann, P. Bleuler, A. Giuggiola, E.G. Pannatier, W. Landolt, P. Schleppi and A. Rigling 2010. Effect of irrigation on needle morphology, shoot and stem growth in a drought-exposed *Pinus sylvestris* forest. Tree Physiology. 30:346-360.

Dobbertin, M., B. Wermelinger, C. Bigler, M. Bürgi, M. Carron, B. Forster, U. Gimmi and A. Rigling 2007. Linking increasing drought stress to Scots pine mortality and bark beetle infestations. The Scientific World Journal. 7:231-239.

Domec, J.-C. and D.M. Johnson 2012. Does homeostasis or disturbance of homeostasis in minimum leaf water potential explain the isohydric versus anisohydric behavior of *Vitis vinifera* L. cultivars? Tree Physiology. 32:245-248.

Domec, J.-C., A. Noormets, J.S. King, G.E. Sun, S.G. McNulty, M.J. Gavazzi, J.L. Boggs and E.A. Treasure 2009. Decoupling the influence of leaf and root hydraulic conductances on stomatal conductance and its sensitivity to vapour pressure deficit as soil dries in a drained loblolly pine plantation. Plant, Cell & Environment. 32:980-991.

Donovan, L.A., J.H. Richards and M.J. Linton 2003. Magnitude and mechanisms of disequilibrium between predawn plant and soil water potentials. Ecology. 84:463-470.

Dore, M.H.I. 2005. Climate change and changes in global precipitation patterns: what do we know? Environment international. 31:1167-1181.

Duan, H., R.A. Duursma, G. Huang, R.A. Smith, B. Choat, A.P. O'Grady and D.T. Tissue 2014. Elevated [CO_2] does not ameliorate the negative effects of elevated temperature on drought-induced mortality in *Eucalyptus radiata* seedlings. Plant, Cell & Environment. 37:1598-1613.

Duursma, R.A., P. Kolari, M. Peramaki, E. Nikinmaa, P. Hari, S. Delzon, D. Loustau, H. Ilvesniemi, J. Pumpanen and A. Makela 2008. Predicting the decline in daily maximum transpiration rate of two pine stands during drought based on constant minimum leaf water potential and plant hydraulic conductance. Tree Physiology. 28:265.

Eamus, D., N. Boulain, J. Cleverly and D.D. Breshears 2013. Global change-type drought-induced tree mortality: vapor pressure deficit is more important than temperature per se in causing decline in tree health. Ecology and evolution. 3:2711-2729.

Eilmann, B., N. Buchmann, R. Siegwolf, M. Saurer, P. Cherubini and A. Rigling 2010. Fast response of Scots pine to improved water availability reflected in tree-ring width and δ13C. Plant, Cell & Environment. 33:1351-1360.

Espeleta, J.F., J.B. West and L.A. Donovan 2009. Tree species fine-root demography parallels habitat specialitzation across a sandhill soil resource gradient. Ecology. 90:1773-1787.

Espino, S. and H.J. Schenk 2011. Mind the bubbles: achieving stable measurements of maximum hydraulic conductivity through woody plant samples. Journal of Experimental Botany. 62:1119-1132.

Ewers, B.E., D.S. Mackay, S.T. Gower, D.E. Ahl, S.N. Burrows and S.S. Samanta 2002. Tree species effects on stand transpiration in northern Wisconsin. Water Resources Research. 38:1–11.

Ewers, B.E. and R. Oren 2000. Analyses of assumptions and errors in the calculation of stomatal conductance from sap flux measurements. Tree Physiology. 20:579-589.

Filella, I., J. Llusià, J. Piñol and J. Peñuelas 1998. Leaf gas exchange and fluorescence of *Phillyrea latifolia*, *Pistacia lentiscus* and *Quercus ilex* saplings in severe drought and high temperature conditions. Environmental and Experimental Botany. 39:213-220.

Ford, C.R., K.J. Elliott, B.D. Clinton, B.D. Kloeppel and J.M. Vose 2012. Forest dynamics following eastern hemlock mortality in the southern Appalachians. Oikos. 121:523–536.

Ford, C.R., M.A. McGuire, R.J. Mitchell and R.O. Teskey 2004. Assessing variation in the radial profile of sap flux density in *Pinus* species and its effect on daily water use. Tree Physiology. 24:241-249.

Franklin, J.F., H.H. Shugart and M.E. Harmon 1987. Tree death as an ecological process. BioScience. 37:550-556.

Galiano, L., J. Martínez-Vilalta and F. Lloret 2010. Drought-Induced Multifactor Decline of Scots Pine in the Pyrenees and Potential Vegetation Change by the Expansion of Co-occurring Oak Species. Ecosystems. 13:978-991.

Galiano, L., J. Martínez-Vilalta and F. Lloret 2011. Carbon reserves and canopy defoliation determine the recovery of Scots pine 4 yr after a drought episode. New Phytologist. 190:750-759.

Galiano, L., J. Martínez-Vilalta, S. Sabaté and F. Lloret 2012. Determinants of drought effects on crown condition and their relationship with depletion of carbon reserves in a Mediterranean holm oak forest. Tree Physiology. 32:478-489.

Galvez, D.A., S.M. Landhäusser and M.T. Tyree 2013. Low root reserve accumulation during drought may lead to winter mortality in poplar seedlings. New Phytologist. 198:139-148.

Garbelotto, M. 2004. Root and butt rot diseases. *In* The encyclopedia of forest sciences Eds. J. Burley, J. Evans and J.A. Youngquist. Elsevier, Oxford, UK, pp. 750-758.

Garcia-Forner, N., H.D. Adams, S. Sevanto, A.D. Collins, L.T. Dickman, P.J. Hudson, M.J.B. Zeppel, M.W. Jenkins, H. Powers and J. Martínez-Vilalta 2016a. Responses of two semiarid conifer tree species to reduced precipitation and warming reveal new perspectives for stomatal regulation. Plant, Cell & Environment. 39:38-49.

Garcia-Forner, N., A. Sala, C. Biel, R. Savé and J. Martínez-Vilalta 2016b. Individual traits as determinants of time to death under extreme drought in *Pinus sylvestris* L. Tree Physiology

Gaylord, M.L., T.E. Kolb, W.T. Pockman, J.A. Plaut, E.A. Yepez, A.K. Macalady, R.E. Pangle and N.G. McDowell 2013. Drought predisposes piñon-juniper woodlands to insect attacks and mortality. New Phytologist. 198:567-578.

Gibbs, H.K., A.S. Ruesch, F. Achard, M.K. Clayton, P. Holmgren, N. Ramankutty and J.A. Foley 2010. Tropical forests were the primary sources of new agricultural land in the 1980s and 1990s. Proceedings of the National Academy of Sciences. 107:16732-16737.

Giuggiola, A., H. Bugmann, A. Zingg, M. Dobbertin and A. Rigling 2013. Reduction of stand density increases drought resistance in xeric Scots pine forests. Forest Ecology and Management. 310:827-835.

Giuggiola, A., J. Ogée, A. Rigling, A. Gessler, H. Bugmann and K. Treydte 2015. Improvement of water and light availability after thinning at a xeric site: which matters more? A dual isotope approach. New Phytologist. 210:108-121.

Gollan, T., N.C. Turner and E.D. Schulze 1985. The responses of stomata and leaf gas exchange to vapour pressure deficits and soil water content. Oecologia. 65:356-362.

Granier, A. 1985. Une nouvelle méthode pour la mesure du flux de sève brute dans le tronc des arbres. Annales des Sciences Forestières. 42:193-200.

Grossiord, C., S. Sevanto, T.E. Dawson, H.D. Adams, A.D. Collins, L.T. Dickman, B.D. Newman, E.A. Stockton and N.G. McDowell 2016. Warming combined with more extreme precipitation regimes modifies the water sources used by trees. New Phytologist

Gruber, A., D. Pirkebner, C. Florian and W. Oberhuber 2012. No evidence for depletion of carbohydrate pools in Scots pine (*Pinus sylvestris* L.) under drought stress. Plant Biology. 14:142-148.

Grulke, N.E., R.A. Minnich, T.D. Paine, S.J. Seybold, D.J. Chavez, M.E. Fenn, P.J. Riggan and A. Dunn 2008. Chapter 17 Air Pollution Increases Forest Fusceptibility To Wildfires: A Case Study in the San Bernardino Mountains in Southern California. *In* Wildland Fires and Air Pollution. Developments in environmental science Eds. A. Bytnerowicz, M. Arbaugh, A. Riebau and C. Andersen. Elsevier Publishers, The Hague, Netherlands, pp. 365-403.

Guardiola-Claramonte, M., P.A. Troch, D.D. Breshears, T.E. Huxman, M.B. Switanek, M. Durcik and N.S. Cobb 2011. Decreased streamflow in semi-arid basins following drought-induced tree die-off: A counter-intuitive and indirect climate impact on hydrology. Journal of Hydrology. 406:225-233.

Gutiérrez Merino, E. 1989. Dendroclimatological study of *Pinus sylvestris* L. in southern Catalonia (Spain). Tree-Ring Bulletin. 49:1-9.

Hacke, U.G., J.S. Sperry and J. Pittermann 2000. Drought experience and cavitation resistance in six shrubs from the Great Basin, Utah. Basic and Applied Ecology. 1:31-41.

Hacke, U.G., V. Stiller, J.S. Sperry, J. Pittermann and K.A. McCulloh 2001. Cavitation fatigue. Embolism and refilling cycles can weaken the cavitation resistance of xylem. Plant Physiology. 125:779-786.

Hampe, A. and R.J. Petit 2005. Conserving biodiversity under climate change: the rear edge matters. Ecology letters. 8:461-467.

Hanewinkel, M., D.A. Cullmann, M.-J. Schelhass, G.-J. Nabuurs and N.E. Zimmermann 2013. Climate change may cause severe loss in the economic value of European forest land. Nature Climate Change. 3:203-207.

Hartmann, H., H.D. Adams, W.R.L. Anderegg, S. Jansen and M.J.B. Zeppel 2015. Research frontiers in drought-induced tree mortality: crossing scales and disciplines. New Phytologist. 205:965-969.

Hartmann, H. and S. Trumbore 2016. Understanding the roles of nonstructural carbohydrates in forest trees - from what we can measure to what we want to know. New Phytologist. 211:386-403.

Hartmann, H., W. Ziegler, O. Kolle and S. Trumbore 2013a. Thirst beats hunger-declining hydration during drought prevents carbon starvation in Norway spruce saplings. New Phytologist. 200:340-349.

Hartmann, H., W. Ziegler and S. Trumbore 2013b. Lethal drought leads to reduction in nonstructural carbohydrates in Norway spruce tree roots but not in the canopy. Functional Ecology. 27:413-427.

Heiniger, U., F. Theile, A. Rigling and D. Rigling 2011. Blue-stain infections in roots, stems and branches of declining *Pinus sylvestris* trees in a dry inner alpine valley in Switzerland. Forest Pathology. 41:501-509.

Hendrick, R.L. and K.S. Pregitzer 1996. Temporal and depth-related patterns of fine root dynamics in northern hardwood forests. Journal of Ecology. 84:167-176.

Hereş, A.M., J. Martínez-Vilalta and B.C. López 2012. Growth patterns in relation to drought-induced mortality at two Scots pine (*Pinus sylvestris* L.) sites in NE Iberian Peninsula. Trees-Structure and Function. 26:621-630.

Hereter, A. and J.R. Sánchez 1999. Experimental areas of Prades and Montseny. *In* Ecology of Mediterranean Evergreen Oak Forests Eds. F. Rodà, J. Retana, C.A. Gracia and J. Bellot. Springer-Verlag, Berlin. 15-27 pp.

Hoch, G. and C. Körner 2003. The carbon charging of pines at the climatic treeline: a global comparison. Oecologia. 135:10-21.

Hoch, G., M. Popp and C. Körner 2002. Altitudinal increase of mobile carbon pools in *Pinus cembra* suggests sink limitation of growth at the Swiss treeline. Oikos. 98:361-374.

Hoch, G., A. Richter and C. Körner 2003. Non-structural carbon compounds in temperate forest trees. Plant, Cell & Environment. 26:1067-1081.

Hoffmann, W.A., R.M. Marchin, P. Abit and O.L. Lau 2011. Hydraulic failure and tree dieback are associated with high wood density in a temperate forest under extreme drought. Global Change Biology. 17:2731-2742.

Holmgren, M., L. Gómez-Aparicio, J.L. Quero and F. Valladares 2012. Non-linear effects of drought under shade: reconciling physiological and ecological models in plant communities. Oecologia. 169:293-305.

Hothorn, T., F. Bretz and P. Westfall 2008. Simultaneous inference in general parametric models. Biometrical journal. 50:346-363.

Hubbard, R.M., C.C. Rhoades, K. Elder and J. Negron 2013. Changes in transpiration and foliage growth in lodgepole pine trees following mountain pine beetle attack and mechanical girdling. Forest Ecology and Management. 289:312-317.

IPCC 2013. Climate Change 2013: The Physical Science Basis. Contribution of Working Group I to the Fifth Assessment Report of the Intergovernmental Panel on Climate Change (IPCC). Cambridge University Press, Cambridge, United Kingdom and New York, NY, USA. 1535 p.

IPCC 2014. Climate Change 2014: Synthesis Report. Contribution of Working Groups I, II and III to Fifth Assessment Report of the Intergovernmental Panel on Climate Change (IPCC). Geneva, Switzerland. p. 151.

Irvine, J. and J. Grace 1997. Continuous measurements of water tensions in the xylem of trees based on the elastic properties of wood. Planta. 202:455-461.

Irvine, J., B.E. Law, M.R. Kurpius, P.M. Anthoni, D. Moore and P.A. Schwarz 2004. Age-related changes in ecosystem structure and function and effects on water and carbon exchange in ponderosa pine. Tree Physiology. 24:753-763.

Irvine, J., M.P. Perks, F. Magnani and J. Grace 1998. The response of *Pinus sylvestris* to drought: stomatal control of transpiration and hydraulic conductance. Tree physiology. 18:393-402.

Johnson, A.H. and T.G. Siccama 1983. Acid deposition and forest decline. Environmental science & technology. 17:294-305.

Johnson, D.M., M.E. Sherrard, J.-C. Domec and R.B. Jackson 2014. Role of aquaporin activity in regulating deep and shallow root hydraulic conductance during extreme drought. Trees. 28:1323-1331.

Johnson, D.M., R. Wortemann, K.A. McCulloh, L. Jordan-Meille, E. Ward, J.M. Warren, S. Palmroth and J.-C. Domec 2016. A test of the hydraulic vulnerability segmentation hypothesis in angiosperm and conifer tree species. Tree Physiology:tpw031.

Jones, H.G. 1998. Stomatal control of photosynthesis and transpiration. Journal of Experimental Botany. 49:387-398.

Klein, T. 2014. The variability of stomatal sensitivity to leaf water potential across tree species indicates a continuum between isohydric and anisohydric behaviours. Functional Ecology. 28:1313-1320.

Klein, T., G. Di Matteo, E. Rotenberg, S. Cohen and D. Yakir 2013. Differential ecophysiological response of a major Mediterranean pine species across a climatic gradient. Tree Physiology. 33:26-36.

Kolb, T.E. and J.E. Stone 2000. Differences in leaf gas exchange and water relations among species and tree sizes in an Arizona pine-oak forest. Tree Physiology. 20:1-12.

Kozlowski, T.T. 1992. Carbohydrate sources and sinks in woody plants. The Botanical Review. 58:107-222.

Kutscha, N.P. and I.B. Sachs 1962. Color tests for differentiating heartwood and sapwood in certain softwood tree species. Forestry Products Laboratory Report Number 2246

La Porta, N., P. Capretti, I.M. Thomsen, R. Kasanen, A.M. Hietala and K. Von Weissenberg 2008. Forest pathogens with higher damage potential due to climate change in Europe. Canadian Journal of Plant Pathology. 30:177-195.

Lagergren, F. and A. Lindroth 2002. Transpiration response to soil moisture in pine and spruce trees in Sweden. Agricultural and forest meteorology. 112:67-85.

Le Quéré, C., G.P. Peters, R.J. Andres, R.M. Andrew, T. Boden, P. Ciais, P. Friedlingstein, R.A. Houghton, G. Marland, R. Moriarty, S. Sitch, P. Tans, A. Arneth, A. Arvanitis, D.C.E. Bakker, L. Bopp, J.G. Canadell, L.P. Chini, S.C. Doney, A. Harper, I. Harris, J.I. House, A.K. Jain, S.D. Jones, E. Kato, R.F. Keeling, K. Klein Goldewijk, A. Körtzinger, C. Koven, N. Lefèvre, F. Maignan, A. Omar, T. Ono, G.-H. Park, B. Pfeil, B. Poulter, M.R. Raupach, P. Regnier, C. Rödenbeck, S. Saito, J. Schwinger, J. Segschneider, B.D. Stocker, T. Takahashi, B. Tilbrook, S. van Heuven, N. Viovy, R. Wanninkhof, A. Wiltshire and S. Zaehle 2014. Global carbon budget 2013. Earth Syst. Sci. Data. 6:235-263.

Leuzinger, S., C. Bigler, A. Wolf and C. Körner 2009. Poor methodology for predicting large-scale tree die-off. Proceedings of the National Academy of Sciences. 106

Li, M.H., W.F. Xiao, S.G. Wang, G.W. Cheng, P. Cherubini, X.H. Cai, X.L. Liu, X.D. Wang and W.Z. Zhu 2008. Mobile carbohydrates in Himalayan treeline trees I. Evidence for carbon gain limitation but not for growth limitation. Tree Physiology. 28:1287-1296.

Limousin, J.M., S. Rambal, J.M. Ourcival, A. Rocheteau, R. Joffre and R. Rodriguez Cortina 2009. Long term transpiration change with rainfall decline in a Mediterranean *Quercus ilex* forest. Global Change Biology. 15:2163-2175.

Linares, J.C., J.J. Camarero and J.A. Carreira 2009. Interacting effects of climate and forest-cover changes on mortality and growth of the southernmost European fir forests. Global Ecology and Biogeography. 18:485–497.

Liu, J., M.A. Equiza, A. Navarro-Rodenas, S.H. Lee and J.J. Zwiazeck 2014. Hydraulic adjustments in aspen (*Populus tremuloides*) seedlings following defoliation involve root and leaf aquaporins. Planta. 240:553-564.

Llorens, P., R. Poyatos, J. Latron, J. Delgado, I. Oliveras and F. Gallart 2010. A multi-year study of rainfall and soil water controls on Scots pine transpiration under Mediterranean mountain conditions. Hydrological Processes. 24:3053-3064.

Lloret, F. 2012. Vulnerabilidad y resiliencia de ecosistemas forestales frente a episodios extremos de sequía. Revista Ecosistemas. 21:85-90.

Lloret, F., A. Escudero, J.M. Iriondo, J. Martínez-Vilalta and F. Valladares 2012. Extreme climatic events and vegetation: the role of stabilizing processes. Global Change Biology. 18:797-805.

Lloret, F., D. Siscart and C. Dalmases 2004. Canopy recovery after drought dieback in holm-oak Mediterranean forests of Catalonia (NE Spain). Global Change Biology. 10:2092-2099.

Maherali, H. and E.H. DeLucia 2000. Xylem conductivity and vulnerability to cavitation of ponderosa pine growing in contrasting climates. Tree physiology. 20:859-867.

Maherali, H. and E.H. DeLucia 2001. Influence of climate-driven shifts in biomass allocation on water transport and storage in ponderosa pine. Oecologia. 129:481-491.

Martin-StPaul, N.K., J.-M. Limousin, H. Vogt-Schilb, J. Rodríguez-Calcerrada, S. Rambal, D. Longepierre and L. Misson 2013. The temporal response to drought in a Mediterranean evergreen tree: comparing a regional precipitation gradient and a throughfall exclusion experiment. Global Change Biology. 19:2413-2426.

Martin-StPaul, N.K., D. Longepierre, R. Huc, S. Delzon, R. Burlett, R. Joffre, S. Rambal and H. Cochard 2014. How reliable are methods to assess xylem vulnerability to cavitation? The issue of 'open vessel' artifact in oaks. Tree Physiology. 34:894-905.

Martínez-Vilalta, J., D. Aguadé, M. Banqué, J. Barba, J.C. Yuste, L. Galiano, N. Garcia, M. Gómez, A.M. Hereş, B.C. López, F. Lloret, J. Retana, O. Sus, J. Vayreda and A. Vilà-Cabrera 2012a. Las poblaciones ibéricas de pino albar ante el cambio climático: con la muerte en los talones. Revista Ecosistemas. 21:15-21.

Martínez-Vilalta, J., H. Cochard, M. Mencuccini, F. Sterck, A. Herrero, J.F.J. Korhonen, P. Llorens, E. Nikinmaa, A. Nolè, R. Poyatos, F. Ripullone, U. Sass-Klaassen and R. Zweifel 2009. Hydraulic adjustment of Scots pine across Europe. New phytologist. 184:353-364.

Martínez-Vilalta, J. and N. Garcia-Forner 2016. Water potential regulation, stomatal behaviour and hydraulic transport under drought: deconstructing the iso/anisohydric concept. Plant, Cell & Environment

Martínez-Vilalta, J., E. Korakaki, D. Vanderklein and M. Mencuccini 2007. Below-ground hydraulic conductance is a function of environmental conditions and tree size in Scots pine. Functional Ecology. 21:1072-1083.

Martínez-Vilalta, J., F. Lloret and D.D. Breshears 2012b. Drought-induced forest decline: causes, scope and implications. Biology Letters. 8:689-691.

Martínez-Vilalta, J., B.C. López, N. Adell, L. Badiella and M. Ninyerola 2008. Twentieth century increase of Scots pine radial growth in NE Spain shows strong climate interactions. Global Change Biology. 14:2868-2881.

Martínez-Vilalta, J., B.C. López, L. Loepfe and F. Lloret 2012c. Stand-and tree-level determinants of the drought response of Scots pine radial growth. Oecologia. 168:877-888.

Martínez-Vilalta, J., M. Mangirón, R. Ogaya, M. Sauret, L. Serrano, J. Peñuelas and J. Piñol 2003. Sap flow of three co-occurring Mediterranean woody species under varying atmospheric and soil water conditions. Tree physiology. 23:747-758.

Martínez-Vilalta, J. and J. Piñol 2002. Drought-induced mortality and hydraulic architecture in pine populations of the NE Iberian Peninsula. Forest Ecology and Management. 161:247-256.

Martínez-Vilalta, J., R. Poyatos, D. Aguadé, J. Retana and M. Mencuccini 2014. A new look at water transport regulation in plants. New Phytologist. 204:105-115.

Martínez-Vilalta, J., E. Prat, I. Oliveras and J. Piñol 2002. Xylem hydraulic properties of roots and stems of nine woody species from a holm oak forest in NE Spain. Oecologia. 133:19-29.

Martínez-Vilalta, J., A. Sala, D. Asensio, L. Galiano, G. Hoch, S. Palacio, F.I. Piper and F. Lloret 2016. Dynamics of non-structural carbohydrates in terrestrial plants: a global synthesis. Ecological Monographs. 86:495-516.

Martínez-Vilalta, J., A. Sala and J. Piñol 2004. The hydraulic architecture of Pinaceae-a review. Plant Ecology. 171:3-13.

Martinez-Vilalta, J., D. Vanderklein and M. Mencuccini 2007. Tree height and age-related decline in growth in Scots pine (*Pinus sylvestris* L.). Oecologia. 150:529-544.

Maseda, P.H. and R.J. Fernández 2006. Stay wet or else: three ways in which plants can adjust hydraulically to their environment. Journal of Experimental Botany. 57:3963-3977.

Matthias, D., W. Beat, B. Christof, B. Matthias, C. Mathias, F. Beat, G. Urs and R. Andreas 2007. Linking increasing drought stress to Scots pine mortality and bark beetle infestations. The Scientific World Journal. 7:231-239.

Maurel, C., L. Verdoucq, D.-T. Luu and V. Santoni 2008. Plant aquaporins: membrane channels with multiple integrated functions. Annu. Rev. Plant Biol. 59:595-624.

McCulloh, K.A., D.M. Johnson, F.C. Meinzer and B. Lachenbruch 2011. An annual pattern of native embolism in upper branches of four tall conifer species. American journal of botany. 98:1007-1015.

McCulloh, K.A., D.M. Johnson, F.C. Meinzer and D.R. Woodruff 2014. The dynamic pipeline: hydraulic capacitance and xylem hydraulic safety in four tall conifer species. Plant, Cell & Environment. 37:1171-1183.

McDowell, N., W.T. Pockman, C.D. Allen, D.D. Breshears, N. Cobb, T. Kolb, J. Plaut, J. Sperry, A. West, D.G. Williams and E.A. Yepez 2008. Mechanisms of plant survival and mortality during drought: why do some plants survive while others succumb to drought? New Phytologist. 178:719-739.

McDowell, N.G. 2011. Mechanisms linking drought, hydraulics, carbon metabolism, and vegetation mortality. Plant Physiology. 155:1051-1059.

McDowell, N.G., D.J. Beerling, D.D. Breshears, R.A. Fisher, K.F. Raffa and M. Stitt 2011. The interdependence of mechanisms underlying climate-driven vegetation mortality. Trends in Ecology & Evolution. 26:523-532.

McDowell, N.G. and S. Sevanto 2010. The mechanisms of carbon starvation: how, when, or does it even occur at all? New Phytologist. 186:264-266.

McDowell, N.G., A.P. Williams, C. Xu, W.T. Pockman, L.T. Dickman, S. Sevanto, R. Pangle, J. Limousin, J. Plaut, D.S. Mackay, J. Ogee, J.C. Domec, C.D. Allen, R.A. Fisher, X. Jiang, J.D. Muss, D.D. Breshears, S.A. Rauscher and C. Koven 2016. Multi-scale predictions of massive conifer mortality due to chronic temperature rise. Nature Climate Change. 6:295-300.

Meier, I.C. and C. Leuschner 2008. Belowground drought response of European beech: fine root biomass and carbon partitioning in 14 mature stands across a precipitation gradient. Global Change Biology. 14:2081-2095.

Meinzer, F.C., D.M. Johnson, B. Lachenbruch, K.A. McCulloh and D.R. Woodruff 2009. Xylem hydraulic safety margins in woody plants: coordination of stomatal control of xylem tension with hydraulic capacitance. Functional Ecology. 23:922-930.

Meinzer, F.C., D.R. Woodruff, D.E. Marias, K.A. McCulloh and S. Sevanto 2014. Dynamics of leaf water relations components in co-occurring Iso-□and anisohydric conifer species. Plant, Cell & Environment. 37:2577-2586.

Mencuccini, M. 2003. The ecological significance of long-distance water transport: short-term regulation, long-term acclimation and the hydraulic costs of stature across plant life forms. Plant, Cell & Environment. 26:163-182.

Mencuccini, M. and J. Grace 1995. Climate influences the leaf area/sapwood area ratio in Scots pine. Tree physiology. 15:1-10.

Mencuccini, M., J. Grace and M. Fioravanti 1997. Biomechanical and hydraulic determinants of tree structure in Scots pine: anatomical characteristics. Tree Physiology. 17:105-113.

Mencuccini, M., F. Minunno, Y. Salmon, J. Martínez-Vilalta and T. Hölttä 2015. Coordination of physiological traits involved in drought-induced mortality of woody plants. New Phytologist. 208:396-409.

Mitchell, P.J., A.P. O'Grady, D.T. Tissue, D.A. White, M.L. Ottenschlaeger and E.A. Pinkard 2013. Drought response strategies define the relative contributions of hydraulic dysfunction and carbohydrate depletion during tree mortality. New Phytologist. 197:862-872.

Morton, D.C., R.S. DeFries, Y.E. Shimabukuro, L.O. Anderson, E. Arai, F. del Bon Espirito-Santo, R. Freitas and J. Morisette 2006. Cropland expansion changes deforestation dynamics in the southern Brazilian Amazon. Proceedings of the National Academy of Sciences. 103:14637-14641.

Nadezhdina, N., J. Čermák and R. Ceulemans 2002. Radial patterns of sap flow in woody stems of dominant and understory species: scaling errors associated with positioning of sensors. Tree Physiology. 22:907-918.

Nadezhdina, N., J. Čermák, J. Gašpárek, V. Nadezhdin and A. Prax 2006. Vertical and horizontal water redistribution in Norway spruce (*Picea abies*) roots in the Moravian Upland. Tree Physiology. 26:1277-1288.

Naidoo, R., A. Balmford, R. Costanza, B. Fisher, R.E. Green, B. Lehner, T.R. Malcolm and T.H. Ricketts 2008. Global mapping of ecosystem services and conservation priorities. Proceedings of the National Academy of Sciences. 105:9495-9500.

Nardini, A., M. Battistuzzo and T. Savi 2013. Shoot desiccation and hydraulic failure in temperate woody angiosperms during an extreme summer drought. New Phytologist. 200:322-329.

Nardini, A., M.A.L. Gullo, P. Trifilò and S. Salleo 2014. The challenge of the Mediterranean climate to plant hydraulics: responses and adaptations. Environmental and Experimental Botany. 103:68-79.

Navarro Cerrillo, R.M., M.A. Varo, S. Lanjeri and R.H. Clemente 2007. Cartografía de defoliación en los pinares de pino silvestre (*Pinus sylvestris* L.) y pino salgareño (*Pinus nigra* Arnold.) en la Sierra de los Filabres. Revista Ecosistemas. 16:163-171.

Navarro, L.M. and H.M. Pereira 2012. Rewilding abandoned landscapes in Europe. Ecosystems. 15:900-912.

Newman, E.I. 1969. Resistance to water flow in soil and plant. I. Soil resistance in relation to amounts of root: theoretical estimates. Journal of Applied Ecology. 6:1-12.

Ninyerola, M., X. Pons and J.M. Roure 2007a. Monthly precipitation mapping of the Iberian Peninsula using spatial interpolation tools implemented in a Geographic Information System. Theoretical and Applied Climatology. 89:195-209.

Ninyerola, M., X. Pons and J.M. Roure 2007b. Objective air temperature mapping for the Iberian Peninsula using spatial interpolation and GIS. International Journal of Climatology. 27:1231-1242.

North, G.B. and P.S. Nobel 1997. Root-soil contact for the desert succulent *Agave deserti* in wet and drying soil. New Phytologist. 135:21-29.

O'Brien, M.J., D.F.R.P. Burslem, A. Caduff, J. Tay and A. Hector 2015. Contrasting nonstructural carbohydrate dynamics of tropical tree seedlings under water deficit and variability. New Phytologist. 205:1083-1094.

O'Brien, M.J., S. Leuzinger, C.D. Philipson, J. Tay and A. Hector 2014. Drought survival of tropical tree seedlings enhanced by non-structural carbohydrate levels. Nature Climate Change. 4:710-714.

Oberhuber, W. 2001. The role of climate in the mortality of Scots pine (*Pinus sylvestris* L.) exposed to soil dryness. Dendrochronologia. 19:45-55.

Offenthaler, I., P. Hietz and H. Richter 2001. Wood diameter indicates diurnal and long-term patterns of xylem water potential in Norway spruce. Trees. 15:215-221.

Ogaya, R. 2003. Plant ecophysiological responses to a field experimental drought in the Prades holm oak forest. *In* Departament de Biologia Animal, de Biologia Vegetal i d'Ecologia. Universitat Autònoma de Barcelona, Cerdanyola del Vallès, p. 117.

Ogaya, R., A. Barbeta, C. Başnou and J. Peñuelas 2015. Satellite data as indicators of tree biomass growth and forest dieback in a Mediterranean holm oak forest. Annals of Forest Science. 72:135-144.

Ogaya, R. and J. Peñelas 2004. Phenological patterns of *Quercus ilex*, *Phillyrea latifolia*, and *Arbutus unedo* growing under a field experimental drought. Ecoscience. 11:263-270.

Ogaya, R. and J. Peñuelas 2007. Tree growth, mortality, and above-ground biomass accumulation in a holm oak forest under a five-year experimental field drought. Plant Ecology. 189:291-299.

Ogle, K., R.W. Lucas, L.P. Bentley, J.M. Cable, G.A. Barron-Gafford, A. Griffith, D. Ignace, G.D. Jenerette, A. Tyler, T.E. Huxman, M.E. Loik, S.D. Smith and D.T. Tissue 2012. Differential daytime and night-time stomatal behavior in plants from North American deserts. New Phytologist. 194:464-476.

Oishi, A.C., R. Oren and P.C. Stoy 2008. Estimating components of forest evapotranspiration: a footprint approach for scaling sap flux measurements. Agricultural and forest meteorology. 148:1719-1732.

Oliva, J., J. Julio Camarero and J. Stenlid 2012. Understanding the role of sapwood loss and reaction zone formation on radial growth of Norway spruce (*Picea abies*) trees decayed by *Heterobasidion annosum* s.l. Forest Ecology and Management. 274:201-209.

Oliva, J., J. Stenlid and J. Martínez-Vilalta 2014. The effect of fungal pathogens on the water and carbon economy of trees: implications for drought-induced mortality. New Phytologist. 203:1028-1035.

Oren, R., J.S. Sperry, G.G. Katul, D.E. Pataki, B.E. Ewers, N. Phillips and K.V.R. Schäfer 1999. Survey and synthesis of intra and interspecific variation in stomatal sensitivity to vapour pressure deficit. Plant, Cell & Environment. 22:1515-1526.

Palacio, S., P. Millard, M. Maestro and G. Montserrat-Martí 2007. Non-structural carbohydrates and nitrogen dynamics in Mediterranean sub-shrubs: an analysis of the functional role of overwintering leaves. Plant Biology. 9:49-58.

Pammenter, N.W. and C. Van Der Willigen 1998. A mathematical and statistical analysis of the curves illustrating vulnerability of xylem to cavitation. Tree Physiology. 18:589-593.

Pan, Y., R.A. Birdsey, J. Fang, R. Houghton, P.E. Kauppi, W.A. Kurz, O.L. Phillips, A. Shvidenko, S.L. Lewis and J.G. Canadell 2011. A large and persistent carbon sink in the world's forests. Science. 333:988-993.

Pangle, R.E., J.-M. Limousin, J.A. Plaut, E.A. Yepez, P.J. Hudson, A.L. Boutz, N. Gehres, W.T. Pockman and N.G. McDowell 2015. Prolonged experimental drought reduces plant hydraulic conductance and transpiration and increases mortality in a piñon-juniper woodland. Ecology and evolution. 5:1618-1638.

Pataki, D.E., R. Oren and N. Phillips 1998. Responses of sap flux and stomatal conductance of *Pinus taeda* L. trees to stepwise reductions in leaf area. Journal of Experimental Botany. 49:871-878.

Peguero-Pina, J.J., D. Sancho-Knapik, E. Barrón, J.J. Camarero, A. Vilagrosa and E. Gil-Pelegrín 2014. Morphological and physiological divergences within *Quercus ilex* support the existence of different ecotypes depending on climatic dryness. Annals of Botany. 114:301-313.

Perämäki, M., E. Nikinmaa, S. Sevanto, H. Ilvesniemi, E. Siivola, P. Hari and T. Vesala 2001. Tree stem diameter variations and transpiration in Scots pine: an analysis using a dynamic sap flow model. Tree Physiology. 21:889-897.

Pereira Blanco, E., F. Lloret Maya, J. Curiel Yuste and J. Barba Ferrer 2014. Response of fine root respiration to variations in biotic and abiotic factors in a mixed Mediterranean forest affected by drought-induced secondary succession. *In* Departament de Biologia Animal, Biologia Vegetal i Ecologia. Universitat Autònoma de Barcelona, Cerdanyola del Vallès, p. 27.

Phillips, N. and R. Oren 1998. A comparison of daily representations of canopy conductance based on two conditional time-averaging methods and the dependence of daily conductance on environmental factors. Annales des Sciences Forestières. 55:217-235.

Pinheiro, J. and D.M. Bates 2000. Mixed-effects Models in S and S-Plus. Springer Verlag, Berlin.

Piper, F.I. 2011. Drought induces opposite changes in the concentration of non-structural carbohydrates of two evergreen *Nothofagus* species of differential drought resistance. Annals of Forest Science. 68:415-424.

Piper, F.I. and A. Fajardo 2016. Carbon dynamics of *Acer pseudoplatanus* seedlings under drought and complete darkness. Tree Physiology

Plaut, J.A., W.D. Wadsworth, R. Pangle, E.A. Yepez, N.G. McDowell and W.T. Pockman 2013. Reduced transpiration response to precipitation pulses precedes mortality in a piñon-juniper woodland subject to prolonged drought. New Phytologist. 200:375-387.

Plaut, J.A., E.A. Yepez, J. Hill, R. Pangle, J.S. Sperry, W.T. Pockman and N.G. McDowell 2012. Hydraulic limits preceding mortality in a piñon-juniper woodland under experimental drought. Plant, Cell & Environment. 35:1601-1617.

Poyatos, R., D. Aguadé, L. Galiano, M. Mencuccini and J. Martínez-Vilalta 2013. Drought-induced defoliation and long periods of near-zero gas exchange play a key role in accentuating metabolic decline of Scots pine. New Phytologist. 200:388-401.

Poyatos, R., P. Llorens, J. Piñol and C. Rubio 2008. Response of Scots pine (*Pinus sylvestris* L.) and pubescent oak (*Quercus pubescens* Willd.) to soil and atmospheric water deficits under Mediterranean mountain climate. Annals of Forest Science. 65:306-306.

Poyatos, R., J. Martínez-Vilalta, J. Čermák, R. Ceulemans, A. Granier, J. Irvine, B. Köstner, F. Lagergren, L. Meiresonne, N. Nadezhdina, R. Zimmermann, P. Llorens and M. Mencuccini 2007. Plasticity in hydraulic architecture of Scots pine across Eurasia. Oecologia. 153:245-259.

Pratt, R.B., A.L. Jacobsen, A.R. Ramirez, A.M. Helms, C.A. Traugh, M.F. Tobin, M.S. Heffner and S.D. Davis 2014. Mortality of resprouting chaparral shrubs after a fire and during a record drought: physiological mechanisms and demographic consequences. Global Change Biology. 20:893-907.

Quentin, A.G., A.P. O'Grady, C.L. Beadle, D. Worledge and E.A. Pinkard 2011. Responses of transpiration and canopy conductance to partial defoliation of *Eucalyptus globulus* trees. Agricultural and forest meteorology. 151:356-364.

Quentin, A.G., E.A. Pinkard, M.G. Ryan, D.T. Tissue, L.S. Baggett, H.D. Adams, P. Maillard, J. Marchand, S.M. Landhäusser, A. Lacointe, Y. Gibon, W.R.L. Anderegg, S. Asao, O.K. Atkin, M. Bonhomme, C. Claye, P.S. Chow, A. Clément-Vidal, N.W. Davies, L.T. Dickman, R. Dumbur, D.S. Ellsworth, K. Falk, L. Galiano, J.M. Grünzweig, H. Hartmann, G. Hoch, S.

Hood, J.E. Jones, T. Koike, I. Kuhlmann, F. Lloret, M. Maestro, S.D. Mansfield, J. Martínez-Vilalta, M. Maucourt, N.G. McDowell, A. Moing, B. Muller, S.G. Nebauer, Ü. Niinemets, S. Palacio, F. Piper, E. Raveh, A. Richter, G. Rolland, T. Rosas, B. Saint Joanis, A. Sala, R.A. Smith, F. Sterck, J.R. Stinziano, M. Tobias, F. Unda, M. Watanabe, D.A. Way, L.K. Weerasinghe, B. Wild, E. Wiley and D.R. Woodruff 2015. Non-structural carbohydrates in woody plants compared among laboratories. Tree Physiology. 35:1146-1165.

Quero, J.L., F.J. Sterck, J. Martínez-Vilalta and R. Villar 2011. Water-use strategies of six co-existing Mediterranean woody species during a summer drought. Oecologia. 166:45-57.

Reichstein, M., M. Bahn, P. Ciais, D. Frank, M.D. Mahecha, S.I. Seneviratne, J. Zscheischler, C. Beer, N. Buchmann and D.C. Frank 2013. Climate extremes and the carbon cycle. Nature. 500:287-295.

Rigling, A., C. Bigler, B. Eilmann, E. Feldmeyer-Christe, U. Gimmi, C. Ginzler, U. Graf, P. Mayer, G. Vacchiano and P. Weber 2013. Driving factors of a vegetation shift from Scots pine to pubescent oak in dry Alpine forests. Global Change Biology. 19:229-240.

Rodríguez-Calcerrada, J., M. Li, R. López, F.J. Cano, J. Oleksyn, O.K. Atkin, P. Pita, I. Aranda and L. Gil 2016. Drought-induced shoot dieback starts with massive root xylem embolism and variable depletion of nonstructural carbohydrates in seedlings of two tree species. New Phytologist

R Core Team (2009). R: A language and environment for statistical computing. R Foundation for Statistical Computing, Vienna, Austria. URL https://www.R-project.org/

R Core Team (2013). R: A language and environment for statistical computing. R Foundation for Statistical Computing, Vienna, Austria. URL https://www.R-project.org/

R Core Team (2014). R: A language and environment for statistical computing. R Foundation for Statistical Computing, Vienna, Austria. URL https://www.R-project.org/

R Core Team (2016). R: A language and environment for statistical computing. R Foundation for Statistical Computing, Vienna, Austria. URL https://www.R-project.org/

Rosas, T., L. Galiano, R. Ogaya, J. Peñuelas and J. Martínez-Vilalta 2013. Dynamics of non-structural carbohydrates in three Mediterranean woody species following long-term experimental drought. Frontiers in Plant Science. 4:400.

Running, S.W. 1980. Field estimates of root and xylem resistances in *Pinus contorta* using root excision. Journal of Experimental Botany. 31:555-569.

Sack, L. and N.M. Holbrook 2006. Leaf hydraulics. Annu. Rev. Plant Biol. 57:361-381.

Sala, A. 2009. Lack of direct evidence for the carbon-starvation hypothesis to explain drought-induced mortality in trees. Proceedings of the National Academy of Sciences. 106:68.

Sala, A. and M. Mencuccini 2014. Ecosystem science: Plump trees win under drought. Nature Climate Change. 4:666-667.

Sala, A., F. Piper and G. Hoch 2010. Physiological mechanisms of drought induced tree mortality are far from being resolved. New Phytologist. 186:274-281.

Sala, A., D.R. Woodruff and F.C. Meinzer 2012. Carbon dynamics in trees: feast or famine? Tree Physiology. 32:764-775.

Salmon, Y., J.M. Torres-Ruiz, R. Poyatos, J. Martinez-Vilalta, P. Meir, H. Cochard and M. Mencuccini 2015. Balancing the risks of hydraulic failure and carbon starvation: a twig scale analysis in declining Scots pine. Plant, Cell & Environment. 38:2575-2588.

Sevanto, S., T. Holtta, A. Hirsikko, T. Vesala and E. Nikinmaa 2005a. Determination of thermal expansion of green wood and the accuracy of tree stem diameter variation measurements. Boreal environment research. 10:437-445.

Sevanto, S., T. Holtta, T. Markkanen, M. Peramaki, E. Nikinmaa and T. Vesala 2005b. Relationships between diurnal xylem diameter variation and environmental factors in Scots pine. Boreal environment research. 10:447-458.

Sevanto, S., N.G. McDowell, L.T. Dickman, R. Pangle and W.T. Pockman 2014. How do trees die? A test of the hydraulic failure and carbon starvation hypotheses. Plant, Cell & Environment. 37:153-161.

Sicard, P., A. Augustaitis, S. Belyazid, C. Calfapietra, A. de Marco, M. Fenn, A. Bytnerowicz, N. Grulke, S. He and R. Matyssek 2016. Global topics and novel approaches in the study of air pollution, climate change and forest ecosystems. Environmental pollution. 213:977-987.

Simonneau, T., R. Habib, J.P. Goutouly and J.G. Huguet 1993. Diurnal changes in stem diameter depend upon variations in water content: direct evidence in peach trees. Journal of Experimental Botany. 44:615-621.

Sperry, J. 2013. Cutting-edge research or cutting-edge artefact? An overdue control experiment complicates the xylem refilling story. Plant, Cell & Environment. 36:1916-1918.

Sperry, J.S., U.G. Hacke, R. Oren and J.P. Comstock 2002. Water deficits and hydraulic limits to leaf water supply. Plant, Cell & Environment. 25:251-263.

Sperry, J.S. and D.M. Love 2015. What plant hydraulics can tell us about responses to climate-change droughts. New Phytologist. 207:14-27.

Tardieu, F. and T. Simonneau 1998. Variability among species of stomatal control under fluctuating soil water status and evaporative demand: modelling isohydric and anisohydric behaviours. Journal of Experimental Botany. 49:419-432.

Team, R.C. 2016. R: A language and environment for statistical computing. R Foundation for Statistical Computing, Vienna, Austria.

Thabeet, A., M. Vennetier, C. Gadbin-Henry, N. Denelle, M. Roux, Y. Caraglio and B. Vila 2009. Response of *Pinus sylvestris* L. to recent climatic events in the French Mediterranean region. Trees. 23:843-853.

Torres-Ruiz, J.M., H. Cochard, S. Mayr, B. Beikircher, A. Diaz-Espejo, C.M. Rodriguez-Dominguez, E. Badel and J.E. Fernández 2014. Vulnerability to cavitation in *Olea europaea* current-year shoots: further evidence of an open-vessel artifact associated with centrifuge and air-injection techniques. Physiologia plantarum. 152:465-474.

Trenberth, K.E., A. Dai, G. van der Schrier, P.D. Jones, J. Barichivich, K.R. Briffa and J. Sheffield 2014. Global warming and changes in drought. Nature Climate Change. 4:17-22.

Tyree, M.T. and F.W. Ewers 1991. The hydraulic architecture of trees and other woody plants. New Phytologist. 119:345-360.

Ueda, M. and E.i. Shibata 2001. Diurnal changes in branch diameter as indicator of water status of Hinoki cypress *Chamaecyparis obtusa*. Trees. 15:315-318.

Urli, M., J.-B. Lamy, F. Sin, R. Burlett, S. Delzon and A.J. Porté 2015. The high vulnerability of *Quercus robur* to drought at its southern margin paves the way for *Quercus ilex*. Plant Ecology. 216:177-187.

Urli, M., A.J. Porté, H. Cochard, Y. Guengant, R. Burlett and S. Delzon 2013. Xylem embolism threshold for catastrophic hydraulic failure in angiosperm trees. Tree Physiology. 33:672-683.

Van Mantgem, P.J., N.L. Stephenson, J.C. Byrne, L.D. Daniels, J.F. Franklin, P.Z. Fule, M.E. Harmon, A.J. Larson, J.M. Smith and A.H. Taylor 2009. Widespread increase of tree mortality rates in the western United States. Science. 323:521-524.

Vandeleur, R.K., G. Mayo, M.C. Shelden, M. Gilliham, B.N. Kaiser and S.D. Tyerman 2009. The role of plasma membrane intrinsic protein aquaporins in water transport through roots: diurnal and drought stress responses reveal different strategies between isohydric and anisohydric cultivars of grapevine. Plant Physiology. 149:445-460.

Vayreda, J., J. Martínez-Vilalta, M. Gracia, J.G. Canadell and J. Retana 2016. Anthropogenic-driven rapid shifts in tree distribution lead to increased dominance of broadleaf species. Global Change Biology. 22:3984-3995.

Vertui, F. and F. Tagliaferro 1998. Scots pine (*Pinus sylvestris* L.) die-back by unknown causes in the Aosta Valley, Italy. Chemosphere. 36:1061-1065.

Vilà-Cabrera, A., J. Martínez-Vilalta, L. Galiano and J. Retana 2013. Patterns of forest decline and regeneration across Scots pine populations. Ecosystems. 16:323-335.

Vilà-Cabrera, A., J. Martínez-Vilalta and J. Retana 2014. Variation in reproduction and growth in declining Scots pine populations. Perspectives in Plant Ecology, Evolution and Systematics. 16:111-120.

Vilà-Cabrera, A., J. Martínez-Vilalta, J. Vayreda and J. Retana 2011. Structural and climatic determinants of demographic rates of Scots pine forests across the Iberian Peninsula. Ecological Applications. 21:1162-1172.

Warren, J.M., F.C. Meinzer, J.R. Brooks and J.C. Domec 2005. Vertical stratification of soil water storage and release dynamics in Pacific Northwest coniferous forests. Agricultural and forest meteorology. 130:39-58.

Wermelinger, B., A. Rigling, D. Schneider Mathis and M. Dobbertin 2008. Assessing the role of bark- and wood-boring insects in the decline of Scots pine (*Pinus sylvestris*) in the Swiss Rhone valley. Ecological Entomology. 33:239-249.

Whitehead, D. and P.G. Jarvis 1981. Coniferous forests and plantations. *In* Water deficits and plant growth, edited by: Kozlowski, TT, Academic Press, New York, NY, VI, pp. 49-152.

Williams, A.P., C.D. Allen, A.K. Macalady, D. Griffin, C.A. Woodhouse, D.M. Meko, T.W. Swetnam, S.A. Rauscher, R. Seager and H.D. Grissino-Mayer 2012. Temperature as a potent driver of regional forest drought stress and tree mortality. Nature Climate Change. 3:292-297.

Woodward, F.I. 1987. Climate and plant distribution. Cambridge University Press, Cambridge. 174 p.

Zhang, J., S. Huang and F. He 2015. Half-century evidence from western Canada shows forest dynamics are primarly driven by competition followed by climate. Proceedings of the National Academy of Sciences. 12:4009-4014.

Zweifel, R., A. Rigling and M. Dobbertin 2009. Species-specific stomatal response of trees to drought - a link to vegetation dynamics? Journal of Vegetation Science. 20:442-454.

Zweifel, R., K. Steppe and F.J. Sterck 2007. Stomatal regulation by microclimate and tree water relations: interpreting ecophysiological field data with a hydraulic plant model. Journal of Experimental Botany. 58:2113-2131.

Supplemental Material 1

Drought-induced defoliation and long periods of near-zero gas exchange play a key role in accentuating metabolic decline of Scots pine

Table S1. Characteristics of the measured trees: defoliation class (D, defoliated; ND, non-defoliated), diameter at breast height (DBH), height *(h)*, basal area (A_b), sapwood area (A_s), maximum leaf area (A_L), leaf-to-sapwood area ratio (A_L:A_S) and number of primary branches ($N_{branches}$).

Code	**Class**	**Green needles**	**DBH**	***h***	A_b	A_s	A_L	A_L:A_S	$N_{branches}$
		%	(cm)	(m)	cm^2	cm^2	m^2	m^2cm^{-2}	
703	D	40	39.1	13					
365	D	30	36.2	13.1					
364	D	40	40.1	11.5	1262.9	430.0	19.53	0.045	36
704	D	50	48	11.2	1809.6	652.1	16.64	0.026	32
706	D	50	38.8	14.6	1182.4	397.3	20.89	0.053	27
707	D	45	24.9	11.5	487.0	114.7	6.69	0.058	19
714	D	50	40.9	14.9	1313.8	450.7	16.52	0.037	25
542	D	45	42.6	14.5	1425.3	496.0	19.46	0.039	26
544	D	45	28.4	16.1	633.5	174.2	8.53	0.049	21
699	D	40	45.7	15.7	1640.3	583.3	15.23	0.026	20
693	D	35	42.8	11.7	1438.7	501.4	10.47	0.021	19
711	ND	90	46.5	15.2	1698.2	606.8	32.91	0.054	23
712	ND	80	59.4	14.4	2771.2	1042.8	93.33	0.089	30
713	ND	80	26.7	8.2	559.9	144.3	19.94	0.138	34
715	ND	100	45.8	14.1	1647.5	586.2	37.02	0.063	31
716	ND	80	43.8	14.9	1506.7	529.0	31.63	0.060	35
717	ND	100	41.7	15.2	1365.7	471.7	25.84	0.055	25
572	ND	100	44.7	17.3	1569.3	554.5	45.99	0.083	37
561	ND	80	35.5	16.1	989.8	319.0	17.06	0.053	19
562	ND	80	38.3	18	1152.1	385.0	37.24	0.097	38
725	ND	100	41	14.4	1320.3	453.3	23.03	0.051	28
Defoliated			38.9±2.1	13.4±0.5	1244±145	422±59	**14.9±1.7**	**0.039±0.004**	**25±2**
Non-defoliated			42.3±2.7	14.8±0.8	1458±182	509±74	**36.4±6.9**	**0.074±0.009**	**30±2**

The two bottom rows show mean (±SE) for defoliated and non-defoliated trees. Numbers in bold represent statistically significant differences ($P < 0.05$). Trees 365 and 703 died before sensor installation.

Table S2. Summary of sap flow of defoliated and non-defoliated Scots pine trees, for different periods of years 2010 and 2011. Sap flow is expressed on a leaf (J_L), sapwood (J_S) and tree (J_T) basis.

		J_L (kg m^{-2} leaves d^{-1})			J_S (g cm^{-2} sapwood d^{-1})			J_T (kg d^{-1})		
		Defoliated	**Non-defoliated**	**%**	**Defoliated**	**Non-defoliated**	**%**	**Defoliated**	**Non-defoliated**	**%**
Year	Period									
2010										
	May-Jun	2.18 ± 0.24 [a]	1.11 ± 0.21 [b]	197	72.32 ± 5.11 [a]	71.7 ± 11.09 [a]	101	31.30 ± 1.25 [a]	37.75 ± 1.71 [a]	83
	Jul-Aug	**0.56 ± 0.07 [a]**	**0.39 ± 0.09 [b]**	144	**22.08 ± 2.52 [a]**	**29.27 ± 5.47 [a]**	75	**9.50 ± 0.74 [a]**	**15.69 ± 1.16 [b]**	61
	Sep-Oct	**0.66 ± 0.09 [a]**	**0.39 ± 0.10 [b]**	170	**20.68 ± 1.99 [a]**	**23.68 ± 4.61 [a]**	87	**9.18 ± 0.72 [a]**	**12.34 ± 1.00 [a]**	74
2011										
	May-Jun	1.53 ± 0.19 [a]	0.77 ± 0.14 [b]	200	49.07 ± 4.00 [a]	50.52 ± 8.49 [a]	97	21.71 ± 1.08 [a]	25.92 ± 1.43 [a]	84
	Jul-Aug	**0.16 ± 0.02 [a]**	**0.09 ± 0.01 [b]**	174	**6.83 ± 1.21 [a]**	**7.58 ± 1.13 [a]**	90	**2.68 ± 0.41 [a]**	**3.74 ± 0.49 [a]**	72
	Sep-Oct	**0.12 ± 0.02 [a]**	**0.05 ± 0.01 [b]**	222	**3.99 ± 0.68 [a]**	**3.45 ± 0.65 [a]**	116	**1.57 ± 0.30 [a]**	**2.01 ± 0.48 [a]**	78

Data show means and standard errors among trees of defoliated and non-defoliated classes within a period. Different lowercase letters represent statistically significant differences ($P < 0.05$) between defoliated and non-defoliated trees. Numbers in bold represent statistically significant differences ($P < 0.05$) for a given period across years.

Table S3. Shoot and leaf parameters (mean ± standard error) for different growth cohorts in defoliated and non-defoliated Scots pines.

	2008		2009		2010	
	Defoliated	**Non-defoliated**	**Defoliated**	**Non-defoliated**	**Defoliated**	**Non-defoliated**
Shoot growth (mm)	20.82 ± 1.13 [a]	22.45 ± 1.11 [a]	19.95 ± 1.27 [a]	28.48 ± 1.50 [b]	16.26 ± 1.01 [a]	22.94 ± 1.46 [b]
Shoot growth with needles (mm)	16.34 ± 1.05 [a]	17.17 ± 1.24 [a]	13.65 ± 1.68 [a]	17.66 ± 1.97 [a]	13.66 ± 0.89 [a]	18.01 ± 1.30 [a]
Needles per shoot	56 ± 4 [a]	58 ± 3 [a]	43 ± 5 [a]	44 ± 3 [a]	46 ± 3 [a]	55 ± 3 [b]
Needle density (cm^{-1})	35.47 ± 2.40 [a]	39.76 ± 3.85 [a]	32.05 ± 1.88 [a]	29.74 ± 1.57 [a]	36.19 ± 2.75 [a]	32.15 ± 1.35 [a]
Average Needle Area (cm^2)	0.36 ± 0.02 [a]	0.4 ± 0.01 [a]	0.27 ± 0.01 [a]	0.25 ± 0.01 [a]	0.33 ± 0.02 [a]	0.36 ± 0.01 [a]
Specific leaf area ($cm^2\ g^{-1}$)	28.42 ± 0.35 [a]	26.54 ± 0.65 [a]	31.21 ± 0.49 [a]	29.06 ± 0.40 [a]	33.82 ± 1.23 [a]	31.31 ± 0.52 [b]

Different lowercase letters represent statistically significant differences ($P < 0.05$) between defoliated and non-defoliated trees.

Supplemental Material 2

The role of defoliation and root pathogen infection in driving the mode of drought-related physiological decline in Scots pine (*Pinus sylvestris* L.)

Supplementary equations of the linear models used in the study

Equation S1:

$$RV1 = \beta_0 + \beta_1 \cdot Defoliation + \beta_2 \cdot Infection + \beta_3 \cdot Defoliation \cdot Infection + \varepsilon$$

Equation S2:

$$RV2 = \beta_0 + \gamma_0 + \beta_1 \cdot Organ + \beta_2 \cdot Defoliation + \beta_3 \cdot Infection + \beta_4 \cdot Organ \cdot Defoliation + \beta_5 \cdot Organ \cdot Infection + \varepsilon$$

Equation S3:

$$RV3 = \beta_0 + \gamma_0 + \beta_1 \cdot Month + \beta_2 \cdot Defoliation + \beta_3 \cdot Infection + \beta_4 \cdot Month \cdot Defoliation + \beta_5 \cdot Month \cdot Infection + \varepsilon$$

Equation S4:

$$RV4 = \beta_0 + \gamma_0 + \beta_1 \cdot Tissue + \beta_2 \cdot Month + \beta_3 \cdot Defoliation + \beta_4 \cdot Infection + \beta_5 \cdot Tissue \cdot Month + \beta_6 \cdot Tissue \cdot Defoliation + \beta_7 \cdot Tissue \cdot Infection + \beta_8 \cdot Month \cdot Defoliation + \beta_9 \cdot Month \cdot Infection + \varepsilon$$

Equation S5:

$$RV5 = \beta_0 + \gamma_0 + \beta_1 \cdot Month + \beta_2 \cdot Defoliation + \beta_3 \cdot Infection + \beta_4 \cdot Month \cdot Defoliation + \beta_5 \cdot Month \cdot Infection + \beta_6 \cdot Month \cdot Defoliation \cdot Infection + \varepsilon$$

Where RV is the Response Variable, β_0 is the overall intercept and β_1 to β_9 are parameters adjusting the fixed effects, γ_0 is the random effect associated with tree and ε is the error term.

Table S1. Main characteristics of the studied trees.

Tree ID	Species	Defolation (%)	Defoliation Class	DBH (cm)	BAI (cm^2)	Infestation	Pathogen
1601	Scots pine	25	D	26.5	16.82	NI	
1602	Scots pine	80	ND	37.5	20.97	NI	*P. pini*
1604	Scots pine	75	ND	40	19.72	NI	
1605	Scots pine	30	D	29	6.83	I	*Onnia* sp.
1606	Scots pine	25	D	35	12.08	NI	*P. pini*
1607	Scots pine	60	ND	39.5	17.98	NI	
1608	Scots pine	85	ND	36.3	11.60	NI	
1609	Scots pine	75	ND	28.2	11.02	NI	
1610	Scots pine	85	ND	40.1	18.26	NI	
1611	Scots pine	65	ND	40	20.36	I	*Onnia* sp.
1612	Scots pine	80	ND	35.8	19.94	I	*Onnia* sp.
1613	Scots pine	75	ND	27	19.51	NI	
1614	Scots pine	90	ND	24.2	16.11	NI	
1616	Scots pine	25	D	27	22.94	NI	
1617	Scots pine	35	D	38.6	18.56	I	*Onnia* sp.
1637*	Scots pine	10	D	45.5	19.74	NI	
1638	Scots pine	15	D	44	22.58	NI	
1639	Scots pine	25	D	41.5	11.18	NI	
1640	Scots pine	40	D	39	16.70	NI	
1621	Scots pine	25	D	47	11.52	I	*Onnia* sp.

Abbreviations: D, Defoliated tree; ND, Non-defoliated tree; DBH, Diameter at Breast Height; BAI, Basal Area Increment (calculated from the three newest rings); NI, Non-Infected; I, Infected. Crown status represents the percentage of green needles. *= tree that died during the study.

Supplemental Material 3

Roots hydraulic constraints during drought-induced decline in Scots pine

Table S1. Summary of the fitted linear mixed models with stem pressure difference (ΔP_{bc}) and below-crown hydraulic resistance (R_{bc}) as response variables.

VPD MODEL	**log(ΔP)**	**log(R_{bc})**
Parameter	**R^2 = 0.81**	**R^2 = 0.60**
Intercept	-3.21 ± 0.31***	-1.42 ± 0.46**
Non-defoliated	ni	0.72 ± 0.69 (ns)
VPD	0.84 ± 0.18***	0.10 ± 0.38 (ns)
VPD^2	-0.32 ± 0.07***	0.07 ± 0.14 (ns)
Non-defoliated:VPD	ni	-2.00 ± 0.65**
Non-defoliated:VPD^2	ni	0.76 ± 0.24**
SWC MODEL	**log(ΔP)**	**log(R_{bc})**
Parameter	**R^2 = 0.79**	**R^2 = 0.85**
Intercept	-1.41 ± 0.42***	-4.81 ± 0.51***
Non-defoliated	-2.09 ± 0.61*	-1.99 ± 0.74*
log(SWC)	0.46 ± 0.12***	-1.77 ± 0.13***
Non-defoliated:log(SWC)	-0.60 ± 0.19**	-0.82 ± 0.20***

For factors, the coefficients indicate the difference between each level of a given variable and its reference level. In models the reference defoliation class was "Defoliated". The values are the estimate ± SE. Abbreviations: ns, no significant differences; *0.01 < P < 0.05; **0.001 < P < 0.01; ***P < 0.001; ni, not included in the model. Conditional R^2 values are given for each model.

Supplemental Material 4

Comparative drought responses of *Quercus ilex* L. and *Pinus sylvestris* L. in a montane forest undergoing a vegetation shift

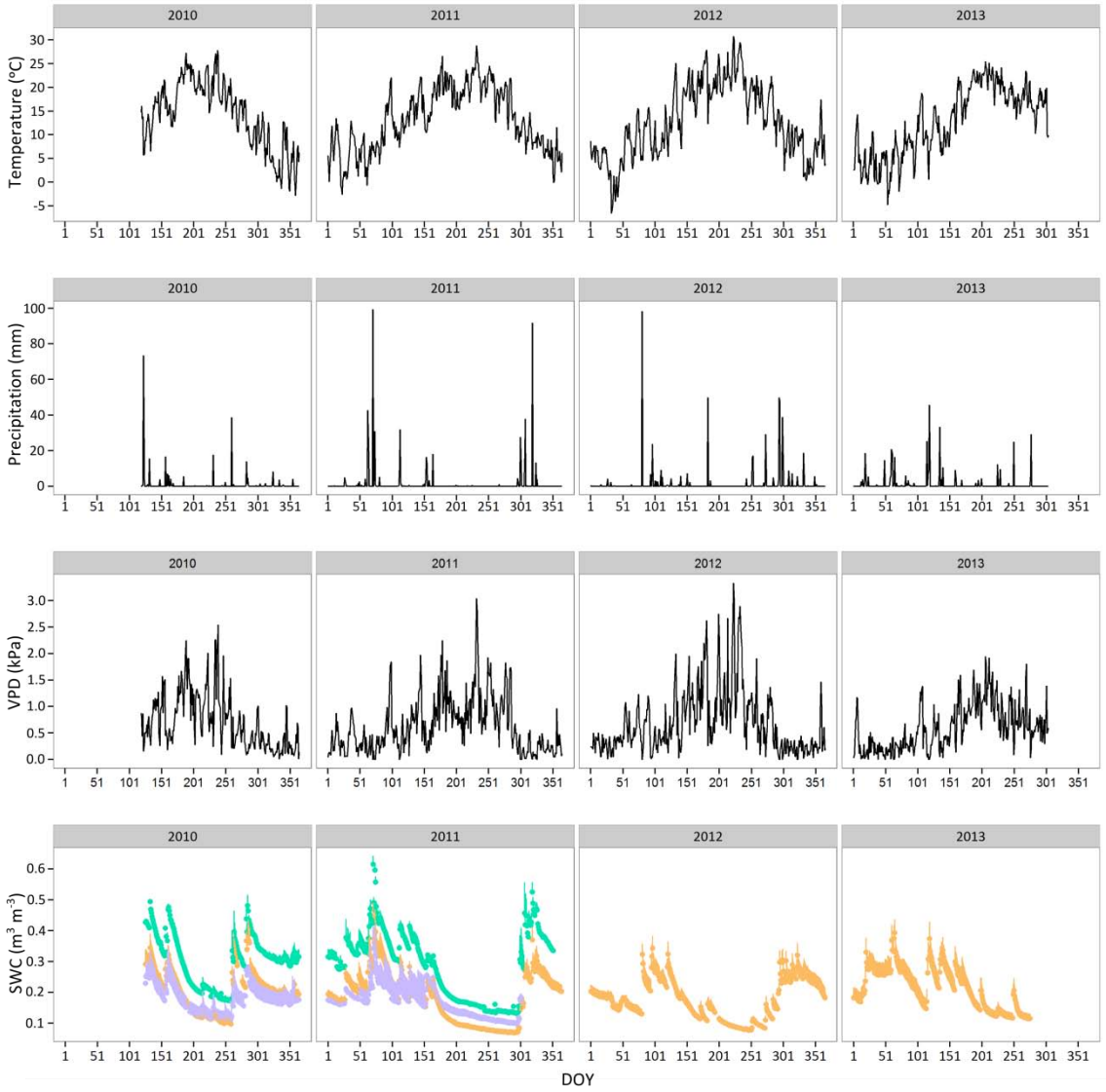

Figure S1. Seasonal course of temperature, precipitation, vapor pressure deficit (VPD), and soil water content (SWC): Orange symbols, mixed stand from Tillar valley; green symbols, pure Scots pine stand from Tillar valley; purple symbols, pure Holm oak stand from Tillar valley) over the study period; DOY, day of year. Error bars indicate +1 SE (only positive SEs are depicted to improve trend clarity). Note that SWC values > ~0.5 m^3 m^{-3} may be anomalous as a result of sensor malfunction (or inadequate calibration) under exceptionally wet conditions.

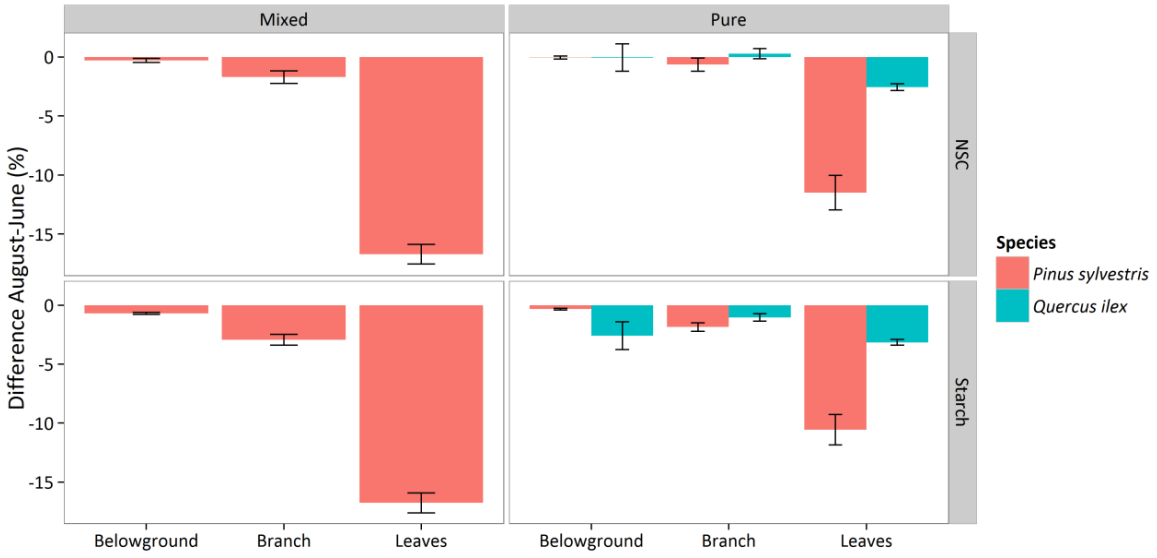

Figure S2. Absolute difference between August and June in measured total non-structural carbohydrates ($\Delta NSC_{Aug\text{-}Jun}$, upper panels) and starch ($\Delta Starch_{Aug\text{-}Jun}$, bottom panels). Values are given for different organs, stand types (columns), and species. Average values for Scots pine and holm oak trees are shown. Error bars indicate ±1 SE.

Table S1. Summary of the fitted quantile regressions (95th percentile) with stomatal conductance ($G_{s,md}$) as response variable. The lower and upper bounds of the confidence intervals are also indicated in brackets.

Species	Log (SWC)				log (VPD)			
	Mixed		Pure		Mixed		Pure	
	Intercept	Slope	Intercept	Slope	Intercept	Slope	Intercept	Slope
Scots pine	5.19 (4.94–5.43)	1.94 (1.83-2)	6.83 (6.6–7.93)	3.32 (3.1–3.78)	1.68 (1.62–1.78)	−1.04 (−1.29– −0.76)	2.26 (2.16–2.3)	−1.52 (−1.67– −1.46)
Holm oak	3.3 (2.74–4.03)	1.09 (0.75–1.41)	4.24 (3.66–4.47)	1.77 (1.37–1.89)	1.05 (1.02–1.08)	−0.75 (−0.81– −0.7)	0.87 (0.84–0.89)	−0.64 (−0.69– −0.58)

Table S2. Summary of the fitted linear mixed models with predawn water potential (Ψ_{PD}), midday water potential (Ψ_{MD}) and the difference between them ($\Delta\Psi$) as response variables.

SWC MODEL	**Ψ_{PD}**	**Ψ_{MD}**	**$\Delta\Psi$**
Parameter	R^2 = 0.76	R^2 = 0.78	R^2 = 0.35
Intercept	0.89 ± 0.31 **	−0.11 ± 0.30 (ns)	−0.79 ± 0.20 ***
Holm oak	1.91 ± 0.52 **	2.04 ± 0.50 ***	0.70 ± 0.15 ***
Pure stand	−0.46 ± 0.51 (ns)	−0.80 ± 0.49 (ns)	−0.81 ± 0.14 ***
SWC	1.06 ± 0.15 ***	0.82 ± 0.15 ***	16.50 ± 2.52 ***
SWC^2	ne	ne	−44.45 ± 7.07 ***
Holm oak:Pure stand	4.31 ± 0.95 ***	3.59 ± 0.92 **	0.24 ± 0.11 *
Holm oak:SWC	1.31 ± 0.25 ***	1.53 ± 0.24 ***	−2.79 ± 0.98 **
Pure stand:SWC	−0.04 ± 0.30 (ns)	-0.32 ± 0.29 (ns)	ni
Holm oak:Pure stand:SWC	2.26 ± 0.51 ***	1.95 ± 0.49 ***	ni
Pure stand:SWC^2	ne	ne	16.17 ± 2.82 ***
VPD MODEL	Ψ_{PD}	Ψ_{MD}	$\Delta\Psi$
Parameter	R^2 = 0.37	R^2 = 0.47	R^2 = 0.12
Intercept	−0.78 ± 0.17 ***	−1.37 ± 0.16 ***	0.51 ± 0.03 ***
Holm oak	−0.14 ± 0.28 (ns)	−0.44 ± 0.26 (ns)	0.25 ± 0.05 ***
VPD	−0.44 ± 0.16 **	−0.36 ± 0.15 *	ni
Holm oak:VPD	−0.65 ± 0.25 **	−0.62 ± 0.23 **	ni

For factors, the coefficients indicate the difference between each level of a given variable and its reference level. In all models, the reference species was Scots pine and the reference stand type was “Mixed stand.” The values are the estimate ± SE. Only interactions between factors present in at least one best-fitting model of all response variables are depicted in the table. Abbreviations: ns, not significant; * 0.01 < P < 0.05; ** 0.001 < P < 0.01; *** P < 0.001; ne, not evaluated in the best model; ni, not included. Conditional R^2 values are given for each model. Note that SWC was log-transformed in some models (Ψ_{PD} and Ψ_{MD}) to better capture the functional relationship.

Table S3. Summary of the linear mixed effect models of whole-tree leaf-specific hydraulic conductance (k_{S_L}) as response variable.

Parameter	k_{S_L}
SWC MODEL	R^2 **= 0.47**
Intercept	−3.46 ± 1.90 *
Holm oak	−2.43 ± 1.71 (ns)
Pure stand	−1.39 ± 2.10 ***
SWC	1.05 ± 1.25 ***
Holm oak:Pure stand	8.23 ± 2.82 **
VPD MODEL	R^2 **= 0.11**
Intercept	8.75 ± 8.09 ***
Pure stand	−5.18 ± 1.31 ***
VPD	ni

For factors, the coefficients indicate the difference between each level of a given variable and its reference level. In all models, the reference species was Scots pine and the reference stand type was "Mixed stand." The values are the estimate ± SE. Only interactions between factors present in at least one best-fitting model of all response variables are depicted in the table. Abbreviations: ns, not significant; * 0.05 <P < 0.1; ** 0.001 <P < 0.01; *** P < 0.001; ni, not included. Conditional R^2values are given for each model.

Table S4. Summary of the fitted linear mixed models with percent loss of hydraulic conductivity (PLC) measured on branches on belowground organs as response variables.

Parameter	**PLC (Branches)**	**PLC (Belowground)**
SWC MODEL	R^2 **= 0.78**	R^2 **= 0.87**
Intercept	0.68 ± 0.17***	0.96 ± 0.15 ***
Holm oak	1.13 ± 0.07***	1.41 ± 0.26 ***
Pure stand	0.27 ± 0.07**	0.42 ± 0.25 (ns)
SWC	−1.11 ± 0.08***	−1.15 ± 0.08 ***
Holm oak:Pure stand	ni	−2.10 ± 0.48 ***
Holm oak:SWC	ni	0.26 ± 0.13 *
Pure stand: SWC	ni	−0.02 ± 0.15 (ns)
Holm oak:Pure stand:SWC	ni	−0.86 ± 0.25 ***
VPD MODEL	R^2 **= 0.68**	R^2 **= 0.58**
Intercept	3.02 ± 0.06 ***	3.31 ± 0.05 ***
Holm oak	1.25 ± 0.08 ***	0.87 ± 0.07 ***
Pure stand	−0.18 ± 0.08 *	ni
VPD	0.65 ± 0.09 ***	0.34 ± 0.05 ***
Holm oak:VPD	−0.19 ± 0.12 (ns)	ni
Pure stand:VPD	−0.36 ± 0.12**	ni

For factors, the coefficients indicate the difference between each level of a given variable and its reference level. In all models, the reference species was Scots pine and the reference stand type was “Mixed stand.” The values are the estimate ± SE. Only interactions between factors present in at least one best-fitting model of all response variables are depicted in the table. Abbreviations: ns, not significant; * 0.01 < P < 0.05; ** 0.001 < P < 0.01; *** P < 0.001; ni, not included in the best model. Conditional R^2values are given for each model. Note that SWC and VPD were log-transformed to better capture the functional relationship.

Table S5. Summary of the absolute difference of NSC ($\Delta NSC_{Aug\text{-}Jun}$) and Starch ($\Delta Starch_{Aug\text{-}Jun}$) and the relative difference of NSC ($\Delta NSC_{Aug\text{-}Jun,rel}$) and starch ($\Delta Starch_{Aug\text{-}Jun,rel}$) as response variables.

Parameter	**$\Delta NSC_{Aug\text{-}Jun}$**	**$\Delta NSC_{Aug\text{-}Jun,rel}$**	**$\Delta Starch_{Aug\text{-}Jun}$**	**$\Delta Starch_{Aug\text{-}Jun,rel}$**
	R^2 = 0.78	**R^2 = 0.17**	**R^2 = 0.77**	**R^2 = 0.11**
Intercept	0.51 ± 0.95 (ns)	−0.23 ± 0.17 (ns)	−0.76 ± 0.84 (ns)	−0.66 ± 0.17 ***
Holm oak	−0.01 ± 1.17 (ns)	0.43 ± 0.17*	−2.25 ± 1.04 *	0.45 ± 0.17 *
Branches	−2.21 ± 1.34 (ns)	0.30 ± 0.21 (ns)	−2.18 ± 1.19*	−0.06 ± 0.21(ns)
Leaves	−18.01 ± 1.34 ***	−0.52 ± 0.21*	−15.96 ± 1.19 ***	−0.51 ± 0.21 *
Pure stand	−0.55 ± 1.34 (ns)	ni	0.42 ± 1.19 (ns)	ni
Holm oak:Branches	0.93 ± 1.66 (ns)	ni	3.06 ± 1.47 *	ni
Holm oak:Leaves	8.96 ± 1.66 ***	ni	9.66 ± 1.47 ***	ni
Branches: Pure stand	1.61 ± 1.90 (ns)	ni	0.67 ± 1.68 (ns)	ni
Leaves: Pure stand	6.56 ± 1.90 ***	ni	5.73 ± 1.68 **	ni

For factors, the coefficients indicate the difference between each level of a given variable and its reference level. In all models, the reference species was Scots pine and the reference stand type was "Mixed stand." The values are the estimate ± SE. Only interactions between factors present in at least one best-fitting model of all response variables are depicted in the table. Abbreviations: ns, not significant; * 0.05 < *P* < 0.1; ** 0.001 < *P* < 0.01; *** *P* < 0.001; ni, not included in the best model. Conditional R^2values are given for each model.

Agraïments

Arribats en aquest punt, toca escriure una de les parts més importants de la tesi. Si més no, la que serà llegida abans que la resta per a la majoria a qui aquesta tesi li arribi a les mans.

Primer de tot voldria donar les gràcies al Jordi i al Rafa, els meus directors de tesi. Sense ells, aquesta tesi no hauria quedat tal i com la podeu llegir en aquest exemplar. Des de la beca que vaig obtindre durant la carrera per fer la "col·laboració en una empresa" (on vaig fer el minuciós treball de soldar i muntar les sondes de Granier) fins al doctorat, amb el màster entremig, hem passat moltes hores plegats: incloent des de les sortides de camp al Barranc del Tillar fins a les reunions. Les vivències viscudes al barranc del Tillar durant aquests anys seran difícils d'oblidar: punxar la roda del cotxe a l'Espluga del Francolí, atropellament del genoll del Rafa entre dos cotxes (sense cap mal major), temperatures baixes extremes (amb nevades incloses) i temperatures altes extremes (amb risc d'incendi inclòs), esmorzars al Casal de l'Espluga i el dinar post-desmantellament dels aparells a l'hostal del Senglar, despertar-se aviat per fer mesures "predawn" quan encara se sentia la música de la festa major de l'Espluga... i tantes altres coses que tothom qui ha anat al Tillar segurament li ha passat. Però, sobretot, gràcies per donar-me la oportunitat per fer aquesta tesi amb vosaltres i per guiar-me, ensenyar-me tantes coses i aconsellar-me en tot moment en l'elaboració d'aquesta tesi.

En segon lloc, aquesta tesi també és obra dels meus pares. Gràcies a ells, vaig poder estudiar la carrera de Biologia a la UAB i començar una nova etapa fora de Riudoms. Si ma mare no m'hagués fet les fiambreres amb menjar durant els primers anys de la carrera o mun pare no m'hagués portat cada diumenge a l'estació de Les Borges del Camp per agafar el tren, ara potser aquesta tesi no existiria. També gràcies a tu Meri. Durant aquests últims mesos i setmanes has tingut prou paciència com per aguantar-me tot i el meu estat de nervis per finalitzar la tesi. Tu has patit, tant com jo, les últimes setmanes de la tesi.

Arriba ara el moment de parlar del -116. Per qui llegeixi aquestes línies i no conegui el -116, dir-vos que és el despatx on he treballat durant aquests anys de tesi, amb l'Ander, l'Adrià i el Jofre. De fet, Ander, podries fer un article de la Viquipèdia sobre el -116. M'és difícil explicar alguna cosa del -116 que no hagin explicat ja anteriorment a les seves respectives tesis l'Adrià o l'Ander. Des del meu punt de vista, he aportat coneixements al despatx sobre les comarques del sud. Poc abans de la meva arribada, la visió de Catalunya del despatx era més aviat barcelonina i el dialecte predominant era el de Barcelona i rodalies. Amb la meva arribada, van obrir els ulls, i van conèixer un altre parlar i noves paraules del territori de l'avellana i el poble natal de Gaudí. No obstant,

també he de reconèixer que amb ells vaig aprendre les noves tendències del Principat, sobretot les centrades en el món dels “skaters” i els “surfers”. Cal destacar que, a banda de treballar, també hem passat grans estones al -116. Però no tot han sigut flors i violes: èpoques fosques amb la persiana baixada, erugues de processionària lliures pel despatx, pols dels cores per tot arreu, música de saxos sonant a tot volum, troncs abandonats pel terra... Perdona Jofre per haver-te “tunejat” el mapa de Cobertes del Sòl de Catalunya que amb bona fe havies penjat a la paret. Tot i les constants humiliacions per motiu geogràfic, gràcies també a vosaltres per aquests anys de companyerisme al despatx. Ep! Em deixava la Janet. La podríem considerar la cinquena membre del despatx. Sempre atent a que no ens faltés berenar i a recordar-nos que teníem les taules molt desordenades. Gràcies a tu també.

També voldria agrair a la Lucía i a la Tere les estones compartides durant la seva ajuda als mostrejos al Barranc del Tillar i a l’alberg Jaume I de l’Espluga. Gràcies també al Josep, al Jorje i a la Mireia per les ajudes compartides al Tillar.

Ja per acabar, no em voldria descuidar a ningú i, per tant, toca agrair al CREAF en general. Durant aquests anys al CREAF he conegut molta gent, amb les quals he compartit dilluns de futbol i dies d’escalada al SAF, dinars, sopars, Cerdanyolades, Diamantades (no tantes... baixar a Barcelona fa mandra), cafè/tertúlia, ajudes en moments d’estancament amb l’R, reunions de boscos... A tots vosaltres, moltes gràcies per fer inoblidable aquesta etapa al CREAF! No voldria acabar aquest apartat sense fer una menció especial al Guillem. Company de carrera, company de pis, company del CREAF i amic. Qui ho diria quan ens vam conèixer aquell llunyà 2005 que acabaríem fent una tesi doctoral. Gràcies a tu també per tots aquests anys i l’ajuda que m’has ofert sempre que ho he necessitat.

Gràcies, CREAF!

Aquesta tesi ha sigut possible gràcies a una beca FPU (Ministeri d’Economia, Cultura i Esport).